



HAL
open science

Methodologies and cross-layer protocols in electromagnetic nanonetworks and ultra-dense wireless ad hoc networks

Farah Hoteit

► **To cite this version:**

Farah Hoteit. Methodologies and cross-layer protocols in electromagnetic nanonetworks and ultra-dense wireless ad hoc networks. Networking and Internet Architecture [cs.NI]. Université Bourgogne Franche-Comté, 2022. English. NNT : 2022UBFCD037 . tel-04041457

HAL Id: tel-04041457

<https://theses.hal.science/tel-04041457>

Submitted on 22 Mar 2023

HAL is a multi-disciplinary open access archive for the deposit and dissemination of scientific research documents, whether they are published or not. The documents may come from teaching and research institutions in France or abroad, or from public or private research centers.

L'archive ouverte pluridisciplinaire **HAL**, est destinée au dépôt et à la diffusion de documents scientifiques de niveau recherche, publiés ou non, émanant des établissements d'enseignement et de recherche français ou étrangers, des laboratoires publics ou privés.

THÈSE DE DOCTORAT

DE L'ÉTABLISSEMENT UNIVERSITÉ BOURGOGNE-FRANCHE-COMTÉ

PRÉPARÉE À L'UNIVERSITÉ DE FRANCHE-COMTÉ

École doctorale n°37

Sciences Pour l'Ingénieur et Microtechniques

Doctorat d'Informatique

par

FARAH HOTEIT

Methodologies and cross-layer protocols in electromagnetic nanonetworks
and ultra-dense wireless ad hoc networks

Méthodologies et protocoles cross-layer dans les nanoréseaux électromagnétiques et les
réseaux ad hoc sans fil ultra-denses

Thèse présentée et soutenue à Montbéliard, le 8 Décembre 2022

Composition du Jury :

M. RONDEAU ÉRIC	Professeur à l'Université de Lorraine	Président
M. THEOLEYRE FABRICE	Ph.D. Directeur de Recherche CNRS	Rapporteur
M. HILT BENOÎT	Maître de conférences HDR à l'Université de Haute-Alsace - UHA	Rapporteur
M. DEDU EUGEN	Maître de conférences HDR à l'Université de Franche-Comté	Directeur de thèse
M. DHOUTAUT DOMINIQUE	Maître de conférences à l'Université de Franche-Comté	Co-directeur de thèse
M. SEAH WINSTON	Professeur à l'Université Victoria de Wellington	Co-encadrant de thèse

ACKNOWLEDGMENTS

First and foremost, I would like to show my sincere gratitude to my research supervisors Mr. Eugen Dedu, Mr. Dominique Dhoutaut and Mr. Winston Seah. They guided my research and helped me grow in my PhD journey. I thank Mr. Eugen for his enthusiasm for the topic, his consistent attention and his precious ideas that motivated me over the past three years. I thank Mr. Dominique Dhoutaut for his technical help, his inestimable explanations and illustrations that I appreciate a lot. And I thank Mr. Winston Seah for giving me valuable insights and visions for my thesis.

I appreciate the jury, Mr. Éric Rondeau, Mr. Fabrice Theoleyre and Mr. Benoît Hilt for being my PhD defense committee and for making honorable points about my thesis.

A special thanks goes to University Bourgogne Franche-Comté and to Pays de Montbéliard Agglomération for the academic and financial support of my research. I thank my doctoral school “Sciences Physiques pour l’Ingénieur et Microtechniques” (ED SPIM, ED37), for giving me the opportunity to pursue this work. I thank Ms. Thérèse Leblois, the director of SPIM and Ms. Aika Rossetti, the administrative staff.

Lastly, I am deeply grateful to my parents, my siblings and my grandmother, who were always there for me to support and encourage me, either physically or through calls. I love you. Distance can never separate us. I also thank my friends and my colleagues for the support and the beautiful memories.

Farah Hoteit

Montbéliard, 20-5-2022

“YOU GET IN LIFE WHAT YOU HAVE THE
COURAGE TO ASK FOR.”

Oprah Winfrey

THESIS CONTEXT

On October 1st 2019, I joined the OMNI team, DISC department in FEMTO-ST institute, University Bourgogne Franche-Comté in Montbéliard, France. My PhD supervisors are Dr. Eugen Dedu, Dr. Dominique Dhoutaut and Pr. Winston Seah. My PhD journey ended on September 30th 2022.

My PhD thesis focuses on the methodologies and the design of cross-layer protocols in ultra-dense wireless ad hoc networks and electromagnetic nanonetworks. Electromagnetic nanonetworks are a topic of interest for OMNI team. Current PhD students working on the same thematic are Ali Medlej and Carole Al Mawla. Additionally, a network simulator called BitSimulator is designed by OMNI specifically for nanonetworks. Authors of BitSimulator are Dominique Dhoutaut, a previous PhD student Thierry Arrabal and Eugen Dedu. Florian Buther, a German previous PhD student, also contributed to the simulator.

We shared this novel topic during many events, as in the following:

- Meeting with researchers in Polytechnic University of Cartagena in Spain. We discussed electromagnetic nanonetworks from the point of view of different layers (November 2019).
- Master thesis supervision of Setareh Nouri. The thesis is called: “Creation of a visualization tool and study of beta parameter in electromagnetic nanonetworks” (October 2020 - January 2021).
- Presentations of nanonetworks in RSD Research Autumn School: “Reproducibility and Experimental Research in Networks and Systems” in Strasbourg, France (October 2021), and in GDR RSD Days: “Journées du GDR Réseaux et Systèmes Distribués” in Rennes, France (April 2022). These presentations made us introduce nanonetworks to researchers in France and build connections with them.

PUBLICATIONS

My PhD journey resulted in four conferences papers, as listed here:

The following paper appears in Chapter 4, Section 4.3:

Hoteit et al. (2022b) Farah Hoteit, Eugen Dedu, Winston K.G. Seah, Dominique Dhoutaut. Ring-based forwarder selection to improve packet delivery in ultra-dense networks. WCNC, Austin, Texas, USA, 2022.

The following paper appears in Chapter 4, Section 4.4:

Hoteit et al. (2022d) Farah Hoteit, Dominique Dhoutaut, Winston K.G. Seah, Eugen Dedu. Expanded ring-based forwarder selection to improve packet delivery in ultra-dense nanonetworks. IWCMC, Dubrovnik, Croatia, 2022.

The following paper appears in Chapter 4, Section 4.5:

Hoteit et al. (2022c) Farah Hoteit, Dominique Dhoutaut, Winston K.G. Seah, Eugen Dedu. Dynamic ring-based forwarder selection to improve packet delivery in ultra-dense nanonetworks. ACM NanoCom, Barcelona, Catalunya, Spain, 2022.

The following paper appears Chapter 5:

Hoteit et al. (2022a) Farah Hoteit, Eugen Dedu, Winston K.G. Seah, Dominique Dhoutaut. Influence of beta and source packet rate on electromagnetic nanocommunications. IC-PADS, Nanjing, China, 2022.

BESIDES RESEARCH

Besides my research, I had the opportunity to be a teaching assistant at IUT Belfort-Montbéliard, University Franche-Comté (November 2020 - June 2021). I taught the following courses for Bachelor, Réseaux et Télécommunications (RT) Department: Acquisition and Information Coding, Internet Technology, Introduction to Web Development and Dynamic Web. I also followed doctoral school courses of 145.25 hours in different fields: Sciences, Scientific Tools, Research Ethics and Scientific Integrity, Open Science and General Training.

CONTENTS

I	Introduction and Context	1
1	Introduction	3
1.1	Context	3
1.1.1	Nanodevice's hardware architecture	4
1.1.2	Applications of electromagnetic nanonetworks	9
1.1.2.1	In-body applications	9
1.1.2.2	Software Defined Metamaterials applications	11
1.1.2.3	Wireless robotic materials applications	11
1.1.2.4	Industrial applications	12
1.1.2.5	Military applications	13
1.1.2.6	Agriculture and environmental applications	13
1.1.2.7	Smart cities applications	13
1.2	Thesis contributions	14
1.3	Outline of the PhD thesis dissertation	15
2	State of Art	17
2.1	Introduction	17
2.2	State of the art	17
2.2.1	Density in ultra-dense wireless ad hoc networks and electromagnetic nanonetworks	17
2.2.2	Physical layer and MAC sublayer of EM nanonetworks	18
2.2.2.1	Terahertz Channel	18
2.2.2.2	Data modulation and Multiple access schemes	19
2.2.3	Network and Transport layers of EM nanonetworks	21

2.2.3.1	Applicability of traditional ad hoc network layer protocols in ultra-dense networks	21
2.2.3.2	Network layer protocols of EM nanonetworks	23
2.2.3.3	Transport layer protocols of EM nanonetworks	25
2.2.4	Conclusion	25
3	Programming and simulation environment	26
3.1	Introduction	26
3.2	Available electromagnetic nanonetwork simulators	26
3.2.1	Nano-Sim	26
3.2.2	TeraSim	27
3.2.3	Vouivre	27
3.2.4	Physical simulators	28
3.3	BitSimulator	28
3.3.1	Guide to BitSimulator	30
3.3.2	Methodology for working with BitSimulator	33
3.4	Conclusion	34
II	Contribution	35
4	Network layer: Ring schemes in ultra-dense networks	37
4.1	Introduction	37
4.2	Related work	40
4.3	Ring scheme	41
4.3.1	Evaluation of ring scheme	45
4.3.1.1	Scenarios	45
4.3.1.2	Effect of ring on pure flooding	47
4.3.1.3	Effect of ring on backoff flooding	49
4.3.1.4	Effect of ring on SLR routing	51
4.3.1.5	Influence of ring on delay	52
4.3.1.6	Influence of ring on traffic	54

4.3.1.7	Evaluation of ring in denser networks	55
4.3.2	Conclusion of ring	56
4.4	Expanded ring scheme	56
4.4.1	Introduction of expanded ring	56
4.4.2	Expanded ring	57
4.4.3	Evaluation of expanded ring	60
4.4.3.1	Scenarios	60
4.4.3.2	Effect of expanded ring on pure flooding	62
4.4.3.3	Effect of expanded ring on SLR	63
4.4.4	Conclusion of expanded ring	64
4.5	Dynamic Ring Scheme	65
4.5.1	Introduction of dynamic ring	65
4.5.2	Dynamic ring	65
4.5.3	Evaluation of dynamic ring	71
4.5.3.1	Scenarios	71
4.5.3.2	Effect of dynamic ring on pure flooding	73
4.5.3.3	Effect of dynamic ring on probabilistic flooding	74
4.5.3.4	Effect of dynamic ring on backoff flooding	75
4.5.3.5	Effect of dynamic ring on SLR	76
4.5.4	Conclusion of dynamic ring	76
4.6	Conclusion	77
5	Transport layer: Beta parameter in nanonetworks	78
5.1	Introduction	78
5.2	Related work	79
5.3	Simulation	80
5.3.1	Scenarios	80
5.3.2	Effect of beta and packet rate on nanocommunications	84
5.3.2.1	Effect of symbol rate beta and source packet rate on ignore and collision	84

5.3.2.2	Effect of beta and source packet rate on packet delivery . .	86
5.3.2.3	Effect of dynamic beta on ignore, collision and packet de- livery	87
5.4	Conclusion	89
6	Reproducibility	90
6.1	Introduction	90
6.2	Details of contribution	90
6.2.1	Reproducibility example	91
6.3	Conclusion	91
III	General conclusion and Future work	93
7	Conclusion and Summary of the PhD thesis	95
7.1	Contributions	96
7.2	Perspectives	96



INTRODUCTION AND CONTEXT

INTRODUCTION

1.1/ CONTEXT

The Internet of Things (IoT) creates an inter-connected world of billions of devices ranging from computers to simple sensors, to enable smart services and applications. Although the Covid-19 virus pandemic has had an effect on the adoption of IoT technologies by the time of this dissertation, IoT is continuously growing and the number of connected IoT devices is estimated to 14.4 billion globally in 2022, according to the latest State of IoT—Spring 2022 report in May 2022 Lueth et al. (2022). The high demand of applications collecting real-time data about the environment requires a large number of wireless connected devices, which then implies looking for low-power devices, deployed densely in the network. Ad hoc networks permit these wireless devices to collaborate without centralization, by establishing unicast or multicast communications.

Similarly, driven by the miniaturization, the Internet of Nano Things (IoNT) connects nanodevices, enabled by nanotechnology, with the internet. Nanotechnology allows the manipulation of materials at the nanoscale. The IoNT may also combine nanonetworks with other networks and technologies, such as Cloud Computing and Big Data Akyildiz et al. (2011). To give an idea about the nanoscale: the diameter of a strand of human DNA is 2.5 nanometers, if we multiply this diameter by 10^6 then we get the size of a rain-drop Initiative. Ralph Merkle, a computer scientist and one of the inventors of public-key cryptography, says: “Nanotechnology will let us build computers that are incredibly powerful. We’ll have more power in the volume of a sugar cube than exists in the entire world today”. Nanotechnology is also paving way for development of integrated nanosensor devices (or nanonodes) as sub- μm scale devices (from 1 to 100 nm), explained in the next section 1.1.1.

Communication among nanodevices in a nanonetwork can be electromagnetic, molecular, acoustic and mechanical. Most promising communications are electromagnetic and molecular Rikhtegar and Keshtgary (2013). Electromagnetic nanocommunications rely

on the modulation and the demodulation of electromagnetic signals between nanodevices and they are the subject of this dissertation. Molecular nanocommunications use molecules as data carriers between nanomachines. In the context of molecular nanocommunications, this year, a group of researchers at the Korea Institute of Science and Technology created molecular machines or nanomachines. These nanomachines use mechanical molecular movements to penetrate and promisingly destroy cancer cells Jeong et al. (2022).

The IoNT may define two architectures: in flat protocols, all nodes in the network are nanonodes with similar capacities. However, in hierarchical protocols, IoNT components are classified into nanonodes, nanorouters (nanocontrollers), nanointerfaces and the gateway. Nanorouters are stronger in resources than nanonodes and thus act as cluster heads to collect data from nanonodes and to forward it to nanointerfaces. The gateway connects the whole system to the external world and the internet.

1.1.1/ NANODEVICE'S HARDWARE ARCHITECTURE

An integrated nanodevice or a nanonode, as illustrated in Fig. 1.1, includes nanocomponents. It is not built yet, due to the size restrictions imposed by the nanoscale, but active research is being done for its components. A promising material for nanocomponents is graphene that is a monolayer of carbon atoms packed into a two-dimensional honeycomb lattice Geim and Novoselov (2010). Nanocomponents are nanosensors, a nanoantenna, a nano-Electromagnetic transceiver (nano-EM transceiver), a nanoactuator, a nanoprocessor, a nanomemory and a nano-power unit. For multimedia nanodevices, nanocomponents can expand to a nanocamera and a nanomicrophone. In the following, some examples are given on each component that may not be yet nanocomponents, but are taking the steps towards miniaturization.

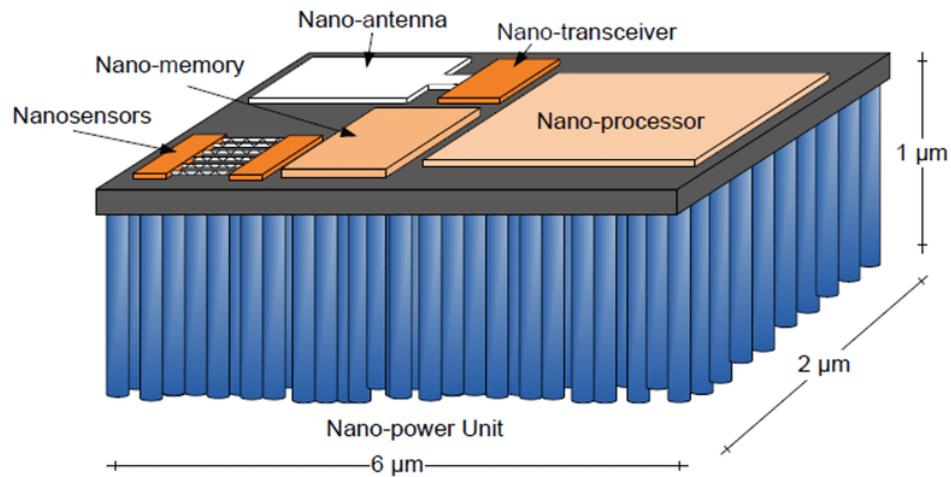


Figure 1.1: The integrated nanodevice's hardware architecture. Source: Mohammad and Shubair (2019).

Nanocameras are based on photo-detectors with high sensitivity. Some steps towards the minuscule cameras have been noticed recently: researchers at Princeton University and the University of Washington developed a camera the size of a coarse grain of salt using a technology called “metasurface” Tseng et al. (2021). Nanomicrophones are based on ultrasonic nanotransducers with high frequency resolution Smith et al. (2012). Again, nanocomponents are still under exploration and development.

Nanosensors, as in Fig. 1.2, are a new generation of sensors, as a nanosensor is not only a tiny sensor, but it also uses the properties of nanomaterials to perform high resolution sensing events/phenomenons. Nanosensors can be chemical, to monitor the concentration levels or the chemical and molecular compositions. They can also be biological, to sense the biomolecular interactions of cells, antibodies and DNA, etc. Physical nanosensors measure the physical properties, such as force, pressure or displacement, etc. Researchers at Karolinska Institutet in Sweden have recently developed nanosensors for detecting pesticides on fruits in a few minutes Li et al. (2022). Also, researchers at Shanghai Jiao Tong University designed a nanowire-based sensor for real-time ammonia (NH₃) monitoring that presents faster response time and lower power consumption than traditional ammonia sensors. Another advantage is the scalable soft lithography fabrication technique of these nanosensors Tang et al. (2019).

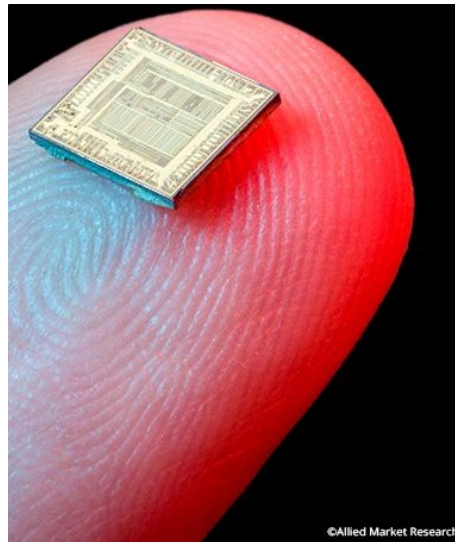


Figure 1.2: Nanosensor. Source: Allied Market Research.

Nanoantennas are responsible for transmitting and receiving signals. They are much smaller than traditional antennas and thus radiate high frequencies. Graphene is proposed for nanoantennas to radiate TeraHertz (THz) radiations, as the resonant frequency of graphene-based nanoantennas can be up to two orders of magnitude below that of non-carbon nanoantennas Jornet and Akyildiz (2010b). Researchers at Drexel University created a titanium carbide nanoantenna using an interesting fabrication technique as the nanoantenna can be “sprayed” directly into any object for it to become a smart IoT device, as seen in Fig. 1.3 Sarycheva et al. (2018). Nano-EM transceivers are the circuits processing the transmitted or received signals by the nanoantennas.



Figure 1.3: A spray-on nanoantenna. Source: Sarycheva et al. (2018).

Nanoactuators allow the interactions with the environment by creating a mechanical motion. An envisioned example of a nanoactuator is a nanoheater that burns cancerous cells detected by a nanosensor in the human body. Other nanoactuators can be physical that use the principle of Nanoelectromechanical systems (NEMS) including medical devices like nanoscissors and nanotweezers for surgery applications in sensitive organs in the body. Fig. 1.4 shows a microimage of fabricated nanotweezers on a nanomanipulator for heating carbon nanotubes Zakharov et al. (2012). MiGriBot (Miniaturized Gripper Robot), designed by University of Franche-Comté, is the fastest pick and place micro-robot by the time of this thesis. MiGriBot can move a micro-object almost 720 times per minute Leveziel et al. (2022).

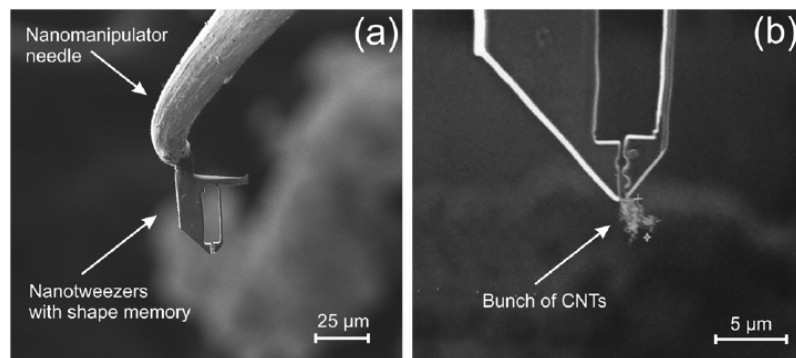


Figure 1.4: Nanotweezers. Source: Zakharov et al. (2012).

Nanoprocessors process the received data. The number of integrated transistors acting as binary switches in the chip determines the computation complexity of a nanoprocessor. In 2019, a microprocessor from 14000 carbon nanotube (Fig. 1.5) transistors promises high-performance and energy-efficient computing Hills et al. (2019). More work will be done on nanoprocessors in the upcoming years.

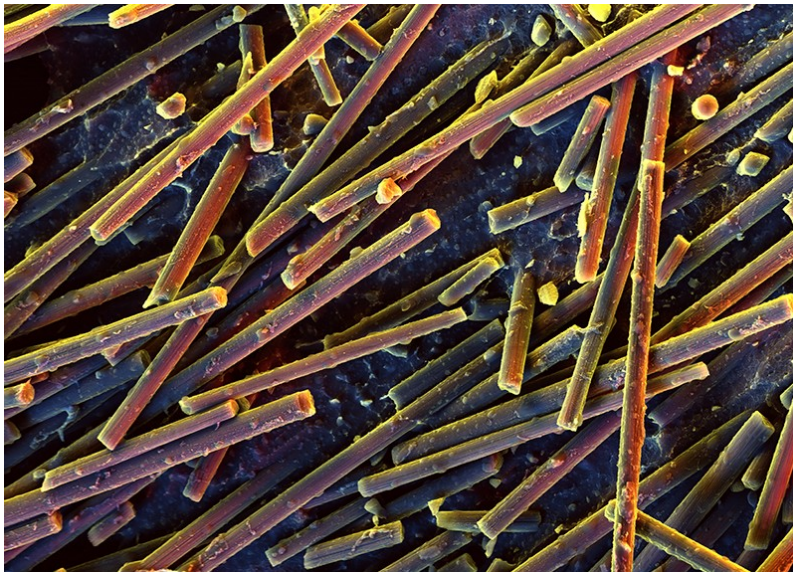


Figure 1.5: Carbon nanotubes. Source: Stefan Diller/ Science Photo Library.

Nanomemories are highly complex to construct. The challenge, defined by the Nobel Prize recipient Prof. Richard Feynman in 1959, is to store one bit of information in a single atom. Researchers at Radboud University, being inspired by Feynman, created an orbitally derived single-atom magnetic memory Kiraly et al. (2018).

Nano-power units constitute an important part of the IoNT architecture, as they provide energy to the nanosensor devices. The goal is to maximize the potential of a nanobattery and to extend its lifetime. Nanobatteries are small batteries that need to be recharged periodically. The current battery technology relies mainly on Lithium-ion batteries. However, battery manufacturing using nanotechnology can lead to greater power density and lower recharging times, compared to the Lithium-ion technology Wong and Dia (2017). Nanobatteries may employ nanomaterials for their anode and cathode parts, such as carbon nanotubes and graphene Soliman et al. (2021). To tackle the issue of the limited power supply of a nanobattery, energy harvesting presents a good platform to collect mechanical (e.g., movements), vibrational (e.g., acoustic signals) or hydraulic energy (e.g., blood flows) from the environment and converting into electrical energy Akyildiz and Jornet (2010a). The power required for a nanodevice is in the range of micro- to milliwatt and a prototype of an integrated nanosystem including a nanogenerator (energy harvester) is shown in Fig. 1.6 Wang (2012). It is important to define the source of energy as its availability depends on the application. Additionally, the size of the capacitor for harvested energy storage is smaller in nanosensors compared with the traditional sensors. Therefore, the energy harvesting systems in Wireless Sensor Networks (WSNs) may not always be suitable for Wireless Nano Sensor Networks (WNSNs) Jornet and Akyildiz (2012b). Another solution for power supply other than energy harvesting is Wireless Power Transfer, that is an external entity that vibrates the nanogenerator to give

a constant energy harvest rate Donohoe et al. (2015). We can conclude that the energy consumption in nanosystems is critical and because packet transmission is the main source of consumption, designing energy efficient routing protocols is key.

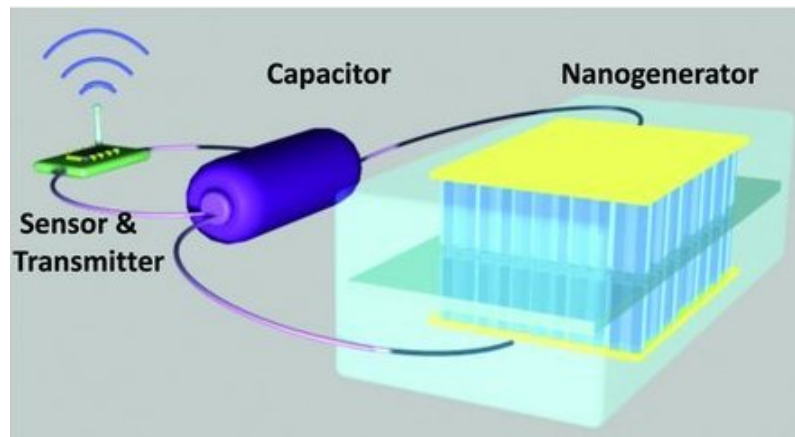


Figure 1.6: Prototype of an integrated nanosystem including a nanogenerator (energy harvester). Source: Wang (2012).

1.1.2/ APPLICATIONS OF ELECTROMAGNETIC NANONETWORKS

The Electromagnetic Nanonetworks or the Wireless Nano Sensor Networks were introduced by Jornet in 2010. They are networks of integrated nanosensor devices that enable a new networking paradigm that is the Internet of Nano Things and that communicate in the THz band Akyildiz and Jornet (2010b). The THz and the Millimeter wave (mmWave) are contemporary communications. The mmWave band, as 60 GHz, can offer high data rates (on the order of 10 Gbps) but requires complex transceiver architectures Rappaport et al. (2011). On the other hand, The THz band (0.1-10 THz) is the preferred band for nanonetworks, as it provides high data rates of up to few terabits per second for very short-range communications between the constrained nanodevices in the scale of tens of millimeters Jornet and Akyildiz (2010a); Singh et al. (2018).

An integrated nanosensor device is under development, which makes the electromagnetic nanonetworks at the conceptual level. Electromagnetic nanonetworks revolutionize various application domains, as nanomachines can perform tasks of sensing and actuation at an unprecedented small scale Ali and Abu-Elkheir (2015). In this section, we list the envisioned application domains of these networks.

1.1.2.1/ IN-BODY APPLICATIONS

Nanomedicine change the world of medicine. Nanosensors are comparable in size to some proteins and that is one reason why they function well inside cells Devreese (2007).

For brain diseases, scientists at Harvard University developed a technique called Nano “moon landing”, that uses hairpin-like nanowires to land neurons to study neuron networks and signals without damaging the cells Zhang (2019). Fig. 1.7 illustrates hybrid in-body nanocommunications as both molecular and electromagnetic, where nanomachines are deployed inside the human body and can be controlled by the external world over the internet and by the healthcare provider Yang et al. (2020). In the context of electromagnetic nanonetworks, in-body applications include health monitoring systems, Drug Delivery Systems (DDSs) and genetic engineering. Steps towards the design and development of in-body THz nanonetworks are being taken. For example, an analytical model for flow-guided nanonetworks is proposed to understand their applicability in this field Canovas-Carrasco et al. (2020). Health systems use nanosensors for monitoring different concentration levels of molecules in the blood and for detection of infectious intra-body agents. Other healthcare systems include vital signs monitoring, detection of cardiovascular abnormalities. DDSs use nanoactuators for delivering nanoparticles and drugs into the body Iovine et al. (2017). Such applications require a large network in the scale of 10^3 to 10^9 nodes with very high node density that exceeds 10^3 nodes per cm^3 Lemic et al. (2021). Several challenges encounter the in-body nanocommunications, such as the safety and reliability of implementing the nanodevices Dressler and Fischer (2015) and the effects of the THz signals on the human body Saeed et al. (2021).

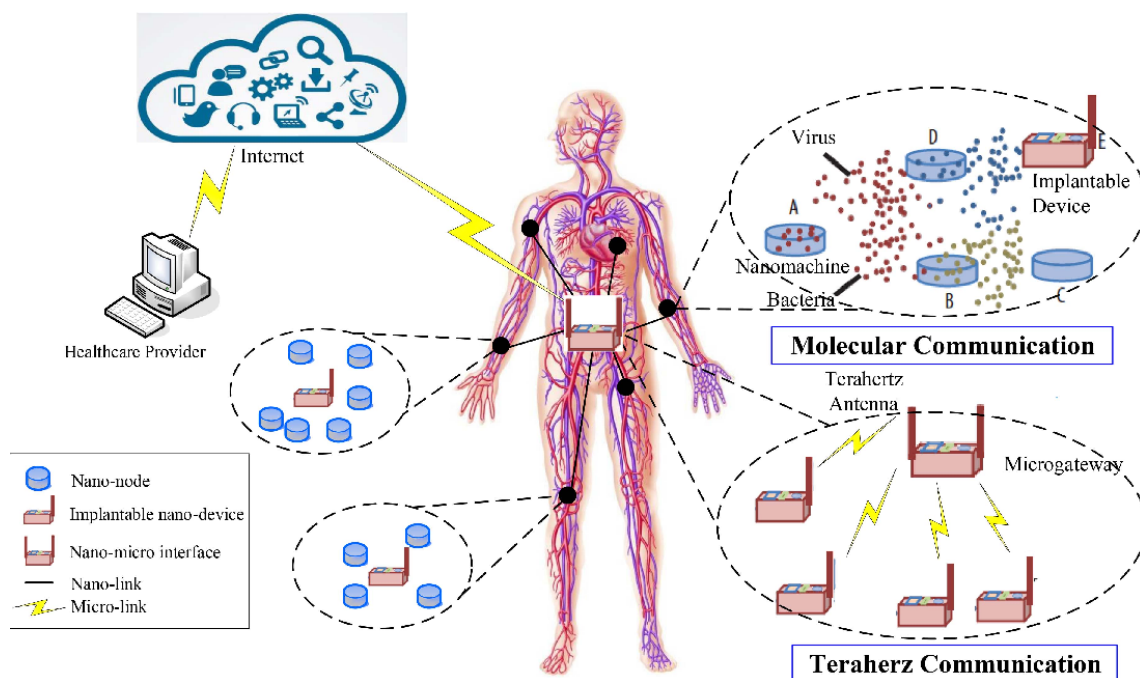


Figure 1.7: In-body nanocommunications. Source: Yang et al. (2020).

1.1.2.2/ SOFTWARE DEFINED METAMATERIALS APPLICATIONS

Software-Defined Metamaterials (SDMs) are an application domain of nanonetworks, where nanonetworks and metamaterials (artificial structures with unnatural properties) are combined, allowing the user to send commands to nanodevices aiming to perform geometrically-altering actions on the metamaterial and tuning of its electromagnetic behavior Liaskos et al. (2015). In a wider perspective of wireless communications, SDMs define a novel concept of programmable wireless environments, capable of mitigating the wireless channel losses Liaskos et al. (2018). Software-Defined Metamaterials, like in-body nanocommunications, demand a large network. Networks are usually in the scale of 10^3 to 10^9 nodes with a local density of 10^2 to 10^4 nodes per cm^2 Lemic et al. (2021).

1.1.2.3/ WIRELESS ROBOTIC MATERIALS APPLICATIONS

While SDMs control the electromagnetic waves, robotic materials enable smart programmable composites that change their shape according to their sensed environment Lemic et al. (2021). Examples of existing robotic materials are depicted in Fig. 1.8 McEvoy and Correll (2015). One application is a beam that can change its shape using variable stiffness control, as seen in Fig. 1.8(C) McEvoy and Correll (2016) Correll et al. (2017). The THz band yields a promising paradigm for controlling robotic materials Lemic et al. (2021). Networks of wireless robotic materials are smaller than both the SDMs and in-body nanonetworks, but they stay large, being composed of 10 to 10^6 nodes with a node degree of one to 100 nodes per cm^2 Lemic et al. (2021).

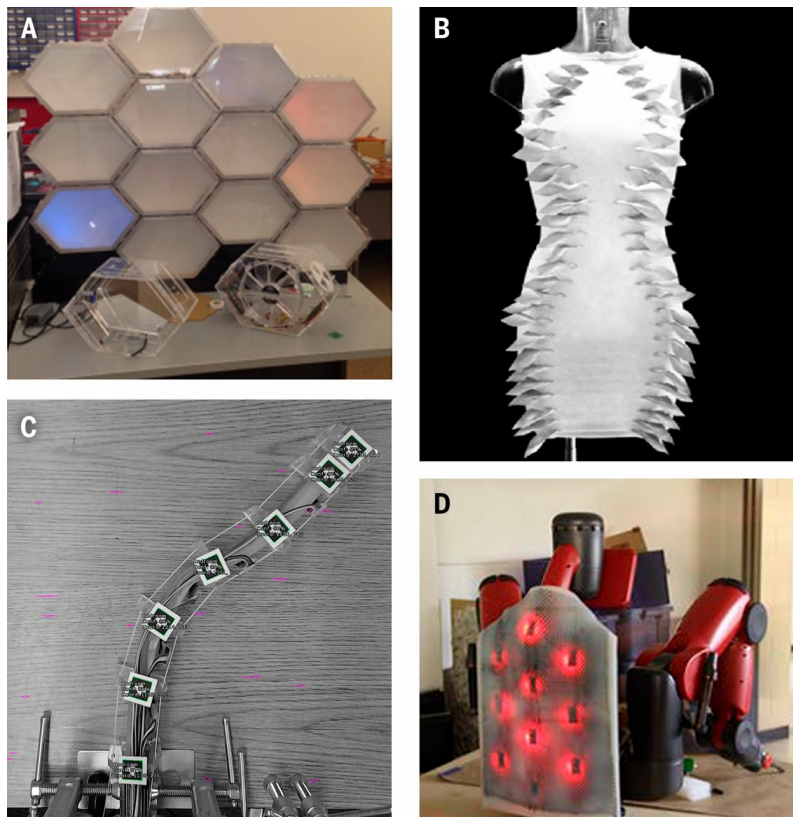


Figure 1.8: Examples of robotic materials McEvoy and Correll (2015), A: a facade that changes its opacity and color by hand gesture recognition Farrow et al. (2014), B: a dress that localizes the direction of incoming sounds and displays them to its wearer by localized flutter Profita et al. (2015), C: a beam that changes its shape using variable stiffness control McEvoy and Correll (2016) and D: a robotic skin that can sense and localize textures Hughes and Correll (2014).

1.1.2.4/ INDUSTRIAL APPLICATIONS

Nanonetworks bring novelties in industrial applications. Nanosensors provide precise and quick sensing information at low costs. On top of that, the THz sensing shows a strong penetration feature and high sensitivity for molecules monitoring Ren et al. (2019). Food and water contamination detection is an application of THz nanonetworks that targets the safety of customers. Future interconnected office is another proposed application where nanosensors and nanoactuators connect to the internet, offering the user a new way of tracking his office belongings Akyildiz and Jornet (2010a). In addition, nanophones and nanocameras are being designed, enabling the Internet of Multimedia Nano Things Jornet and Akyildiz (2012a).

1.1.2.5/ MILITARY APPLICATIONS

The IoNT benefits the military and the nuclear, biological and chemical (NBC) defenses fields. Military nanotechnology opens the door for nanoweapons that include nano-enhanced lasers and self-replicating smart nanorobots (SSN) Del Monte (2017). CubeSats are a category of nanosatellites that are enabled the Software defined radio technology. They have standard sizes (10 cm x 10 cm x 10 cm) or (10 cm x 10 cm x 34 cm) and they are accessible by small organizations due to their low costs Alvarez et al. (2016). CubeSats can be deployed densely for constellations with higher resilience and reliability Fraga-Lamas et al. (2016). In general, miniaturized devices such as nanosensors, nanoactuators, nanodrones and nanorobotics are implemented in smart and energy efficient battlefield monitoring systems for example Fraga-Lamas et al. (2016) and revolutionary military applications are invoked with electromagnetic nanonetworks.

1.1.2.6/ AGRICULTURE AND ENVIRONMENTAL APPLICATIONS

To increase the productions and to improve their quality, smart and sustainable agriculture systems are developed. Again, both the nanosensors and the THz sensing of electromagnetic nanonetworks provide quick and reliable surveillance for the health of leaves and detection of any pesticides in leaves Zahid et al. (2020). Nanonetworks for plant monitoring alert the need for water, fertilizers and pesticides. Nanonetworks may also intervene in animal health monitoring and feed management, where wearable sensors can be installed on cows for example Awasthi et al. (2016). Additionally, distributed air pollution control is an environmental application which utilizes nanofilters Han et al. (2008).

1.1.2.7/ SMART CITIES APPLICATIONS

The IoT and the IoNT play a vital role to enable smart cities, as connected sensors and nanosensors collect and analyze data. Applications of smart cities include structural health of buildings to diminish the risks of sudden collapse Lamonaca et al. (2018) or to maintain historical buildings using vibration and deformation sensors for monitoring. Other applications help the traffic congestion and enable smart cars, smart parking, smart lighting, air quality control and city energy consumption Zanella et al. (2014).

As seen in the above applications, the IoNT adds a new scale in the IoT. Nanosensors, in comparison with conventional devices, provide better precision and sensitivity, faster response and portability Devreese (2007). They can be placed in tiny areas and are lower in costs and in power consumption than macrosensors Javaid et al. (2021).

1.2/ THESIS CONTRIBUTIONS

This thesis focuses on the network and transport layers of electromagnetic nanonetworks and ultra-dense wireless ad hoc networks in general.

Routing is the higher-level decision making that directs network packets from their source towards their destination through intermediate network nodes by specific packet forwarding mechanisms. A simplified classification of routing protocols in wireless ad hoc networks is shown in Fig. 1.9 (Only essential branches are presented).

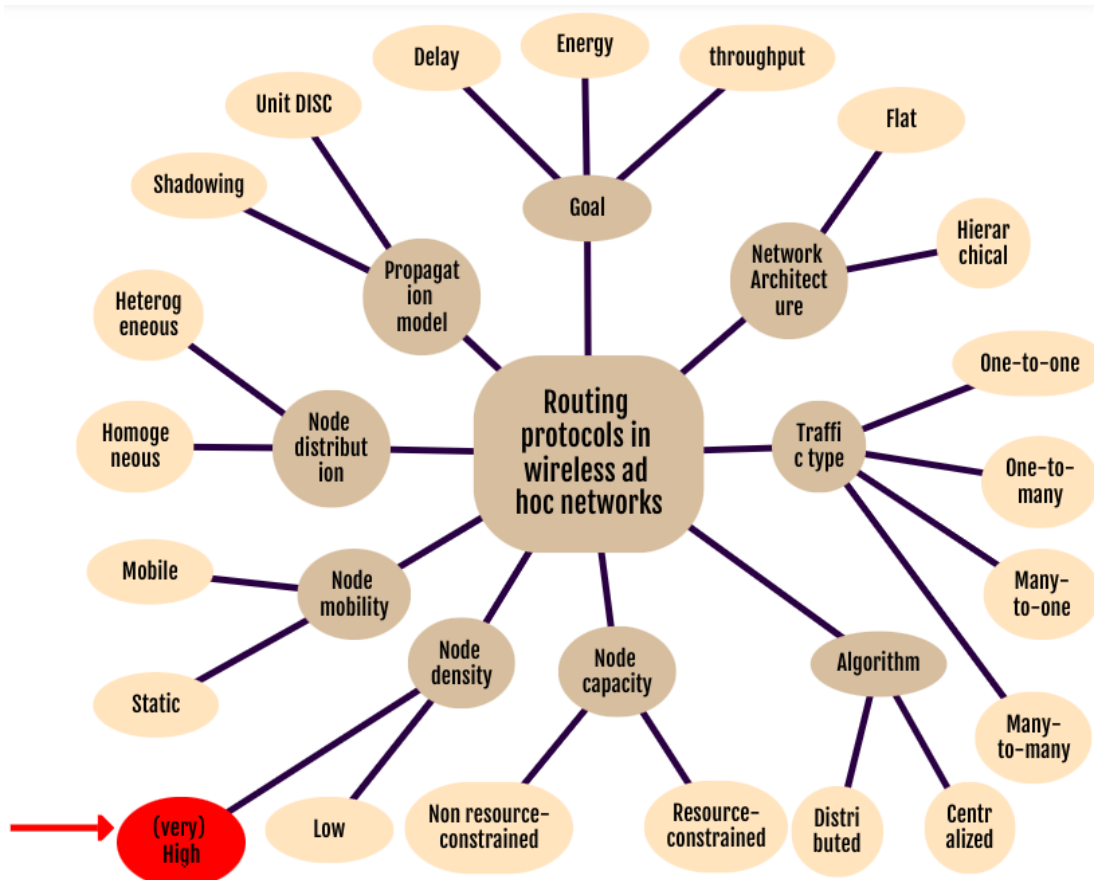


Figure 1.9: Classification of routing protocols in wireless ad hoc networks.

In the node density branch, the lack of routing protocols dealing with high node density is clear. We define the problem as: what if the application requires tens of thousands of nodes in the network? Even more, what if each node has hundreds or even thousands of neighbors? Most communication protocols are no longer applicable in large-scale ultra-dense wireless networks, notably for resource-constrained nodes that cannot store or process data of neighborhood. Moreover, the additional traffic added by the communication protocols congests the network, especially in dense environments. Here, we motivate our first contribution as how to scale-up routing in (resource-constrained) ultra-dense

wireless ad hoc networks and electromagnetic nanonetworks.

In this context, we define the repeated terms throughout the thesis:

Definitions

- Large scale network: is a network with a **large number of nodes**, typically ranging from 10^3 to 10^9 nodes.
- Neighbors of a node: are the adjacent nodes in direct communication range of node. In a wireless channel, all the neighbors of a transmitting node receive its message.
- Ultra-dense wireless network: is a network with **very high node density**, also known as neighbor density, local density or network density, all of which are related to the number of neighbors per node.
- Multi-hop routing: is a communication fashion used when a source node intends to deliver a message to a destination node that is beyond its coverage, the message is retransmitted by intermediate nodes Pešović et al. (2010), going from 1-hop neighbors of the source until reaching the n -hop of the destination.
- Forwarders: are the intermediate nodes in the multi-hop routing, also known as routers or relays James et al. (2015).
- Packet delivery: is the ratio (or percentage) of the number of packets delivered to the destination to the total number of packets sent from source to destination.

The second proposition contributes in the transport layer of electromagnetic nanonetworks, where we study the parameter called beta β 2.2.2.2 that is the symbol rate in the modulation scheme Time Spread On-Off Keying (TS-OOK) and its variants. Along with β , we study the packet source rate and we notice a relationship between these parameters and the congestion in nanonetworks.

1.3/ OUTLINE OF THE PHD THESIS DISSERTATION

In the previous sections of this introductory chapter, we first presented the context of electromagnetic nanonetworks and ultra-dense ad hoc networks, followed by the nanodevice's hardware architecture and the nanonetworks' applications. As shown on Figure 1.9, for the rest of the dissertation, we mainly consider environments where a high to very high node density is possible. As we are going to see in Chapter 2, existing protocols are usually inefficient or problematic in dense wireless nanonetworks. The relative lack of

research on this topic motivated our work and ultimately led to the thesis contributions' section.

The rest of the thesis is structured as follows: Part I, Chapter 2 presents the state of the art on electromagnetic nanonetworks, that may sometimes relate to ultra-dense ad hoc networks as well. This chapter finishes by declaring the goal of the dissertation. Part I, Chapter 3 chooses and explain the programming and simulations environment of this study.

Part II, Chapter 4 is the first contribution of this dissertation and consider the network layer of electromagnetic nanonetworks and (resource-constrained) ultra-dense wireless networks. The chapter proposes in depth analysis of problems and their solutions, it progresses from the ring scheme to the expanded ring and finally to the dynamic ring. Part II, Chapter 5 is the second contribution that explores the influence of beta and the source packet rate in the transport later of electromagnetic nanonetworks. Part II, Chapter 6 is concerned with the reproducibility of the simulation results and research integrity.

Part III concludes this dissertation and offers new insights and potential future work for electromagnetic nanonetworks.

STATE OF ART

2.1/ INTRODUCTION

This part cites research done on electromagnetic nanonetworks and generally ultra-dense ad hoc networks for the different Open Systems Interconnection (OSI) layers of computer networking. It starts with the main common aspect of these networks: the very high density. Then, it goes on presenting protocols for the physical, MAC, network and transport layers.

2.2/ STATE OF THE ART

2.2.1/ DENSITY IN ULTRA-DENSE WIRELESS AD HOC NETWORKS AND ELECTROMAGNETIC NANONETWORKS

An important parameter to design protocols dealing with neighbors in dense networks is the node density, as its estimation can be an input for protocols. The Density Estimator for Dense Networks (DEDeN) Arrabal et al. (2018a) finds the node density of nodes in ultra-dense networks and nanonetworks, as follows. In DEDeN, nodes distributively estimate the local density without having to rely on a full (and very costly) exchange of hello packets. Instead, over the course of multiple rounds, they have an increasing probability to send a small probe packet. At each round, they also count the number of probes received. Knowing the sending probability, they can compute with an increasing confidence their number of neighbors. The implementation of DEDeN in the used network simulator (BitSimulator) can be found in 3.3.1.

2.2.2/ PHYSICAL LAYER AND MAC SUBLAYER OF EM NANONETWORKS

The physical layer of electromagnetic nanonetworks is composed of the THz channel characterization and the description of bit-level transmission between machines. It also includes modulation, coding and error control schemes. In the following section we only focus on the THz channel and the data modulation schemes. The data modulations include multiple access schemes that operate in the Medium Access Control (MAC) sub-layer of the link layer. They allow nanonodes or users to access the shared Terahertz channel, they try to optimize the transmission time and to minimize the collisions.

2.2.2.1/ TERAHERTZ CHANNEL

The THz channel opens the door for a new communication paradigm, as it is demonstrated to support high bit-rates for very small transmission distances between the nanodevices Jornet and Akyildiz (2010a).

However, the THz channel suffers from the path loss and the noise Jornet and Akyildiz (2010a). The path loss includes the spreading loss and the molecular absorption. The spreading loss is the attenuation caused by the wave spreading in the medium and that depends on the wave frequency and the transmission distance. The molecular absorption loss is due to the wave energy being converted into internal kinetic energy in some of the molecules of the medium Goody and Yung (1995). The molecular absorption leads to electronic and molecular noise in the receiver that are both difficult to predict and are neither Gaussian nor white Akyildiz and Jornet (2010a).

The THz channel models for electromagnetic nanonetworks study the nanocommunications and should account for the path loss and the noise when propagating over the short distances between nanodevices. A propagation model for EM communications in the THz Band is proposed based on the radiative transfer theory to compute the path loss and the noise Jornet and Akyildiz (2011).

Other propagation models directly characterize the scenario as in in-body applications, where different human tissues (skin, blood and fat) react differently to the THz radiation and where the positions of the transmitter and the receiver in these tissues also affect the wireless propagation Lemic et al. (2021). In this context, a propagation model containing skin, blood and fat is proposed, in addition to the suggestion that the noise is mainly due to the molecular absorption Yang et al. (2015). Later on, a study adds that the channel noise is also related to the composition of the human tissues and is higher in tissues with higher water vapour Zhang et al. (2016). The interference models are then added to the noise models to express the Signal to Interference plus Noise Ratio (SINR) in the THz in-body nanonetworks and to derive the channel capacity. The node density is shown to

be a factor affecting the SINR Zhang et al. (2017) Lemic et al. (2021).

2.2.2.2/ DATA MODULATION AND MULTIPLE ACCESS SCHEMES

The Terahertz channel with its molecular absorption and the nanoscale impose constraints and requirements that make the traditional physical layer techniques not applicable. Carrier-based modulations cannot be performed by nanotransceivers Jornet and Akyildiz (2014). Instead, simple and lightweight modulation techniques, such as pulse-based modulations, are required for THz nanonetworks and can be cross-layer to further simplify the protocol stack. As seen in the following, the modulations schemes can also be multiple access schemes for the MAC sublayer. As stated by Mamed and Bourgeois (2018), the traditional channel access schemes based on central management entities, such as Frequency Division Multiple Access (FDMA) Afsharinejad et al. (2016) and Temporal Division Multiple Access (TDMA) Suzuki and Budiman (2013) cannot be used for nanonetworks with flat network topology. Nanonetworks cannot benefit from the Carrier Sense Multiple Access with Collision Avoidance (CSMA/CA) as well since there is no carrier-sensing for pulse-based modulations.

Fig. 2.1 Lemic et al. (2021) compares the different pulse-based modulations, starting with the On-Off Keying (OOK). OOK is a modified form of amplitude-shift keying (ASK) modulation, where data is presented as the presence or absence of a carrier wave. OOK avoids the power hungry circuits and paves the way for the main proposed modulation and multiple access scheme in THz nanonetworks, that is the TS-OOK Jornet and Akyildiz (2014). It is a lightweight modulation, as it is convenient for nanomachines to use extremely short electromagnetic pulses. These pulses can be generated by their tiny antennas, and can be detected and processed with limited computation power. The pulse is 100 femtosecond-long ($= T_p$) as a bit 1 with energy, and bit 0 is defined as silence without energy consumption. The ratio between the inter-bit duration T_s and the duration of one bit T_p is known as time spreading ratio (β). TS-OOK, in comparison with OOK, features the parameter β that allows for applications with energy harvesting. β also allows the synchronization and bits at the receiver are decoded at precise times. Generally, the standard values are: $T_p = 100$ fs and $\beta = 1000$. In the article that proposes TS-OOK, authors suggest to interleave bits from concurrent packets (users) at the receiver and confirm the capacity of Tbps of the THz channel.

Variants of TS-OOK have been later proposed to improve it or to adapt it to different scenarios. One of the problems of TS-OOK is that when multiple users transmit with same symbol rate and they collide in one bit, they will collide in all their bits. To tackle this problem, Rate Division Time Spread On-Off Keying (RD TS-OOK) attributes co-prime symbol rates to transmitters during the Physical Layer Aware MAC Protocol for Electromagnetic

Nanonetworks (PHLAME) Handshaking process Pujol et al. (2011). A later research works on the implementation of RD TS-OOK and derives the symbol rate by generating unique prime number at each user node using Prime Mod algorithm, eliminating the need for coordination between the transmitter and the receiver Shrestha et al. (2016).

Symbol rate Hopping TSOOK (SRH-TSOOK) is also a modulation and multiple access scheme based on TS-OOK. The difference is that with SRH-TSOOK, the transmitter hops over different symbol rates following a pseudo-random sequence known by both the transmitter and the receiver, in order to improve the distribution of the channel capacity over the active communications Mabed (2017). Adaptive Symbol Rate Hopping TS-OOK (ASRH-TSOOK) is an improved version of SRH-TSOOK that takes into account the traffic load variation. Each active node estimates its neighboring load to determine the upper limit of the symbol rate range. Accordingly, for lower traffic load, the upper limit of the symbol rate range should be lower Mabed and Bourgeois (2018).

Applications where the energy constraint is more important than the data rates, the Pulse Position Modulation (PPM) generally outperforms the On-Off Keying (OOK) Oppermann et al. (2004). In PPM, while bit 0 is represented by a pulse originating at the time instant 0, bit 1 is shifted in time by the amount of δ from 0 Oppermann et al. (2004). In this context, a modulation scheme combines TS-OOK and the PPM and sends bits as a sequence (instead of bit by bit as in TS-OOK). In comparison with TS-OOK, the proposed scheme achieves higher energy efficiency and lower data rates and is thus useful for in body-centric nanonetworks Vavouris et al. (2018). Another work proposes TH-PPM as a modulation and multiple access scheme for nanonetworks, which couples time-hopping (TH) and M-ary PPM Singh et al. (2018).

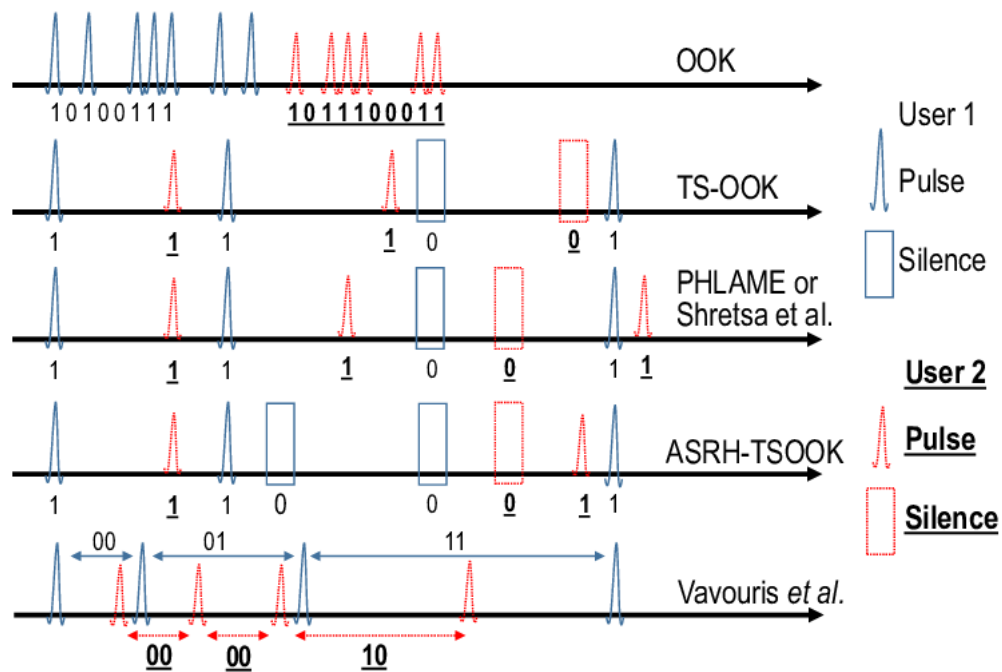


Figure 2.1: Comparison between modulations: Jornet and Akyildiz (2014), Pujol et al. (2011), Mabeed and Bourgeois (2018), Vavouris et al. (2018), user1 in blue and user2 in red. Source: Lemic et al. (2021).

2.2.3/ NETWORK AND TRANSPORT LAYERS OF EM NANONETWORKS

The network layer defines the data exchange between nodes and networks, through packet forwarding and routing. In the following, we discuss the applicability of traditional routing schemes in ultra-dense ad hoc networks, to initiate the urge for new network protocols. Later on, and for electromagnetic nanonetworks, we present the proposed network layer protocols and briefly mention the transport layer.

2.2.3.1/ APPLICABILITY OF TRADITIONAL AD HOC NETWORK LAYER PROTOCOLS IN ULTRA-DENSE NETWORKS

The traditional routing schemes are not directly applicable in nanonetworks and resource-constrained ultra-dense networks, as illustrated in the following cases. Flooding or broadcasting schemes do not need route discovery nor route maintenance and are suitable for the constrained nanodevices. However, in a dense environment, flooding can cause broadcast storms, if not refined.

The Ad hoc On Demand Distance Vector (AODV) is a reactive routing protocol for mobile ad hoc networks (MANETs) and other wireless ad hoc networks like ZigBee. In AODV, each node has a routing table and each entry contains the next hop node, the hop count to

the destination and the sequence number (to determine the freshness of a route). When a node intends to send a message to a destination, it checks its routing table: if there is a route to the destination, it forwards it to the next hop, and if not, it starts the route discovery by broadcasting a Route Request (RREQ) message to all its neighbors Perkins et al. (2003). Storing routing tables in the constrained devices is costly or even unfeasible for ultra-dense neighborhoods.

Dynamic Source Routing (DSR) is a routing for wireless mesh networks. DSR is similar to AODV, in the way that the transmitting node requests a route. However, AODV uses routing tables at intermediate nodes and instead, DSR uses source routing (path addressing) Johnson et al. (2007). In large networks, storing long paths in the packet's header is expensive.

Hierarchical routing arranges routers in a hierarchical manner. In its evaluation of hierarchical routing in large networks, Kleinrock states that smaller routing tables require less storage and processing, but give less precise routing information resulting in longer paths Kleinrock and Kamoun (1977). Hierarchy scales well. In this context, AODV has been modified into a hierarchical version to make it efficient in nanonetworks, making the RREQ packets forwarded only by the intermediate nanorouters, not by the intermediate nanonodes Tairin et al. (2017). However, building a hierarchy is costly for constrained nodes. Adding to that, clustering makes cluster heads exhaust their batteries fast and therefore, cluster heads should be powerful devices or should trade roles with other devices Ducrocq et al. (2013).

The Optimized Link State Routing Protocol (OLSR) is a proactive, table-driven routing protocol for mobile ad hoc networks Clausen and Jacquet (2003). OLSR selects a minimum set of neighboring nodes called MultiPoint Relays (MPRs) such that they cover all the 2nd-hop neighbors. OLSR incurs a high overhead in ultra-dense networks because nodes need to know their 2-hop neighbors.

Greedy forwarding schemes are the main component of geographic routing in WSNs that select forwarders that increase the forwarding progress towards the destination. But, greedy forwarding requires nodes to learn positions of their neighbors or the destination, which is inappropriate for nanonetworks. We can cite several greedy protocols: in Geometric broadcast in dense wireless sensor networks Liang et al. (2014), a node picks a set of neighbors as forwarding candidate nodes located at the boundary of the communication range based on a virtual hexagon-based coverage, without needing a GPS to locate them. The assumption is that each node knows its 1-hop and 2-hop neighbor IDs. The sender calculates the set of common nodes with his 1-hop neighbor to estimate the location of its neighbor. In Contention-based forwarding for mobile ad hoc networks Füzler et al. (2003) and Blind geographic routing for Sensor Networks (BGR) Witt and Turau (2005), nodes set timers and the node whose timer expires first is assumed to be closer

to the destination and thus forwards, whereas the other nodes cancel their transmission. This greedy approach cannot be applied in our context as the location or direction of destination node is unknown to nodes. In edge forwarding Cai et al. (2005), nodes keep track of all their neighbors and require the farthest ones to be forwarders. In Greedy Perimeter Stateless Routing (GPSR) Karp and Kung (2000), a node knows its location and the locations of its neighbors, and packets contain the coordinates of the destination. The neighbor closest to the destination is selected as forwarder. It uses perimeter routing to route around dead ends (mathematically avoiding local minimums). In Vehicular Ad hoc Networks (VANETs), GPS is usually a given unlike nanonetworks and greedy forwarding Sun et al. (2000); Panichpapiboon and Cheng (2013); Rossi et al. (2008) selects the farthest vehicle from the transmitter as the new forwarder.

2.2.3.2/ NETWORK LAYER PROTOCOLS OF EM NANONETWORKS

If we take this further towards electromagnetic nanonetworks, nanodevices require low complexity routing schemes because constrained nanodevices cannot store nor process large routing tables, neighboring information or complex network knowledge in general.

Depending on the application, the routing protocol either delivers the data packets to a destination node or to many nodes (strict unicast or merely zone-cast routing), or it floods the whole network so that every node receives a certain message (flooding). In the following, we present some schemes aiming to reduce the number of forwarders.

Flooding schemes In pure flooding, every node in the network forwards the data packet that it receives for the first time. This flooding is not scalable and results in redundant transmissions and broadcast storms in dense environments. In probabilistic flooding Reina et al. (2015), nodes forward packets with a static probability and discard it otherwise. The probability should be carefully chosen depending on the scenario, in order to guarantee the message delivery with a minimal number of forwarders.

Backoff flooding Arrabal et al. (2018b) is a highly efficient flooding scheme, where the number of forwarders is notably reduced. Only nodes receiving few copies of data packets (less than redundancy r) forward the packet. The count of data copies is done in a time window proportional to the number of neighbors, estimated using the node density estimator DEDeN Arrabal et al. (2018a).

In the Lightweight Self-tuning Data Dissemination for dense nanonetworks (LSDD) Tsioliaridou et al. (2016), nodes classify themselves as forwarders or non-forwarders (passive auditors) using packet-receive statistics (including success or failure on packet reception and integrity checks).

Unicast (or merely zone-cast) schemes In RADAR routing Neupane (2014), the nanonetwork is a circular area and a central entity emits radiation at an angle. Nanonodes found inside the angle of radiation are in the ON-state, and all the other nodes are in the OFF-state. RADAR only consists in blind flooding inside the angle of radiation. Nevertheless, a large angle can still cause a broadcast storm, and the destination node must be in ON-state to receive the packet.

The Deployable Routing System for Nanonetworks (DEROUS) Liaskos et al. (2016) establishes a point-to-point communication in circular and radial paths. In the setup phase, a beacon node set at the center of a 2D circular area sends a packet, and nanonodes self classify as infrastructure (always retransmit) or user (never retransmit) using packet reception quality. During the routing, nanonodes that are between the source and destination become forwarders to finally form a circular or radial routing path. Thus, DEROUS limits the retransmissions to a circle area.

In the Coordinate and Routing system for Nanonetworks (CORONA) Tsioliariidou et al. (2015), the network is a 2D rectangular area with **uniformly** distributed nanonodes and four anchor nodes placed at each corner. During the setup phase, anchors transmit their packets in sequence, allowing nanonodes to set their coordinates as hop counts from the anchors. During the routing phase, only nanonodes that are in a **rhombus area** between source and destination nodes forward the packet.

Stateless Linear-path Routing (SLR) Tsioliariidou et al. (2017) extends CORONA to a 3D cubic space. SLR is an efficient zone-cast routing scheme that uses anchors and a coordinate system for nanonodes that can extend to a 3D environment. The node coordinates are represented as hop counts from the anchors. Thus, space is divided in zones, where all nodes in a zone share the same coordinates. Contrarily to IP networks where the forwarding router is chosen by the preceding router, a nanonode takes the forwarding decision for itself. Only nodes whose coordinates verify the line equation joining the source-destination pair are forwarders. Therefore, SLR limits the zone of forwarding to the path between the source and the destination and thus also reduces the number of forwarders in the network. On the other hand, all the nodes in the zone between the source and the destination are forwarders and there are still some redundant retransmissions that can be eliminated. Fig. 2.2 compares SLR (black) with CORONA (yellow) routing protocols for a communicating source and destination nodes in a given space Tsioliariidou et al. (2017).

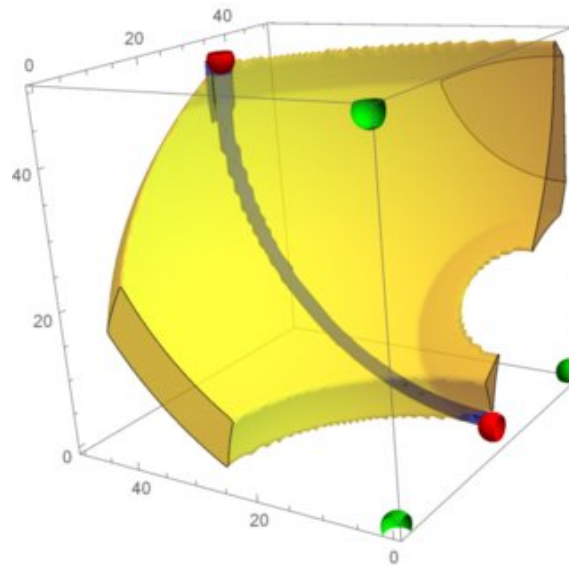


Figure 2.2: Comparison between SLR (black) and CORONA (yellow) routing protocols for a communicating source and destination nodes in a given space. Source: Tsioliariidou et al. (2017).

2.2.3.3/ TRANSPORT LAYER PROTOCOLS OF EM NANONETWORKS

The transport layer generally provides error detection, reliable data transfer and congestion control services. The transport layer of THz nanonetworks remains largely unexplored. Instead of presenting it in this section, we prefer to postpone its details to Chapter 5 5.2. There, we will be able to explain more in depth the specific problems that the transport layer encounters in wireless nanonetworks and we will later propose a solution.

2.2.4/ CONCLUSION

After reviewing the literature, we can declare the goal of this dissertation in three words: "Scalability Under Constraints". The Terahertz channel, the nanoscale and the very high density are all challenges for designing efficient schemes for the protocol stack of nanonetworks and ultra-dense networks in general.

PROGRAMMING AND SIMULATION ENVIRONMENT

3.1/ INTRODUCTION

This part shows the available electromagnetic nanonetwork simulators: Nano-Sim, TeraSim, Vouivre, COMSOL Multiphysics and BitSimulator. This part then selects BitSimulator as the optimal option for this study and offers a simplified BitSimulator guide. Finally, a methodology for working with BitSimulator and a conclusion are given.

3.2/ AVAILABLE ELECTROMAGNETIC NANONETWORK SIMULATORS

This thesis targets ultra-dense networks (thousands of nodes, with hundreds of neighbors per node) and thus requires a highly scalable network simulator. To validate the proposed approaches in this dissertation, we choose the electromagnetic nanonetworks as an example of (resource-constrained) ultra-dense networks. Several simulators of electromagnetic nanonetworks have been proposed that we present in the following. A detailed evaluation of the simulators for electromagnetic nanonetworks can be found in Sahin et al. (2021).

3.2.1/ NANO-SIM

NS-3¹ is a widely used network simulator due to its versatility and its compatibility with different networks of satellites, Wi-Fi, Zigbee, etc. Nano-Sim Piro et al. (2013) is the first ns-3 module designed for electromagnetic nanonetworks that implements TS-LOOK. It is the most used nanonetwork simulator because of its simple protocol stack. However, it has some deficiencies: Nano-Sim is not being upgraded and does not have enough

¹<https://www.nsnam.org>

documentation to be included in ns-3 App Store. Nano-Sim lacks the propagation delay and the energy models. Nano-Sim, at the physical layer TS-OOK, uses the same symbol rate β for communications and considers collisions whenever bits arrive at the receiver at the same time, which is not completely true as destructive collisions in nanonetworks only happen if the a bit 0 is replaced by a bit 1 Dhoutaut et al. (2018). Nano-Sim is heavy and in practice can simulate networks of up to around one thousand nodes. Another limitation of Nano-Sim is that it does not support the visualization modules of ns-3. In this dissertation, both the scalability and visualization are keys. Understanding the β parameter is also one of the contributions. Consequently, Nano-Sim is not the selected simulator for this study.

3.2.2/ TERASIM

TeraSim Hossain et al. (2018) is another ns-3 module for EM nanonetworks that overcomes some of the limitations Nano-Sim. A good feature of TeraSim is the ability to include both nanoscale and macroscale applications together. TeraSim has documentation and is included in ns-3 App Store. TeraSim also considers the propagation delay, the path loss, the molecular absorption and the spreading loss, it also implements energy models and advanced protocols for the different layers. Nevertheless, similarly to Nano-Sim, TeraSim still considers the same β value and sill counts non-destructive collisions as collisions. TeraSim does not support more than one thousand nodes, as its advanced protocol stack imposes huge cost on the CPU, and thus TeraSim is not convenient for large-scale networks. Nodes also cannot be visualized by the advanced ns-3 modules. Therefore, this dissertation cannot make use of TeraSim.

3.2.3/ VOUIVRE

Vouivre Boillot et al. (2015), developed by our laboratory and co-developed by my co-director Dominique Dhoutaut, is a C++ simulator library for EM nanonetworks in Dynamic Physical Rendering Simulator (DPRSim). Vouivre enables wireless communications among node and solves the scalability issue by removing the heavy DPRSim features, and thus can simulate tens of thousands of nodes in the nanonetwork. On the contrary, Vouivre is not widely used and is not being updated. Vouivre focuses on the statistical approach and does not study the effect of the packet payload and bits. Vouivre also does not support visualization. Hence, Vouivre is not the optimal choice of our work.

3.2.4/ PHYSICAL SIMULATORS

Physical simulators such as COMSOL Multiphysics² present a very detailed physical model, which gives accurate results, but is very costly and can simulate only very few nodes.

On the other hand, BitSimulator can simulate hundreds of thousands of nodes and is presented in the following section.

3.3/ BITSIMULATOR

BitSimulator Dhoutaut et al. (2018), also designed by our laboratory, is a fast C++ EM nanonetwork simulator that can simulate hundreds of thousands of nodes, with a node density of hundreds of nodes, on a classical computer. Its scalability is confirmed in the study comparing these nanonetwork simulators Sahin et al. (2021). It also targets both routing and transport layers and is accompanied by a visualization tool called VisualTracer. It permits the use of different β values and only considers the catastrophic collisions at the physical layer, as opposed to Nano-Sim and TeraSim. Hence, it is convenient for this dissertation. It is free software³. All results in BitSimulator are fully reproducible, as shown in Chapter 6, due to the use of random seeds RNG for different runs. My co-director Dominique Dhoutaut and my supervisor Eugen Dedu are co-developers of BitSimulator.

Fig. 3.1 shows the interactions among main C++ classes in BitSimulator. The **Node C++** class along with the **World** class implement the physical and channel access control layer. Nodes have nanotransceivers with configurable range. The TS-OOK model is the default modulation scheme, with 100 fs pulses and a configurable β per frame. **Routing** executes the network layer protocols, usually flooding or SLR. New routing agents can be added. **Application** allows nodes to only send packets while **Server Application** also allows them to receive by registering to a port. Multiple Application(s) and ServerApplication(s) can be attached to a given node. The **Packet** class encapsulates the binary payload along with various headers such as the source, destination, packet and flow identifiers. Packets are passed to a **Server Application** upon correct reception.

²<https://www.comsol.com>

³Available at <http://eugen.dedu.free.fr/bitsimulator>

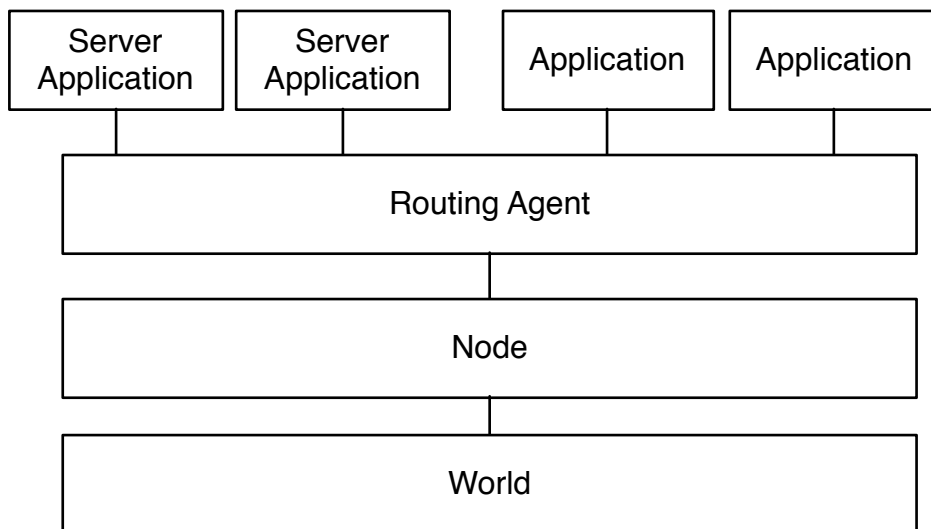


Figure 3.1: Interactions among main C++ classes. Source: Dhoutaut et al. (2018).

Compared to the other simulators, BitSimulator is less known and has the following limitations:

Limitations of BitSimulator

- BitSimulator only simulates nanonetworks.
- All nodes are nanomachines (no nanorouters or gateways).
- Nanoantennas are omnidirectional for both the transmissions and receptions.
- For a given node, transmissions are only done sequentially.
- BitSimulator does not directly consider the path loss, the molecular absorption and the spreading loss. Instead it uses a communication radius, that has to be defined externally.
- BitSimulator does not implement an energy model (energy depleting while being active).
- BitSimulator does not include the link layer.
- The design of mobility models is still limited.
- Only one routing protocol can be selected at a time.

Although having these limitations, BitSimulator is a great option for this dissertation as it provides fast execution, accuracy and scalability.

3.3.1/ GUIDE TO BITSIMULATOR

Inputs of BitSimulator: Scenario BitSimulator simulates a scenario. The input `scenario.xml` defines the scenario parameters and seeds in order to get statistical results that can be reproducible (check Chapter 6, 6.2). Parameters in the scenario are the network dimensions, the number of nodes and their distribution in the network. Nodes can be distributed either following a random uniform (homogeneous) or a Gaussian (normal) distribution. Additionally, different densities can be applied to different areas in the network. Another scenario parameter is the communication range of a node in micrometers. The implemented propagation models are the unit disc model and the normal shadowing model (for more realistic scenarios). The implemented normal shadowing is explained in 21.

The scenario also precises the routing protocol used for the Constant BitRate (CBR) Flows. Current routing protocols are pure flooding, probabilistic flooding, backoff flooding, Stateless Linear-path Routing (SLR) and their derivations. Each flow defines a source node generating a flow of data packets, destined to a node or to the whole network. A packet contains a header and a random binary payload of ones and zeros. Values for the inter-bit interval in a packet (related to beta) and the inter-packet interval can be attributed in the scenario.

The physical layer implements the pulse-based modulation **TS-OOK** (explained in detail in 2.2.2.2). The transmission of packets is sequential. The reception of packets is parallel due to the features of TS-OOK that allows for bits of packets to be interleaved. However, there is a limit for the number of packets that a constrained node can receive at the same time Pujol et al. (2011), that we call the Maximum Concurrent Receptions (MCR). The packet arrival time to the node depends on its distance from the transmitter. Also, the receiving node does not have to listen continuously for bits because the symbol rate beta permits the decoding of bits at precise times.

Options in BitSimulator: Neighbors' list computations, DEDeN, Duty cycling The **neighbors' list computations** are done either statically or dynamically. The static neighbors' list computations are done by default and for all nodes once at the start of the simulation and is then kept for the entire simulation, which is costly. On the other hand, there is a command to enable the dynamic neighbors' list computations, which are done each time a nodes sends a message.

DEDeN may be enabled for the simulation in order for nodes to know their local density. DEDeN generates packets of type INIT and PROBE. INIT packets are broadcast to the network to initiate DEDeN. PROBE packets are sent by nodes to get their estimation of node density. Details on DEDeN can be found in 2.2.1.

Duty cycling may also be enabled for nodes to sleep with a cycle equal to the time between pulses T_s in TS-OOK.

Outputs of BitSimulator BitSimulator uses a discrete event model. The scheduler is the core implementation of BitSimulator. Nodes undergo events that can be either: **SEND, RECEIVE, COLLISION and IGNORE**, ordered in time. SEND events represent the packets (including copies of the same packet) being sent by a source node or a forwarder. SEND events can indicate the number of forwarding nodes, if a unique SEND data packet event of a forwarding node is counted. RECEIVE events are the packets (including copies) being received by by an intermediate node or a destination node. Similarly, the number of receiving nodes (implying the delivery ratio) can be derived from RECEIVE events, if a unique RECEIVE data packet event of a receiving node is counted. COLLISION events are packets **including copies** containing bits that have been altered by more than MaxBitError bits, as they got collided with other packets when attaining the receiving node. Nanonodes are constrained from several points of view: memory, processing power and speed, energy, and various resources. IGNORE events are packets **including copies** that are discarded as they overflow the node's buffer and exceed the node's resources, limited to MCR packets (3.3.1). Running the simulations outputs a log file called **events.log**, which contains lines describing all the events undergone by nodes chronologically ordered. The events.log file is introduced by a dictionary as a set of lines starting with #, which defines how to read the data in lines. Here is extract of events.log, for example:

```
#<lineFormat id="0" key="s" description="packet sent">
# <item type="Integer 64" key="time">simulation time in fs</item>
# <item type="Integer 32" key="nodeID">node ID handling the event</item>
# <item type="Integer 32" key="transmitterID">node ID of the MAC level
transmitter</item>
# <item type="Integer 32" key="beta">beta</item>
# <item type="Integer 32" key="size">packet size in bits</item>
# <item type="Integer 32" key="pktType">packet type</item>
# <item type="Integer 32" key="flow">flow id</item>
# <item type="Integer 32" key="seqno">packet sequence number</item>
#</lineFormat>
0 4900234 1 1 1000 100 0 1 0
```

The above line can be translated using the previous dictionary to: at time 4900234 fs, The

node with ID 1 sends the first packet (packet sequence number = 0) of the flow with ID = 1. The packet is of type DATA (packet type = 0) and of size is 100 bits and beta (related to the inter-bit interval) = 1000. The other output log files are `positions.log` and potentially: `SLRPositions.log`, `neighborsPositions.log` and `densityError.log`. The `positions.log` shows the positions of nodes as coordinates from the network dimensions, ordered by node ID. The `SLRPositions.log` file is for the SLR positions of nodes, for SLR-based routing protocols Tsioliariidou et al. (2017). The `neighborsPositions.log` contains the neighbors list for all nodes, if this option is used. The `densityError.log` includes the neighbors estimation (node density) for all nodes, if DEDeN is enabled.

Visualization tool of BitSimulator: VisualTracer `VisualTracer` is the visualization tool associated to BitSimulator, it can display 2D and 3D nanonetworks. It supports two modes: global and individual. The global mode displays a map of the nanonetwork, by taking the log files as input and displaying nodes in colors, depending on their events (SEND, RECEIVE, COLLISION and IGNORE). The events are either selected for a defined time window or are cumulative for the whole time of the simulation. The number of events is usually notably larger than the number of nodes, especially as a unique event is generated each time a node receives a packet. Histograms are used in VisualTracer to display the number of events in the current time window. In the following, we show some examples of displays from VisualTracer. Fig. 3.2 shows four screenshots recorded at four extremely close consecutive times, with a scenario of 30 000 nodes in the same communication range. At first, four source nodes send packets (first figure) and as BitSimulator simulates the radio propagation, the nodes gradually receive those packets, according to their respective distances from the sources.

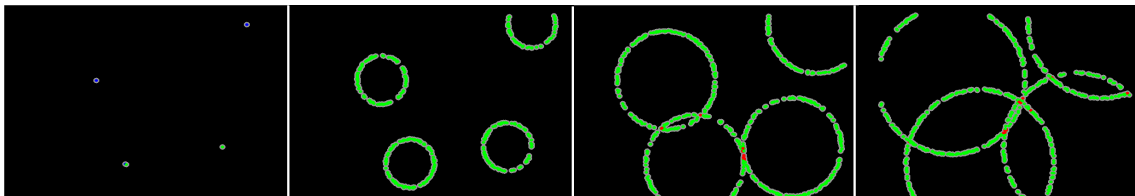


Figure 3.2: VisualTracer's global mode: 30 000 neighbors receiving a few packets over time (4 very small time steps). Source: Dhoutaut et al. (2018).

Fig. 3.3 uses the same scenario with a larger time interval than Fig. 3.2. Fig. 3.3(a) marks the corrupted packets in red lines and histograms (right) show the receptions (green) and the collisions (red). Fig. 3.3(b) chooses a medium time interval and helps understand why and where collisions occurs.

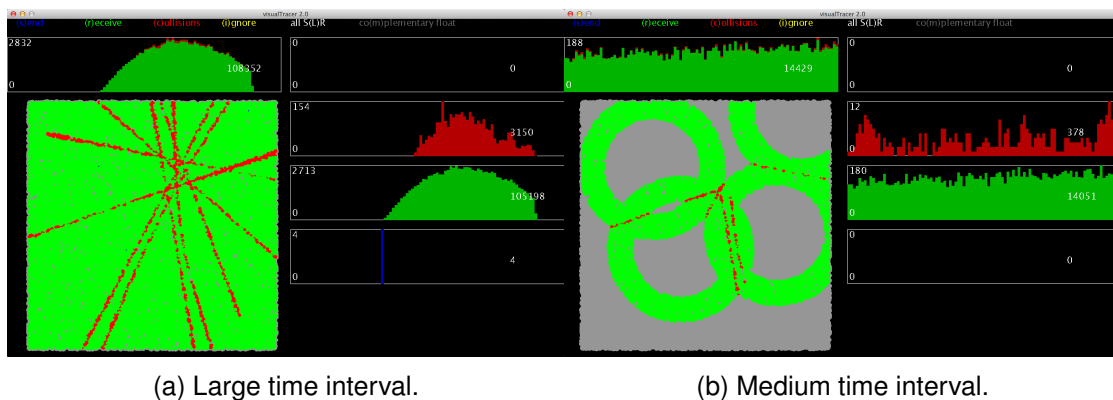


Figure 3.3: VisualTracer's global mode: Propagation delay causing deferred reception. Source: Dhoutaut et al. (2018).

The individual node mode shows a chronogram from the point of view of a particular node. On multiple lines, using a timeline, it shows bits and packets received from neighboring nodes. Due to the inherent interleaved natures of the communications on the channel, it proves especially helpful to detect repetitions and bursts in the collisions. Fig. 3.4 presents four flows: the third and fourth flows have collisions.

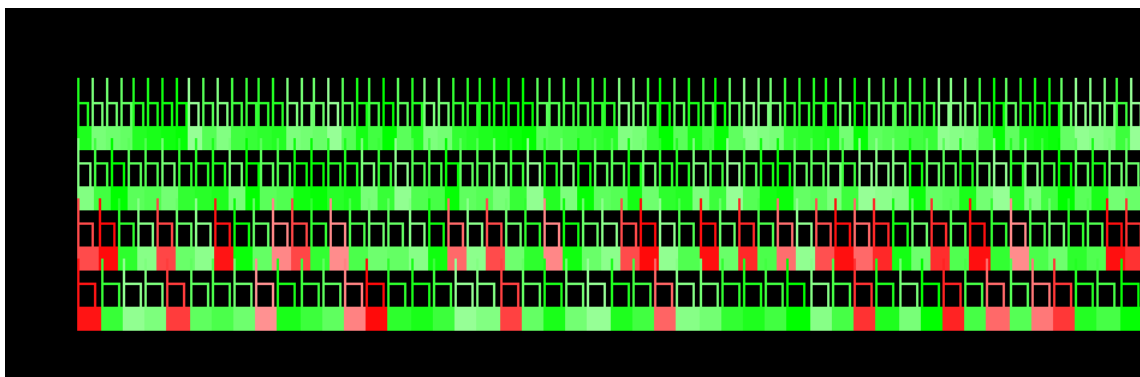


Figure 3.4: VisualTracer's individual mode: four flows scenario, collisions in red. Source: Dhoutaut et al. (2018).

3.3.2/ METHODOLOGY FOR WORKING WITH BITSIMULATOR

Here is the methodology that I adopted for working with BitSimulator:

- Implementation of the proposed work in BitSimulator's source code written in C++, by programming new routing agents and different mechanisms for the network and transport layers.
- Creation and simulation of different scenarios and changing parameters to study their effects.

- Usage of VisualTracer to help validate ideas, as seen in the evaluation figures of this thesis.
- Writing shell files to further analyze and assess the output files.

3.4/ CONCLUSION

As seen in this part, BitSimulator, being compared with other nanonetwork simulators, is the most scalable and suitable environment for the study. Therefore, it is used in the contribution part for the validation of propositions.



CONTRIBUTION

NETWORK LAYER: RING SCHEMES IN ULTRA-DENSE NETWORKS

4.1/ INTRODUCTION

Wireless ad hoc networks, i.e., infrastructure-less radio networks, are nowadays ubiquitous. In these networks, **multi-hop** communications allow to reach a destination beyond the range of a given node with the help of other nodes acting as forwarders James et al. (2015), and the spatial reuse they provide enables higher global and application throughput Kleinrock and Silvester (1978).

With the proliferation of connected objects in the IoT and the IoNT, and their increasing communication ranges (low power wide area networks, LPWAN), the number of neighbors in the communication range of a node is increasing, and networks are becoming ultra-dense. By **ultra-dense** we do not only mean a large number of nodes, but a number of neighbors so high (hundreds or thousands of 1-hop neighbors) that most classical protocols fail or become inefficient (this should not be mixed up with ultra-dense 5G networks (UDN) for example, which concerns the ratio between access points and users).

Nanonetworks, which is chosen to bring further a recent incarnation of ultra-dense networks, are enabled by nanotechnology. Nanotechnology permits the design of integrated devices at the nanoscale and inspires novel applications that can connect to the IoNT. In electromagnetic nanonetworks, nanonodes, deployed densely, radiate signals in the THz band (0.1–10 THz) using graphene antennas Jornet and Akyildiz (2010b).

The scenarios proposed in this dissertation correspond to nanonetwork's applications that require a **very large network size and high node density** such as **software-defined metamaterials and in-body communications** Lemic et al. (2021).

Nanonetworks significantly differ from traditional networks, albeit sharing some characteristics with WSNs. First, due to its size restrictions, a nanodevice faces extreme hardware limitations in its components: transceiver, memory, processor, power unit, etc., which

makes it unable to perform very complex protocols. Hence, and to execute efficient applications, a large number of nodes is required, forming a nanonetwork. In addition, a constrained nanodevice cannot store nor process complete information about its highly dense neighborhood (no matrix multiplication or maintaining long lists of neighbors for example). Given the channel characteristics and very low-level of energy available, the communication ranges in the THz band are very short. To increase coverage, a multi-hop network is required. Due to energy scarcity and hardware simplicity, nanonodes cannot use carrier signals like traditional networks; a lightweight modulation was proposed, TS-OOK Jornet and Akyildiz (2014), explained in 2.2.2.2. On top of those hardware limitations, nanonetworks can be much larger than WSNs, and notably denser, e.g., they may have hundreds or thousands of neighbors in their communication range.

Most classical protocols are inefficient in dense networks. In face of extreme density, they tend to either select too many forwarders or devote too many resources to find a small and optimal subset. In addition, some protocols rely on full neighbor knowledge, which consumes nodes' resources. Our general goal is to adapt those protocols to this context. It is necessary to design new lightweight and highly scalable protocols, with lower overhead.

In this context, we consider the following problem. In a nanonetwork or an ultra-dense network, a source node sends a message to all other network nodes (flooding) or to one destination node in a multi-hop fashion. In a dense network, this generates an avalanche of forwarders, leading to collisions, congestion and useless energy consumption. We look for methods to reduce the number of forwarding nodes, while still achieving a successful message delivery to the intended destination(s).

Current wireless routing protocols are usually not designed for ultra-dense networks. The inefficiency of classical protocols appears for all protocols which ignore the network density. For example, a pure flooding in a network of density 100 nodes quickly leads to the well-known **broadcast storm problem** Tseng et al. (2002): the 100 neighbors that received the initial packet try in turn to send it again in a very short time and space, causing contention on the channel, collisions, waste of energy and packet losses. A simple solution would be to reduce the proportion of forwarders in the network. However, one has to be careful to not decrease it too much, as the reverse problem can manifest itself. If not enough nodes participate in the forwarding of packets, the **die out** problem can appear, where the propagation stops without reaching all the nodes.

The inefficiency of packet propagation has been solved in the past literature, but the proposed methods have various constraints unsuitable for ultra-dense networks: they either use coordinates of all neighbors to compute which of them is nearer the destination, or use heavy storage or computations, or need hardware modules such as geo-positioning system (e.g., Global Positioning System (GPS) or Received Signal Strength Indicator

(RSSI). Generally, the existing methods select too many forwarders, which means that the channel will be encumbered by many copies of the same packet and a lot of power will be drained. On the other hand, trying to select a small and optimal subset of forwarders incurs an initially prohibitive computational and communication overhead.

In this dissertation we propose a simple scheme to select a **ring** of forwarders which solves the problem of too many forwarders and does not have aforementioned constraints. The only assumption we use is that nodes can send packets with different transmission powers. It basically works like this: each node, prior to sending its **first data packet**, sends two control packets at different powers; afterwards all the transmissions occur normally. Nodes near the sender receive both control packets, whereas nodes which have received only one of the two control packets lie on a ring near the border of the communication range. **Only the nodes in the ring forward the subsequent data packets from that node.** Consequently, our scheme **selects** geographically the nodes acting as forwarders, without the need for GPS-like module in nanonodes allowing them to compute distances between two nodes. The final goal is reducing the number of forwarders.

This ring-based forwarder selection method is not meant to be a standalone mechanism, but rather integrated into routing or data delivery protocols. It can be used to implement an optimized global broadcast (i.e., flooding data in the whole network), but can also optimize other unicast or multicast protocols that rely on a local broadcast for their basic operations.

In contrast, we noticed that in long multi-hops path, the number of forwarders progressively increases with the distance from the source. For this, we propose an improved scheme of the ring-based forwarder selection above that we call the **expanded ring**, which selects the forwarders in the rings and never in the inner discs.

Another limitation of the proposed ring is that it is static and manually set. A static ring width contains more forwarders in a dense environment compared to a non-dense environment. A large number of forwarders lead to congestion, while a small number of forwarders cause packet loss. To overcome this limitation, we hereby propose another efficient extension of the ring-based forwarder selection. This scheme, **dynamic ring**, dynamically adapts the **ring width** to the local density.

We implemented the ring and its variants in the nanonetwork simulator BitSimulator. However, despite choosing nanonetworks to validate our method, the ring principle stays the same in any other ultra-dense wireless multi-hop network. We test the rings on different scenarios and different higher layer routing protocols. We mainly analyze the effect of the rings on the number of forwarders, the number of receivers (packet delivery). In the original ring, we also analyzed the delay (transmission time) and the data traffic. We present the results of an extensive evaluation. The results show that the rings are highly efficient compared to without ring. The rings scale-up the routing protocols in dense networks by

optimizing the selection of forwarders and thus reducing the routing cost and increasing the lifetime of a nanonetwork, while keeping a successful packet delivery.

This contribution is organized as follows: Section 4.2 presents the related work. Section 4.3 presents the original ring scheme, Section 4.4 is the expanded ring and Section 4.5 is the dynamic ring.

4.2/ RELATED WORK

The ring schemes are based on a greedy strategy, which aims essentially to minimize the overlapped broadcast in networks. The ring also shares similarities with certain aspects of mobile ad hoc routing protocols such as OLSR and greedy forwarding, discussed in 2.2.3.1.

The traditional protocols in 2.2.3.1, however, have limitations, either in their scalability (when networks are ultra-dense) or in their applicability (when nodes are very simple). Scalability is a problem especially for protocols that need an extended knowledge of their neighborhood (especially if they require knowledge beyond 1-hop). They need a lot of messages and memory to maintain a correct view of their environment. Applicability mainly includes assumptions on the available hardware and resources. GPS, which is a given in VANETs, is not feasible in potentially resource-constraint networks. RSSI, which is often used as an alternative distance measuring technique, may not be available either in very simple transceivers. Memory and computational power may also be heavily restricted.

Finally, like our method, some aforementioned works select forwarders at the border of communication range. Compared to them, our method differs in the constraints, as it considers ultra-dense networks (where nodes can have hundreds or thousands of neighbors), where neither location information nor signal strength measurement are available. Moreover, our method targets ultra-dense networks and can effectively work even if the nodes have constrained resources.

Similarly, All the protocols that are proposed in electromagnetic nanonetworks in 2.2.3.2 may benefit from further enhancements by limiting the number of forwarders at the MAC-level while still maintaining packet delivery to the destination(s). For this, we propose the ring in all its forms that we present in the following: Ring 4.3, Expanded ring 4.4 and Dynamic ring 4.5.

4.3/ RING SCHEME

In a wireless network, when a node sends a packet, all the nodes in its communication range (called **neighbors**) receive it. In a multi-hop transmission, the forwarding nodes are chosen among these neighbors. Depending on the routing algorithm, the forwarding nodes can be all of them (e.g., in pure flooding), or only some of them (e.g., in backoff flooding). In both cases, an inefficiency appears regarding the position of forwarders. For routing purposes, instead of choosing the forwarders randomly, it is more efficient to choose them among furthest neighbors (near the border of communication range), because they lead to fewer hops (or packets generated) towards destination. Our scheme considers this fact, and only selects the forwarders among the border neighboring nodes.

Note that the location information is unavailable to nodes, and thus sectoring for example cannot be performed in flooding schemes. Moreover, the neighborhood and network knowledge is also unavailable so even in a grid-like network where nodes know their own coordinates, they still do not know their neighbors coordinates. Consequently, a node cannot rely on coordinate information. On the contrary, the only key assumption used by the ring protocol is that nodes can change the power used to transmit packets.

Our scheme works as following. Before forwarding **the first data packet**, a node sends two control packets with different powers: one at (or close to) maximum power and the next at a lower power. The nodes having received only the first packet and not the second one form a ring at the edge of the communication radius (the difference of two concentric discs), as shown in Fig. 4.1, lying between *rangeSmall* and *rangeBig*. We call the area that lies between the center and *rangeSmall* the inner disc. Nodes memorize the transmitter ID (no matter the initial source of the packet) and a Boolean value as whether it is on the transmitter's ring or not. Only the nodes within the ring are selected as potential forwarders. (Note that the list of neighbors a node is in the ring of is much smaller than the list of all the neighbors. Also, in a network with mobile nodes, the control packets could be sent several times, e.g., each time the network changes, or at regular predefined intervals.)

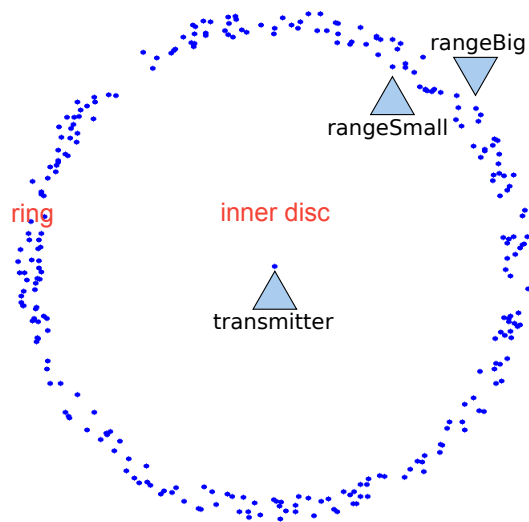


Figure 4.1: Ring principle: only nodes in the ring (between rangeBig and rangeSmall) are potential forwarders of the packet sent by the center.

Depending on the routing algorithm, all the ring nodes (in e.g., pure flooding) or only some of them (e.g., in backoff flooding) will **effectively** forward the packet. The forwarding algorithm is formally presented in Algo. 1. Note that the network is dense enough to always have nodes on the ring with an appropriate ring width.

Algorithm 1: Ring algorithm executed by each node.

```

1 Initially: table = empty, ctrlSent = false
2 Upon packet reception p:
3 n = previous node (sender at MAC-level) of the packet
4 if p is a high-power packet then
5   | table[n,0] = true
6 else if p is a low-power packet then
7   | table[n,1] = true
8 else
9   | // p is a data packet
10  | // check whether it is on the ring of node n, i.e., has received
11  | // high-power packet and has not received low-power packet from n
12  | if table[n,0] == true and table[n,1] == false then
13  |   | if the routing algorithm specifies to forward this packet then
14  |     | if ctrlSent == false then
15  |       | // has not yet sent high-power and low-power packets
16  |         | schedule to send high-power packet
17  |         | schedule to send low-power packet
18  |         | ctrlSent = true
19  |       | end
20  |     | schedule to send the data packet p
21  |   | else
22  |     | discard the packet p
23  |   | end
24  | end
25 end

```

It is worth to note that in the simple unit disc model of propagation (all or nothing, i.e., a packet is received by a node if and only if it is inside the communication range of the sender), the communication range is a circle which results in a perfect ring. Instead, in the more realistic shadowing model, there are obstacles that block the signal path and results in random anisotropic signal strengths. Therefore, mimicking an imperfect transmission range, the packet loss probability increase with the distance from the source. In BitSimulator, to give a better and more complex representation of the real radios and networks, the implemented **shadowing** propagation model performs like this: packets are always received at distance $[0, d]$ from transmitter, received randomly in $[d, CR]$ with decreasing probability from 1 to 0, and lost at distance $>CR$. As such, some nodes may receive the low-power packet, and **not** receive the high-power packet. Our method works in this case too, and the evaluation part uses the shadowing model. Figure 4.2 shows the

effect of shadowing on the communication range of the source node.



Figure 4.2: The communication range of the source hop without (left) and with the shadowing (right).

Figure 4.3 shows the effect of different values of shadowing on the communication range of our scenario. It illustrates the proportion of packets received at a given distance from the center node with Communication Range (CR) = $900\ \mu\text{m}$ and different values of standard deviation. As seen in this figure, when the std deviation is null, the proportion of packets received is 1 if distance from the center node is less than or equal to the communication and 0 otherwise. When the std deviation not null, the proportion of packets received decreases progressively as the distance from the center increases and becomes zero before reaching the communication range. When the shadowing is high, the proportion of packets received at a given distance decreases quicker and the curve slope is higher. This makes farther nodes from the center receive fewer packets.

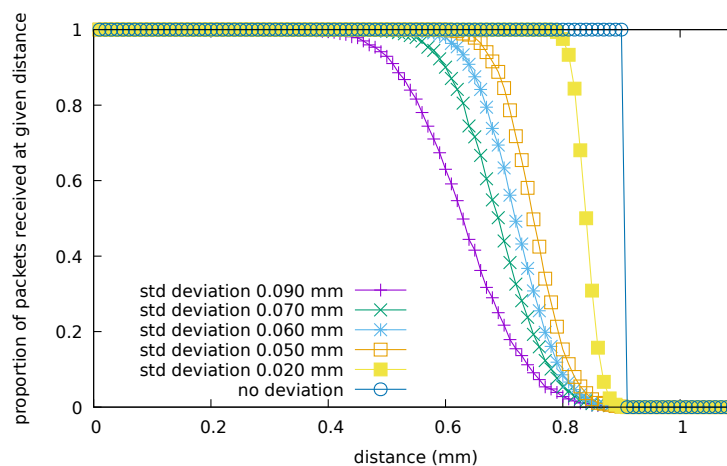


Figure 4.3: Proportion of packets received at a given distance from the center node with CR = $900\ \mu\text{m}$ and different values of std deviation.

4.3.1/ EVALUATION OF RING SCHEME

We evaluate our scheme in an ultra-dense nanonetwork. The modulation scheme is TS-OOK Jornet and Akyildiz (2014), with $T_p = 100$ fs and $\beta = 1000$ Jornet and Akyildiz (2014). There is no explicit mechanism to avoid or detect collisions as it is not required here; nodes access the channel whenever they need to and rely on the inherently low probability of collisions on the very wide channel.

4.3.1.1/ SCENARIOS

The simulation parameters are shown in Table 4.1. The network is a square area. It has (a) 10 000 nodes or (b) 20 000 nodes, distributed in an area of 36 mm². The nodes are placed randomly, using a uniform distribution, and are static. Nodes have omnidirectional antennas and equal communication ranges (except for the particular case of control packets). We use the **shadowing** propagation model 21.

Table 4.1: Simulation parameters.

Size of simulated area	6 mm * 6 mm
Number of nodes	10 000 or 20 000
Communication range	900 μ m
RangeBig	900 μ m
RangeSmall	800 μ m
Data packet size	1003 bit
Control packet sizes	101, 102 bit

The ring is specified by two radiuses, rangeBig and rangeSmall. We chose rangeBig to be equal to the communication range (so that all the nodes can receive it), and rangeSmall smaller (so that it is received only by nodes outside the ring). The ring width is the difference between the two ranges, $w = 900 - 800 = 100 \mu\text{m}$, i.e., $100/900 \approx 11\%$ of the communication range.

For the example scenario used, if we had used the unit disc model, for 10 000 nodes, the average number of neighbors per node would be 616, with a minimum of 167 (for corner nodes) and a maximum of 775. The average number of **ring** neighbors per node would be 122. The 20 000 nodes scenario has 1234 neighbors per node and 259 **ring** neighbors, in average. Using the shadowing propagation model, the average number of neighbors per node is 408 for 10 000 nodes and 819 for 20 000 nodes. This clearly represents an ultra-dense network.

The two control packets have random payload data, and are smaller than data packets. Distinctive values are chosen for data packet size (1003 bits) and control packet sizes

(101 and 102 bits) simply to be easily spotted in the simulation log files.

A given source node (in the middle-top of the networks) generates a CBR flow of 10 packets (or 100 packets in one case) to all the nodes (in flooding) or to a node at the bottom-right of the network (in unicast). The number of hops is $x/CR = 6/.9 \approx 6.7$ hops on each dimension of the network, which is sufficient for testing routing protocols. The interval of time between two consecutive packets is large enough to avoid collisions between them. Given that each node sends the two control packets only once, right before the very first data packet it forwards, the effect of injecting the additional control packets should be reduced for a 10-packet flow.

As already mentioned, the aim of adding the ring to routing protocols is to restrict the forwarders to the ring area at each hop. We show the ring effect on three protocols: two flooding schemes, and a unicast one (SLR) Tsioliariidou et al. (2017).

We present in this section the values of more than 120 simulations: 2 network sizes (10 000 and 20 000 nodes) * 3 routing protocols * 2 scenarios per protocol (with and without ring) * ≥ 10 runs. Except if otherwise stated, each point of simulations shown represents the average of the 10 runs, differing only in the node positions (via a different seed of the random number generator dealing with node placement exclusively). However, for simplicity, we present detailed information for the 10 000 node scenario, and at the end a short comparison with the 20 000 node scenario.

We present the results using several metrics. We reiterate that our method aims to identify better forwarders, which should reduce the number of total forwarders, without impacting the delivery rate. Hence, the first main metric is about **forwarders**, shown as the cumulative number of senders for each packet, averaged for each of the 10 packets and over the 10 runs. The second main metric is about **delivery rate** (number of receivers): in flooding, the cumulative number of receivers for each packet, averaged for each of the 10 packets and over the 10 runs; in SLR, just whether the packet reached the destination (1) or not (0), averaged for each of the 10 packets and over the 10 runs. The third metric we analyze is about **transmission time**, defined as the average time interval between the source sending the first copy of the packet, and the last node (for flooding) or the destination (in SLR) receiving the first copy of it, for each packet over 10 runs. The fourth metric measures the traffic incurred by the two additional packets (control1 and control2). Finally, we show the main finding for the **second scenario** (with 20 000 nodes).

To desynchronize node forwarding in ultra-dense networks and to reduce collisions, nodes choose a random backoff before forwarding, from a fixed window of 10 000 fs in pure flooding, probabilistic flooding and SLR, and from a dynamic window in backoff flooding. The dynamic window is a function of the number of neighbors, given by as DE-DeN and is sufficiently large for the node to count packet copies, as explained in Arrabal et al. (2018b).

To avoid forwarding loops, nodes forward packets they receive for the first time. For this to work, nodes can memorize the source ID and the packet sequence number of the received packets in a list. A nanodevice is assumed to be able to store this, as it is relatively small because a packet does not stay too much time in the network, hence nodes can safely remove old packets if memory is full .

To have an insight on the reduction in the number of forwarders, and to increase the trust on the results, we show table results as average values of 10 runs with 10 packets each. The figures showing the network visually are captured from VisualTracer and show all the cumulative events per packet that occurred in the network with two key colors for nodes: blue for senders and green for receivers (we choose to show the first packet for the first run only as an example). Technical details and information about full reproducibility of our results are provided on a separate web site¹.

4.3.1.2/ EFFECT OF RING ON PURE FLOODING

Pure flooding is the basic broadcasting scheme used for network-wide data dissemination. Nodes do not need any knowledge about the network, they forward each packet they receive for the first time, as explained in 4.3.1.1. Given the high number of packets sent, pure flooding is very inefficient in forwarding, especially in ultra-dense networks. The choice of pure flooding is to show, as a start, the behavior of the ring protocol in its most basic state. The ring protocol is then implemented in advanced routing protocols like backoff flooding and SLR to show its efficiency even for these routings.

The pure flooding with ring restricts the forwarders of a packet, at each hop, to those in the ring area of the sender (instead of the whole communication range). Note that the test to check whether the packet is seen for the first time or not and its memorization as seen are made **before** the test of whether the node is on the ring or not, otherwise a node receiving a packet for the first time and not being in the ring will never forward that packet (even if later it is on the ring of that packet, sent by another transmitter).

We expect that the number of forwarders will be drastically reduced. Table 4.2 confirms this: the use of the ring reduces the number of forwarders by $1 - 2036/10000 \approx 79\%$, while keeping the delivery ratios close to 1.

¹<http://eugen.dedu.free.fr/bitsimulator/wcnc22>

Table 4.2: Results with 10 000 nodes.

	Without ring	With ring
Pure flooding:		
Average number of forwarders per packet	10 000	2 036
Average number of receivers per packet	10 000	10 000
Backoff flooding:		
Average number of forwarders per packet	100	72
Average number of receivers per packet	9 999.99	9 999.7
SLR:		
Average number of forwarders per packet	406	84
Destination reached	100%	99%

We expect that the percentage of forwarders at each hop will no longer be 100% of the neighbors, but smaller. Fig. 4.4 (right) shows visually the spatial effect of the ring on pure flooding. We notice that the forwarders form concentric circles around the initial source, which is coherent with the use of rings. Without ring, the left part of the figure shows that all the 10 000 nodes are forwarders, contrary to routing with ring.

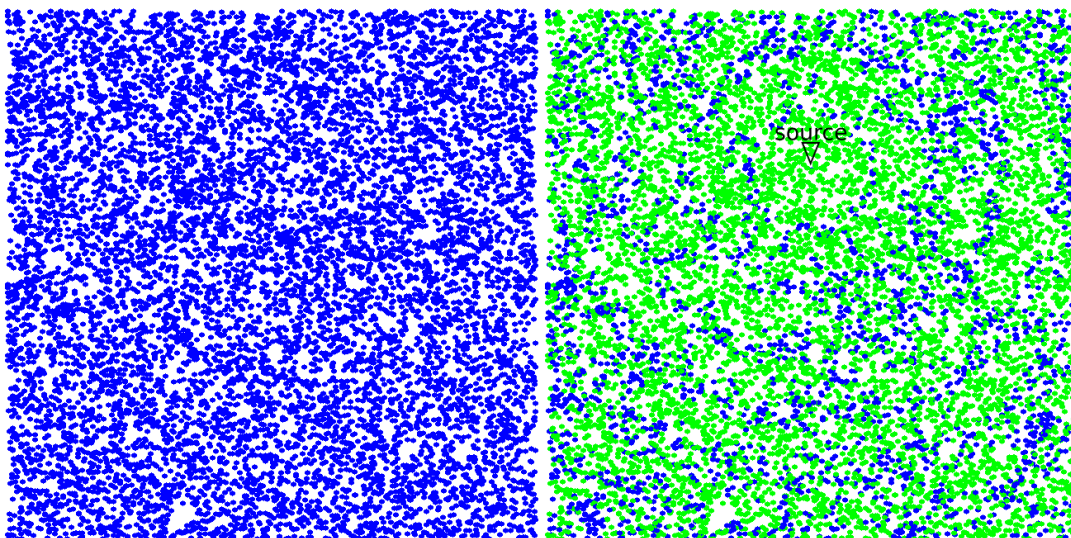


Figure 4.4: Pure flooding without (left) and with the ring (right).

Fig. 4.5 shows the cumulative distribution of the number of forwarders in time, as a percentage of the total number of nodes in the network. The progression for both without and with ring is regular, e.g., there is no sharp increase and the without ring curve increases much more compared to with ring curve.

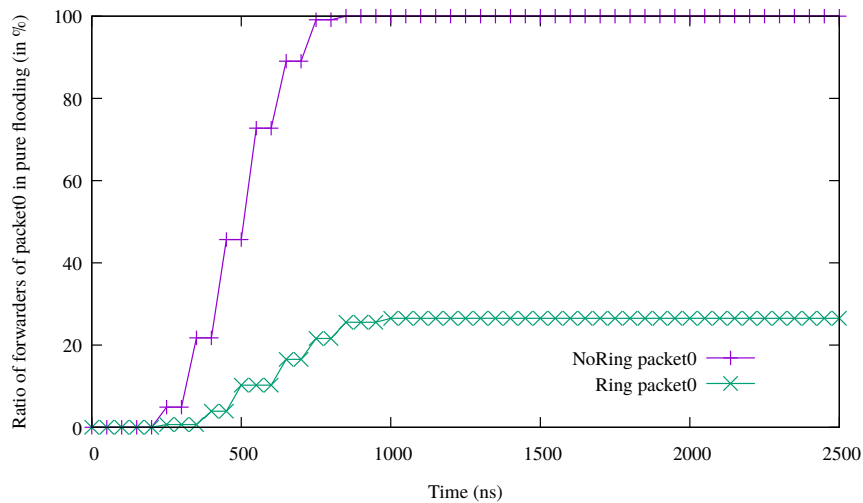


Figure 4.5: Cumulative number of forwarding nodes over time in pure flooding without and with the ring with 10 000 nodes.

To sum up, the ring improves the pure flooding by a wide margin.

4.3.1.3/ EFFECT OF RING ON BACKOFF FLOODING

We want to check the ring effectiveness on an already efficient propagation scheme. Backoff flooding Arrabal et al. (2018b) is a highly efficient variant of flooding, which automatically chooses a very small number of forwarders (no matter the network density), and avoids the use of probabilities. We remind that in backoff flooding, upon reception of a packet, a node chooses a random backoff inside the waiting (contention) window. The window for each node is proportional to its number of neighbors. For that to work, nodes need to know the number of their neighbors, using DEDeN Arrabal et al. (2018a) for example. At the end of the backoff time, if the node has received less than n copies of the message, it forwards the packet, otherwise it discards it without forwarding. In this scenario, the number of copies chosen n is 1.

Adding the ring to the backoff flooding involves two modifications. The first is selecting only the neighbors in the ring to forward packets. The second is on the waiting window size. Again, the time window is proportional to the number of forwarders; in the original backoff flooding, this is the number of neighbors, but when using ring this is the number of ring neighbors. Thus, the waiting time is modified to be proportional to the number of ring neighbors.

Table 4.2 shows that the ring reduces the number of forwarders by $1 - 72/100 = 28\%$, while the delivery ratio is similar (9999.7 vs 9999.99).

Like in pure flooding, we show the distribution in space and time of the forwarders. Fig. 4.6

(right) presents the effect of the ring on backoff flooding, and shows that the forwarders are fewer and farther from each other than without ring.

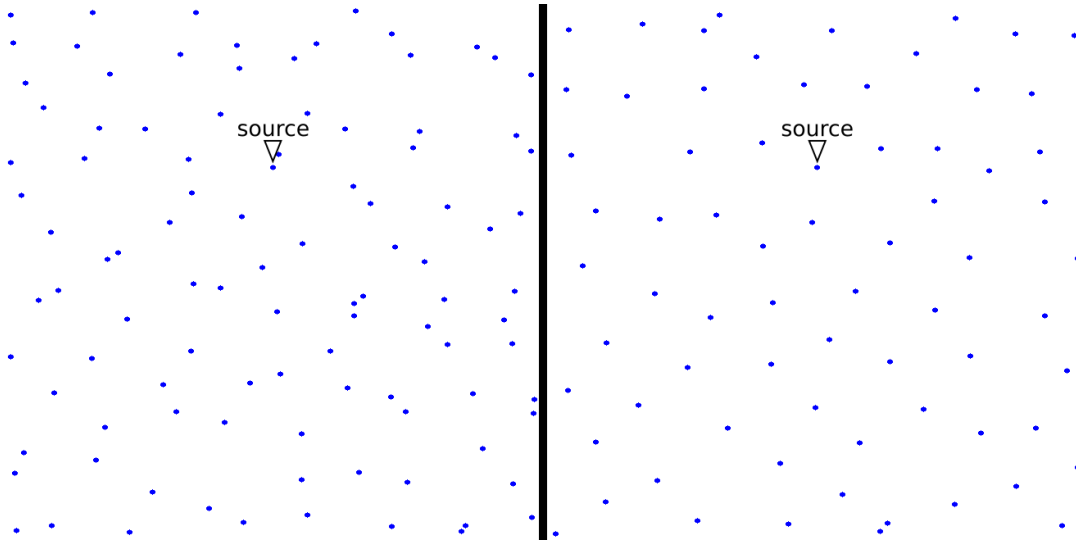


Figure 4.6: Forwarders in backoff flooding without (left) and with the ring (right).

Fig. 4.7 shows the cumulative distribution of the number of forwarders in time, as a percentage of the total number of nodes in the network. Again, the progression for both without and with ring is regular, e.g., there is no sharp increase and the without ring curve increases much more compared to with ring curve.

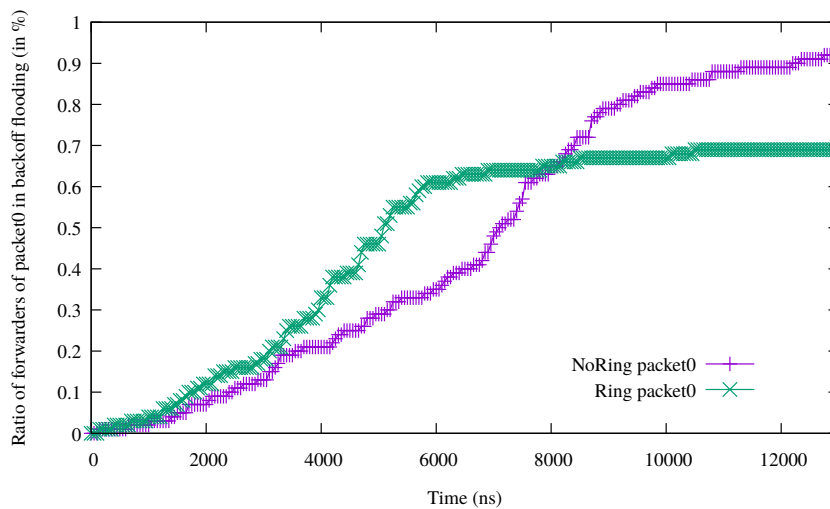


Figure 4.7: Cumulative number of forwarding nodes over time in backoff flooding without and with the ring with 10 000 nodes.

The results show that the ring further increases the efficiency of an already highly efficient backoff flooding.

4.3.1.4/ EFFECT OF RING ON SLR ROUTING

SLR Tsioliariidou et al. (2017) is an addressing and **unicast** (or merely **zone-cast**) routing scheme (i.e., message is sent to one destination only) designed for nanonetworks. In the **setup** phase, a few anchor nodes broadcast a packet in the network with a **hop** field set to 0, forwarded by all the nodes after increasing the hop count, whose effect is to divide the network space in **zones** and allow nodes to set their coordinates as the hop count to each of the anchor. From that time on, upon reception of a packet to **route**, nodes forward it if and only if they are on the line between the source and the destination.

Adding the ring to SLR simply restricts the new forwarders to be in the ring at each hop, as shown in Fig. 4.8 right, i.e., the forwarders are found towards the end of each SLR zone, and fewer than without ring.

The results in Table 4.2 show that the ring reduces the number of forwarders by $1 - 84/406 \approx 79\%$, while the destination at bottom right still receives the message. Fig. 4.8 (right) shows that the ring works as expected, i.e., the forwarders are found towards the end of each SLR zone, and fewer than without ring. Fig. 4.9 shows the cumulative distribution of the number of forwarders in time, as a percentage of the total number of nodes in the network. To conclude, SLR with ring performs better than without ring.

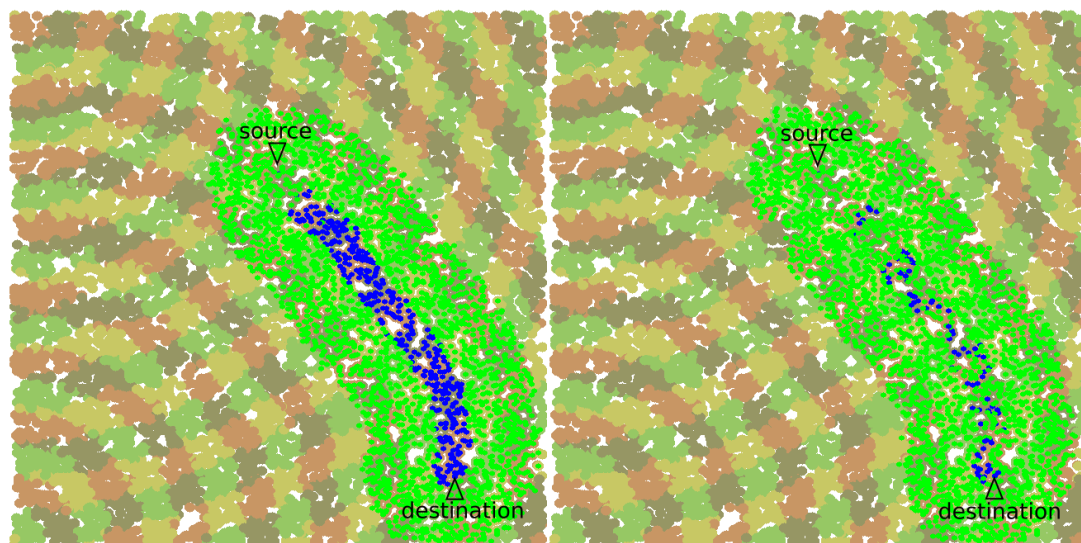


Figure 4.8: SLR without (left) and with the ring (right).

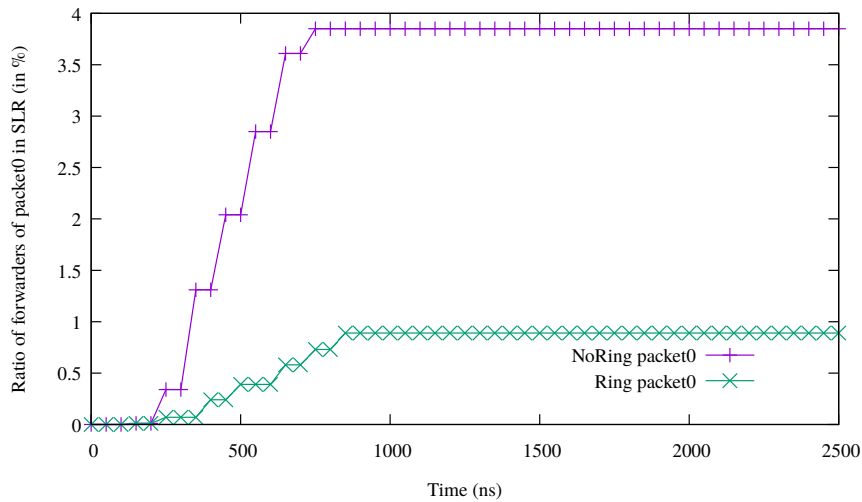


Figure 4.9: Cumulative number of forwarding nodes over time in SLR without and with the ring with 10 000 nodes.

4.3.1.5/ INFLUENCE OF RING ON DELAY

Compared to original versions of protocols, the ring adds the two control packets. This adds delay to the packet delivery. This section studies this delay.

Table 4.3 presents the average transmission time per packet of the 10 packets for all the routing protocols without and with the ring. It shows an increase in the delay for the ring except for backoff flooding (for which the number of neighbors is smaller, hence the contention window is smaller). This delay is due to the presence of control packets that are attached to the first data packet sent by forwarders. After this phase, the transmission time becomes similar to the no-ring approach.

Table 4.3: Average packet transmission time for 10 000 nodes.

	Without ring	With ring	Increase
Pure flooding	618 ns	645 ns	4%
Backoff flooding	13 516 ns	10 590 ns	-21.6%
SLR	493 ns	508 ns	2.9%

Like with the forwarders, to better understand how delay is affected, especially to avoid the particular potential bad case of a last receiver which increases the delay significantly, we show the distribution in **time** of the delay per packet, for one random seed only, as an example. The delay is shown as the cumulative number of unique receiving nodes of a packet (for flooding schemes), and the time of arrival of first copy of the packet to the destination (in SLR).

Fig. 4.10 and Fig. 4.11 shows the cumulative number of receiving nodes over time in the

flooding schemes studied, for four packets (0, 4 and 8) of the 10 packet flow. Fig. 4.10 shows that the without-ring curves almost overlap with the with-ring curves, with a small delay between them. Fig. 4.11 show that ring reaches nodes faster than no ring.

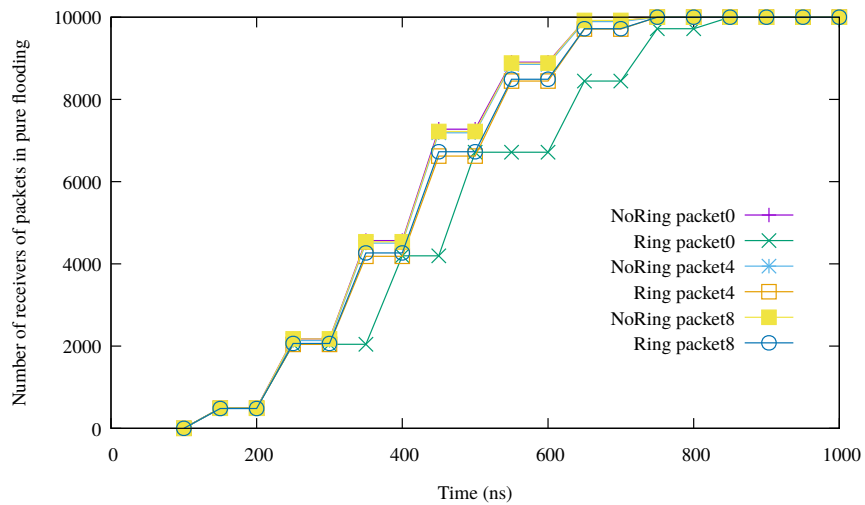


Figure 4.10: Cumulative number of receiving nodes over time in pure flooding without and with the ring with 10 000 nodes.

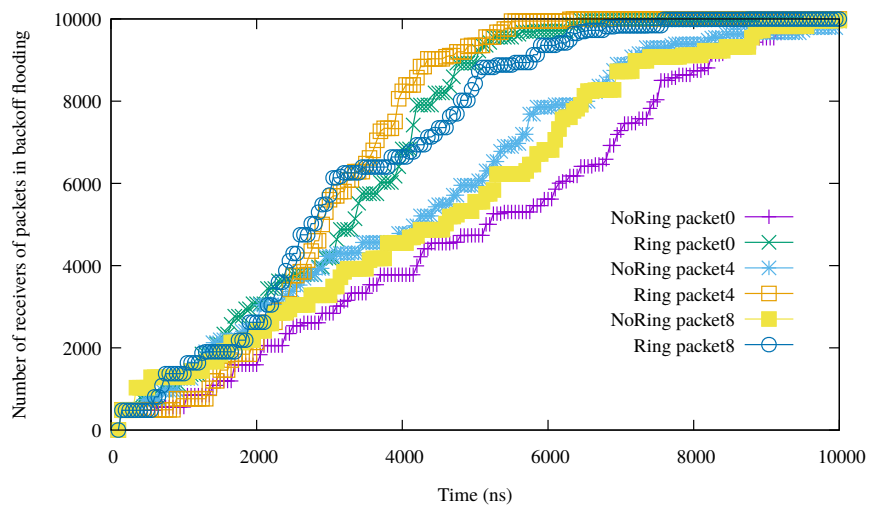


Figure 4.11: Cumulative number of receiving nodes over time in backoff flooding without and with the ring with 10 000 nodes.

Fig. 4.12 shows the arrival time at the destination node in SLR for each of the ten packets. Both curves slightly overlap, and SLR with the ring has an inconsiderable delay over SLR without the ring. Thus, in all the protocols except for backoff flooding, the ring approach has a very small additional delay compared to without the ring.

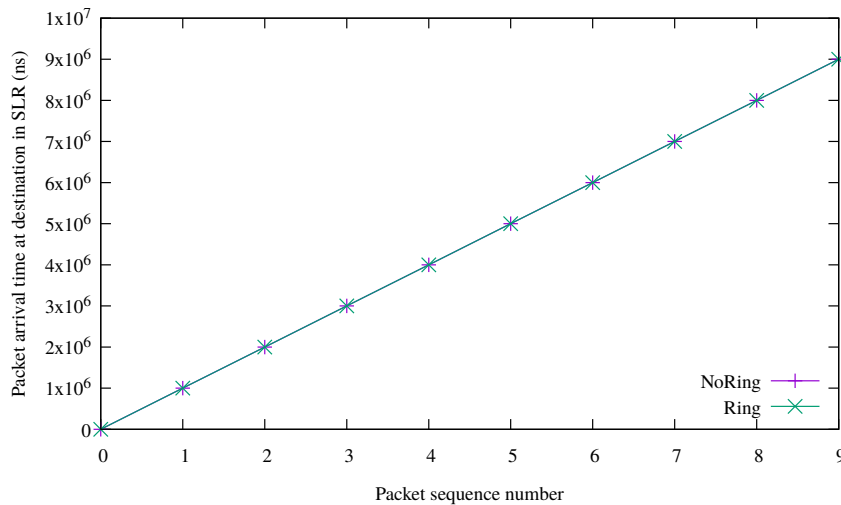


Figure 4.12: Arrival time at destination node in SLR for each packet sequence number with 10 000 nodes (all ten CBR packets for only seed=0 shown).

These curves show that the difference in delay is more visible for the first packet(s), transmissions. We reiterate that control packets are generated only once, right before forwarding the very first data packet. Clearly, the delay for these packets includes the delay of control packets too. Later, this delay decreases progressively until all nodes have previously sent their control packets.

To summarize, the ring adds a slight delay, which is less and less visible with time.

4.3.1.6/ INFLUENCE OF RING ON TRAFFIC

Compared to without ring, the additional two control packets generate additional traffic. However, we emphasize that the control packets for the ring creation are generated **at most once** by each node in static conditions.

In the scenario chosen, the data packet has 1003 bits, and the two control packets have 101 and 102 bits (cf. Table 4.1). Given that the ring leads to a significant decrease of the number of forwarders and hence the number of sent packets, we expect that the ring will reduce the data traffic. Table 4.4 (last column) confirms that the number of packets sent with ring is highly reduced compared to without ring. To conclude, the benefit in reduction of packets generated outweighs by far the additional size of control packets, hence the use of the ring reduces the network traffic. Note that the two control packets may add an additional small transmission delay only for the first packet generated by nodes.

Table 4.4: Total data traffic generated for 10 000 nodes.

	Without ring	With ring	Reduction
Pure flooding	100 030 kbits	21 992 kbits	78%
Backoff flooding	1 012 kbits	861 kbits	19%
SLR	4 079 kbits	905 kbits	77%

4.3.1.7/ EVALUATION OF RING IN DENSER NETWORKS

All the previous results have been obtained in a scenario with 10 000 nodes. For a better confidence in the results, we evaluate the ring in another, denser, network. We keep all the parameters identical, except the number of nodes, increased to 20 000 nodes. The full results are shown in Table 4.5.

Table 4.5: Evaluation results for 20 000 nodes.

	Without ring	With ring
Pure flooding:		
Average number of forwarders per packet	20 000	3 038
Average number of receivers per packet	20 000	19 999.8
Average transmission time per packet	622 ns	638 ns
Backoff flooding:		
Average number of forwarders per packet	103	73
Average number of receivers per packet	20 000	19 999.9
Average transmission time per packet	16 973	13 004 ns
SLR:		
Average number of forwarders per packet	909	155
Destination reached	100%	100%
Average transmission time per packet	469 ns	510 ns

The main finding of these results when compared to previous scenario (10 000 nodes) is that the reduction in the number of forwarders when using the ring as compared to without the ring is generally even higher: for pure flooding, a $1 - 2036/10000 = 79\%$ reduction with 10 000 and $1 - 3038/20000 = 84\%$ reduction with 20 000. For backoff flooding, the reduction is 28% with 10 000 nodes and 29% with 20 000 nodes. For SLR with 10 000 nodes the reduction is 79%, and for 20 000 nodes it is 82%. The average delivery ratio as shown in Table 4.7, is giving 1 or close to 1 values. Thus, the benefit of the ring increases in a denser network.

Table 4.6: Reduction of the number of forwarders from without to with the ring, for both networks of 10 000 and 20 000 nodes.

	10 000	20 000
Pure flooding	79%	84%
Backoff flooding	28%	29%
SLR	79%	82%

Table 4.7: Average delivery ratio with ring in a network of 10 000 nodes vs. 20 000 nodes.

Number of nodes	10 000	20 000
Pure flooding	100%	99.9%
Backoff flooding	99.9%	99.9%
SLR	99%	100%

4.3.2/ CONCLUSION OF RING

Section 4.3 presented a new method to select forwarders in a multi-hop transmission. Using two control packets transmitted once (only before the very first data packet of a forwarder) at different power levels, a ring of nodes near the communication range of a transmitted node are selected as candidate forwarders.

We validated the ring scheme in a simulator with three protocols: two flooding and one destination-oriented protocols. We compared the results using several metrics: number of forwarders, delivery ratio, delay and data traffic, and in two different network node densities of 10 000 and 20 000 nodes. The ring achieves much better performance in both protocols, and for the main metrics (number of forwarders, and delivery ratio), with slightly lower results for the data traffic and the delay. The performance increases with the network density.

4.4/ EXPANDED RING SCHEME

4.4.1/ INTRODUCTION OF EXPANDED RING

The previous Section 4.3 presented the ring in its basic form that works well. However, further analysis shows that it becomes sub-optimally efficient when the number of hops increases. This is visible on Fig. 4.4 (right), where concentric forwarder rings are thinner and better defined close to the source, while wider and blurrier as we get farther.

After diving into the ring behavior and highlighting its limitations, this section consequently

proposes an enhanced version of the ring, that we call the **expanded ring**. This version especially shows benefits in multi-hop communications.

4.4.2/ EXPANDED RING

The expanded ring further reduces the number of forwarders by redefining the ring neighbors and limiting them to those lying in the rings and never in the inner discs of forwarders having a lesser or equal hop count, as seen in Fig. 4.13 (right). In contrast, the ring neighbors in the basic ring are found on any ring, as in Fig. 4.13 (left). Fig. 4.13, has three nodes. A is the source node. B and C are 1st-hop neighbors of A and are forwarders as they are on the ring of A. The pink area includes potential forwarders and is larger in the original ring (left) than the expanded ring (right). We remind that potential forwarders receive the packet the first time and thus should be outside of A (4.3.1.1).

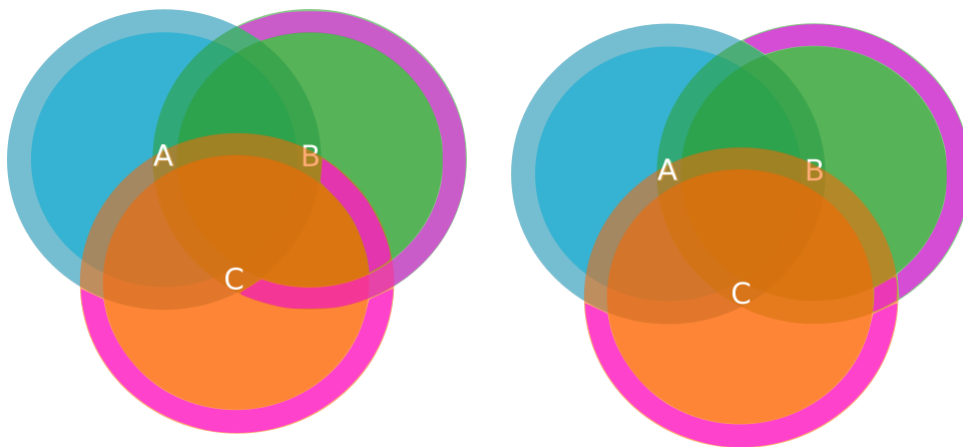


Figure 4.13: Simplified illustration of original ring (left) vs. expanded ring (right). Pink regions contain potential forwarders.

Our aim is to have the initial source node as the center of concentric rings: the n -th ring includes n -hop transmitters, as illustrated in Fig. 4.14 for the first two hops.

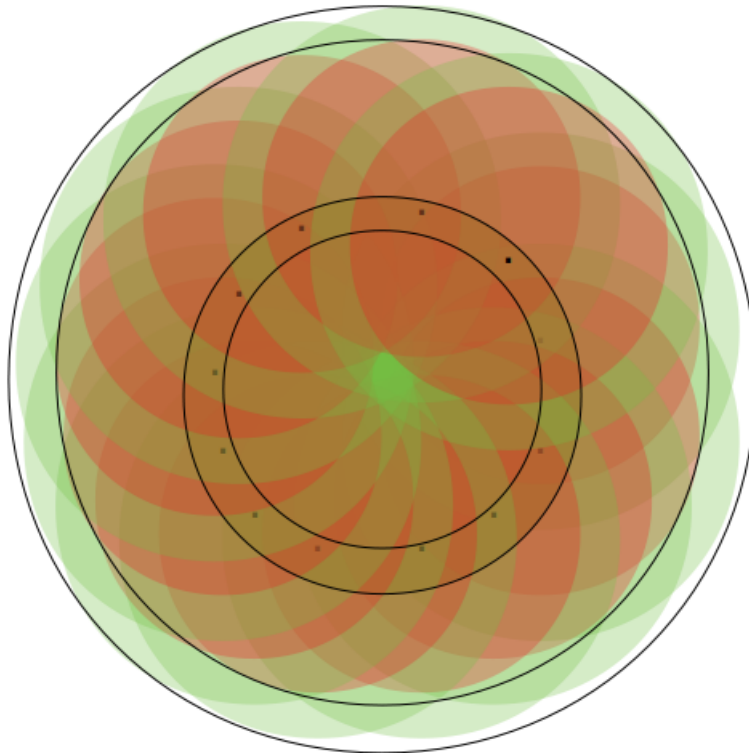


Figure 4.14: Envisioned goal by the expanded ring: forwarders at the first hop are in the inner black ring and forwarders at the second hop are in the external black ring. Nodes (black dots), rings (green) and inner discs (red).

Specifically, the expanded ring uses the same conditions as the basic ring, but with one modification: it is not sufficient anymore to be on the ring area of the node from which it received the packet the first time; the node must also be, for a specified time window w , in the ring of **all** the nodes having sent that packet (or a copy of it). Even if the modification is small, the effects are very different, and need to be evaluated.

The implementation of this scheme is fully presented in Algo. 2. The modifications compared to the basic scheme are at lines 3–7 and 21–23.

Algorithm 2: Expanded ring algorithm.

Data:

rangeBig = defaultCommunicationRange
 amlOnRingMap = [transmitterID, ctrlBig, ctrlSmall]
 needToSendControl = true
 sourceRingMap = [sourceID, hopCount, isOnTransmitterRing]

Result: Perform expanded ring restriction of forwarders

```

1 Upon packet reception (type, sourceID, seqNo, transmitterID)
2 if type is DATA then
3   | isOnTransmitterRing = ctrlBig[transmitterID] AND !ctrlSmall[transmitterID];
4   | if sourceRingMap[sourceID] does not exist then
5   |   | insert [sourceID, hopCount, isOnTransmitterRing] in sourceRingMap
6   | if !isOnTransmitterRing AND hopCount(packet) < hopCount[sourceID] then
7   |   | isOnTransmitterRing[sourceID] = false;
8   | if call amlOnRing AND routing protocol selects me as forwarder then
9   |   | call forwardDataPackets
10 else if type is CONTROL-BIG then
11 |   | ctrlBig[transmitterID] = true
12 else if type is CONTROL-SMALL then
13 |   | ctrlSmall[transmitterID] = true
14 bool function amlOnRing
15 | // I am on the ring if the following conditions are met:
16 | // - I received a ctrlBig packet from this transmitter
17 | // - did NOT receive a ctrlSmall packet from this same transmitter
18 | return ctrlBig[transmitterID] = true AND ctrlSmall[transmitterID] = false;
19 function forwardDataPacket
20 if needToSendControl then
21 |   | send ControlBig with rangeBig
22 |   | send ControlSmall with rangeSmall
23 |   | needToSendControl = false
24 | schedule send data packet event in t
25 Upon scheduled send data packet event
26 if isOnTransmitterRing[sourceID] then
27 |   | send data
  
```

The state diagram is presented in Fig. 4.15. A node can be on the ring or not, and if on the ring then it can be a forwarder or not, depending on the routing protocol operation.

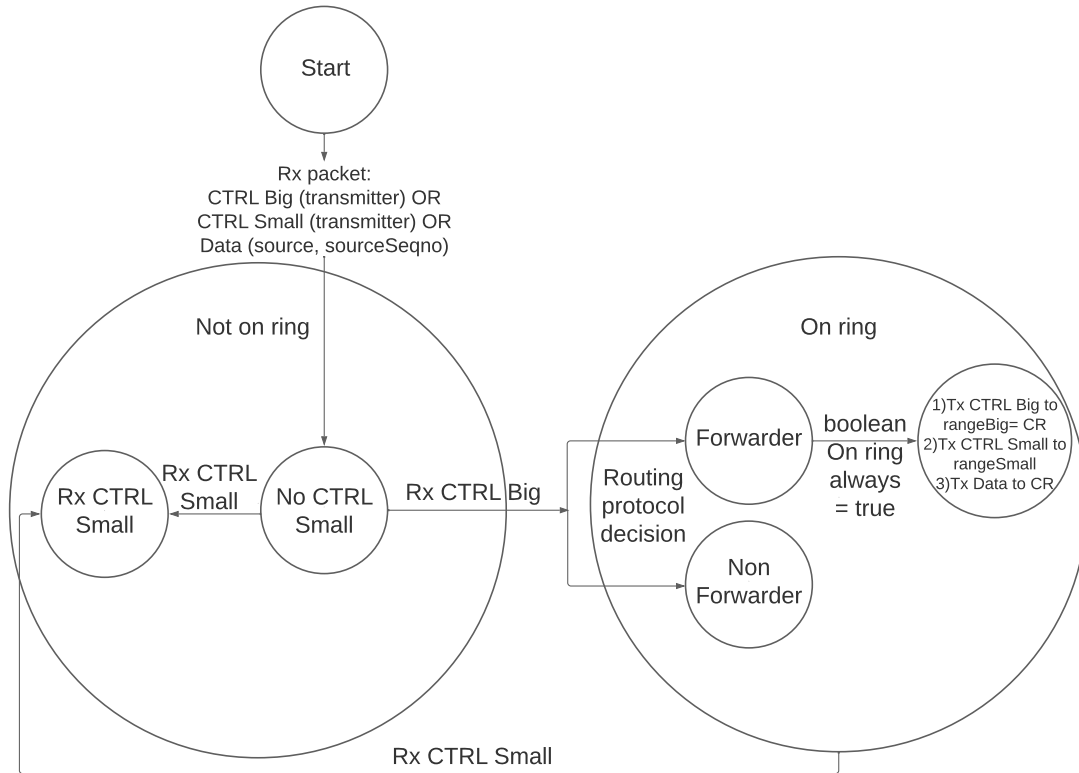


Figure 4.15: State diagram of expanded ring.

4.4.3/ EVALUATION OF EXPANDED RING

This section compares three versions: the proposed scheme, original ring, and no ring, each of them under two routing protocols: pure flooding and SLR.

4.4.3.1/ SCENARIOS

The parameters used are shown in in Table 4.8. The simulated nanonetwork is a square area of 36 mm². 10 000 nodes are randomly placed in three equally sized horizontal bands with different densities: 5500 nodes in the upper band, 3000 nodes in the middle band, and 1500 nodes in the bottom band, yielding a **heterogeneous** network.

Table 4.8: Simulation parameters.

Parameter	Value
Size of simulated area	6 mm * 6 mm
Number of nodes	10 000
Communication range	1000 μ m
RangeBig	1000 μ m
RangeSmall	830 μ m
Data packet size	1003 bit
Control packet sizes	101, 102 bit
Time window w	200 ns

The communication range of a nanonode is $CR = 1000 \mu\text{m}$ and includes 906 neighbors in average. It results in a network width of $x/CR = 6 \text{ mm} / 1 \text{ mm} = 6$ hops horizontally and vertically in the network, appropriate for multi-hop communications. Again, the **shadowing** propagation model is used 21.

Compared to the previous work, on the original ring Section 4.3, the evaluation in the current section uses a slightly different scenario and a heterogeneous network (in terms of node density).

The ring is delimited by two ranges: rangeBig (of high-power control packet) is set to default communication range to increase the forwarding progress, and rangeSmall (of low-power control packet) is chosen empirically to guarantee successful packet delivery. In both old and new protocols we used the same values. We recall that the control packets are sent only once per node, before the very first forwarded data packet, so their cost fades away after 50 data packets. The data packet is a random sequence of 1003 bits of “1”s and “0”s. The high and low-power control packets are also random sequences, of 101 and 102 bits, respectively (these specific values are chosen simply to be spotted easily in the output log files of simulations). The mechanism to avoid endless loops 4.3.1.1 is also taken into account (see Algo. 2). Additionally, a backoff before transmission is used before forwarding any packet in order to reduce collisions.

The scenario includes a source node at the top of the network that transmits a CBR flow of 50 data packets. The destination is either the whole network (for pure flooding) or a destination node, at the bottom-right of the network (for SLR protocol). SLR anchors are at the top-left and bottom-left corners of the network.

The expanded ring is implemented in both pure flooding and SLR. We compare three schemes for both protocols: no ring, original ring, and expanded ring. For each of the six cases, the simulation is done for 10 different RNG seeds, used for the backoff time before transmission. This results in 60 simulations with 50 data packets each.

The evaluation metrics are the number of forwarders and the delivery ratio. Again, the goal of the ring schemes is to reduce the number of forwarders while ensuring a 100% packet delivery to the destination(s).

Table 4.9 shows the average numbers of forwarders and receivers per data packet for each case (three schemes and two protocols), and will be analyzed later.

Table 4.9: Evaluation results with 10 000 nodes averaged for 10 runs and 50 packets each.

	No ring	Original ring	Expanded ring
Pure flooding:			
Forwarders per packet	10 000	2747.3	1111.6
Receivers per packet	10 000	10 000	10 000
SLR:			
Forwarders per packet	901.6	213.2	123.8
Destination reached	100%	100%	98.8%

In order to reproduce the simulation results we provide a separate web site².

4.4.3.2/ EFFECT OF EXPANDED RING ON PURE FLOODING

We remind that in the original ring, the forwarding nodes are required to be on the ring of the first packet received. In contrast, the expanded ring restricts the forwarding nodes to nodes which are on the ring of **all** the packets received in a given time window w .

For pure flooding, the proposed expanded ring adds a restriction to the forwarders: a forwarder has to receive the data packet for the first time (as in pure flooding), but it also has to remain on the ring of all the packets for a given time window w .

Table 4.9 shows that the number of forwarders per packet decreases from 10 000 (without ring) to 2747.3 (with original ring) and to 1111.6 (with expanded ring), i.e., the expanded ring reduces the number of forwarders by 88.8% compared to traditional pure flooding and by 59.5% compared to original ring. Moreover, despite this large decrease in the number of forwarders, both ring schemes allow for the correct distribution of all data packets (100% destination reached).

Fig. 4.16 visually shows that the forwarders are better positioned at the border of communication ranges. The expanded ring clearly shows concentric rings around the source node, as envisioned in goal Figure. 4.14. Those rings are still imperfect as a consequence of the different backoffs before transmission used by transmitters, but are an acceptable trade-off.

²<http://eugen.dedu.free.fr/bitsimulator/iwcmc22>

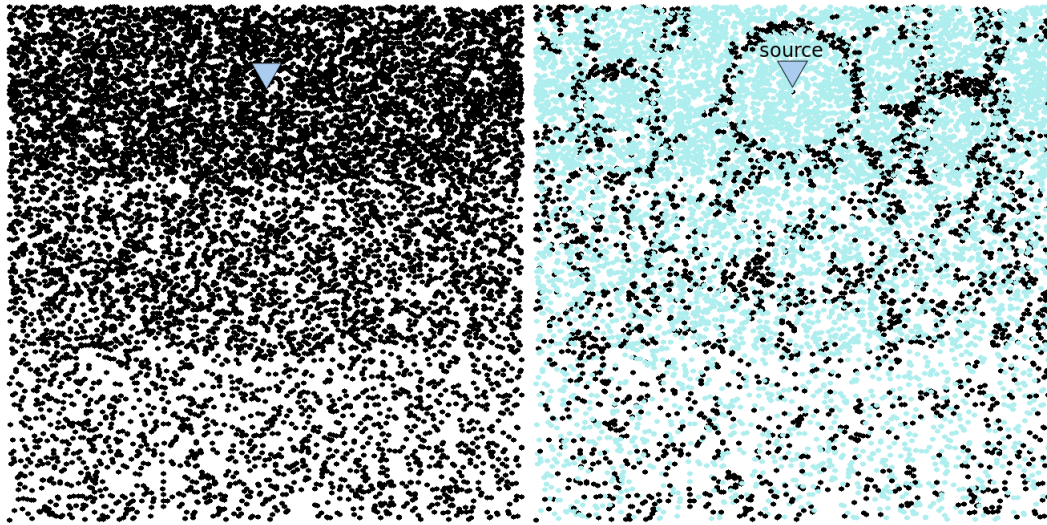


Figure 4.16: Pure flooding without ring (left) and with (right) the expanded ring for the first packet of the first run (forwarders are in black, receivers are in light blue).

4.4.3.3/ EFFECT OF EXPANDED RING ON SLR

A forwarder in the SLR with expanded ring must fulfill the following conditions: it receives the data packet for the first time, it is on the path between the source and destination (as required by SLR), and it is on the rings and never in inner discs for the specified time window w .

A very good reduction rate of 86% is seen in Table 4.9 for the number of forwarders per packet, going from 901 without ring to 123 for expanded ring. The expanded ring also improves the original ring by reducing the number of forwarders by 41.9% from 213.2 to 123.8. The delivery rate to the destination node for the expanded ring stays very high: 98.8%.

Fig. 4.17 shows much fewer forwarders for expanded ring (right) compared to without ring (left) along the path between the source and the destination nodes.

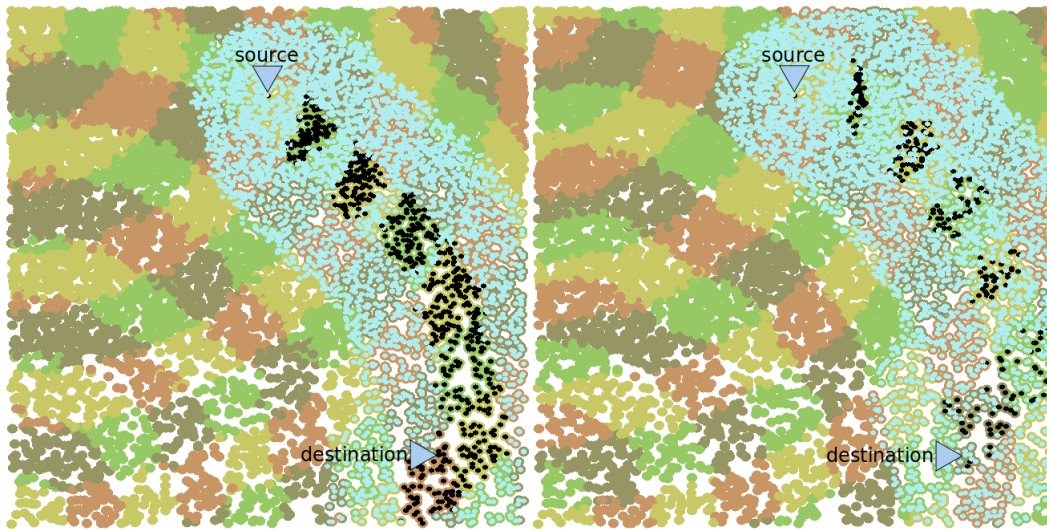


Figure 4.17: SLR without (left) and with (right) the expanded ring for the first packet for the first run (forwarders are in black, receivers are in light blue).

To summarize, the expanded ring scheme is better at selecting forwarders in multi-hop scenarios. When configured with an optimal ring width value, it greatly reduces the number of forwarders compared to traditional protocols (88% and 86% in the simulations).

4.4.4/ CONCLUSION OF EXPANDED RING

Section 4.3 presented the original ring scheme as a forwarder selection method using two control packets. The current Section 4.4 highlighted limitations of the original ring and presented an enhanced version called expanded ring. This version is a multi-hop optimization for the routing schemes in electromagnetic nanonetworks. The expanded ring scheme improves the original ring scheme by redefining nodes on the ring to only those which are always on the rings and never in the inner discs of forwarders having a lesser or equal hop count.

We implemented the expanded ring in BitSimulator, for two routing protocols (pure flooding and a destination-oriented protocol). The expanded ring shows an improvement of the routing protocols over many hops using the main metrics: the number and placement of forwarders, and the packet delivery rate. Forwarders are fewer and generally selected at the border of the communication ranges, which increases the forwarding progress. The packet delivery is successful.

4.5/ DYNAMIC RING SCHEME

4.5.1/ INTRODUCTION OF DYNAMIC RING

The original ring found in Section 4.3 is static. It works well in environments with a constant density of nodes (homogeneous). However, applying this scheme to different environments (for example dense and sparse ones), conducts to rings of the same width containing significantly different number of nodes. Therefore, this section proposes another enhancement to the original ring algorithm, called the *dynamic ring*, which makes nodes configure the ring width automatically, based on a desired number of local ring neighbors and the local density. The following work answers these questions: "How can the original ring adapt its width automatically in a heterogeneous environment? Based on what?".

4.5.2/ DYNAMIC RING

This section starts by discussing a parameter of the dynamic ring that is the number of ring neighbors per hop. This section then presents three dynamic ring methods. The first two acknowledgement methods are inefficient and thus the third method is selected.

In the new scheme, *rangeBig* is kept fixed and equal to the communication range to make the forwarding progress faster, while *rangeSmall* varies and makes the ring thinner or thicker. The challenge is to find the appropriate *rangeSmall* value. This value is inferred from the desired number of ring neighbors per hop, denoted by N . Finding the **optimal** (minimal) set of forwarders among the 1-hop neighbors is an NP complete problem. A recent research Maccari et al. (2018) finds the distributed minimum of MPRs selection in dense mesh networks. However, their definition of a dense network (up to 150 nodes) is still low compared to our own scenario (10 000 nodes), and as the method requires powerful hardware for mesh nodes and a sufficiently stable network, it cannot be applied in our context. The optimal value also depends on the routing protocol used and the desired redundancy. Finding the optimal value for various applications is out of the scope of this section. For now, we consider that the network user tests and finds a low, but sufficiently high value of ring neighbors N to guarantee delivery.

An efficient dynamic ring scheme executed by nodes takes into account the network's high density and the nanodevice's hardware constraints. However, one has to be careful when choosing a method to adjust the ring width. In the following, two acknowledgment methods are presented briefly and are shown to not be efficient in nanonetworks. They are followed by a dynamic ring method that is demonstrated to work in nanonetworks in Section 4.5.3.

First method: dynamic ring with implicit acknowledgment In this method, a forwarding node starts with any value for *rangeSmall*, and updates it based on the number of acknowledgments received compared to the required number N of forwarders. The considered (implicit) acknowledgments are the copies received by the node from forwarders belonging to its own forwarding ring. If the number of forwarders is equal to N , then the ring width is fine; whereas a smaller number of forwarders requires a thicker ring and vice-versa.

This evident method has two drawbacks. The first one is that N , a unique value for all nodes, only sometimes applies to **partial** rings. These partial rings do not contain “old forwarders”, i.e., nodes that have already seen the same data packet before and that will not retransmit it to avoid forwarding loops, as detailed in 4.3.1.1. For instance, in Fig. 4.18 (a), A is the first transmitter and its whole ring, including B, forwards. In Fig. 4.18 (b), showing the second hop, only the yet uncovered region of the ring of B, i.e., the pink region at right that has not yet received the data packet, will forward and will be counted as acknowledgments. Thus, the ring of B is much smaller than the ring of A, yet the value N erroneously applies for both of them. Subsequent images in the same Fig. 4.18 illustrate that, as the number of hops increases, the ring (the pink areas), that represent new forwarders at each hop and that are counted as acknowledgments, have smaller and smaller surfaces and number of nodes.

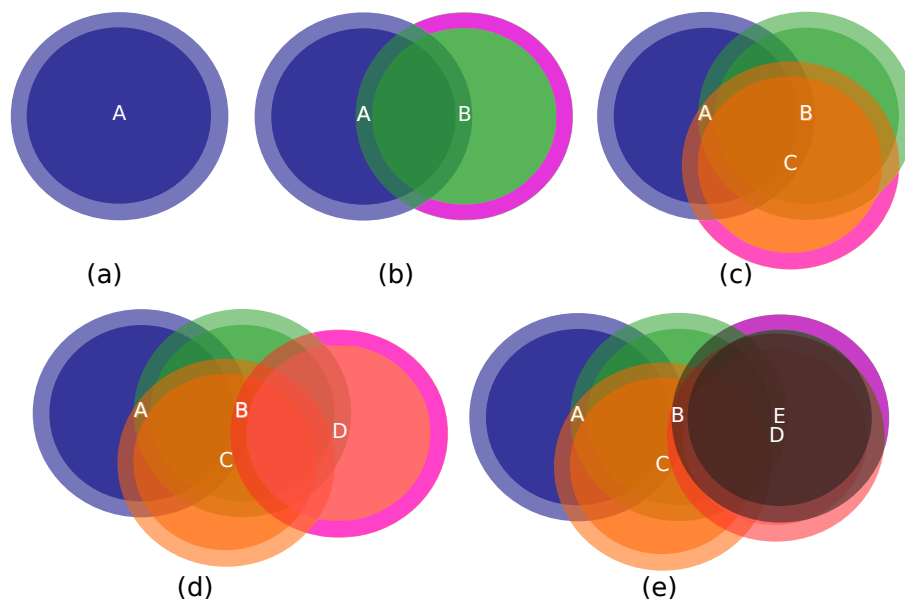


Figure 4.18: Drawbacks of dynamic ring with implicit ack: only the pink areas include new forwarders that will send the data packets counted as acknowledgments.

The second drawback is that a nanonode may not be able to count the acknowledgments, as they are in the order of hundreds. This is due to the high local density and the hardware constraints. The resource constraints of a nanonode in energy, memory and data pro-

cessing require the node to use large backoffs before transmission window at the MAC level to avoid further collisions.

Second method: dynamic ring with explicit acknowledgment To solve the misleading number of acknowledgments given by the previous method, the explicit acknowledgment method makes a ring neighbour (either forwarder or not), after receiving its data packet, generate a new control packet to be received by the transmitter for the acknowledgment counts. Still, this method suffers from another misleading ring neighbours count (instead of forwarders count), where ring neighbours with already seen data packets are ignored. Indeed, as shown in Fig. 4.19 (a), A is the first transmitter, B and C are ring neighbours of A and so they send their corresponding acknowledgments to it; again in Fig. 4.19 (b), B is the second transmitter, A and C need to send their corresponding acknowledgments to it, although A has already seen the data. Another problem with this method is the high traffic caused by the additional control packet, wasting energy and generating collisions.

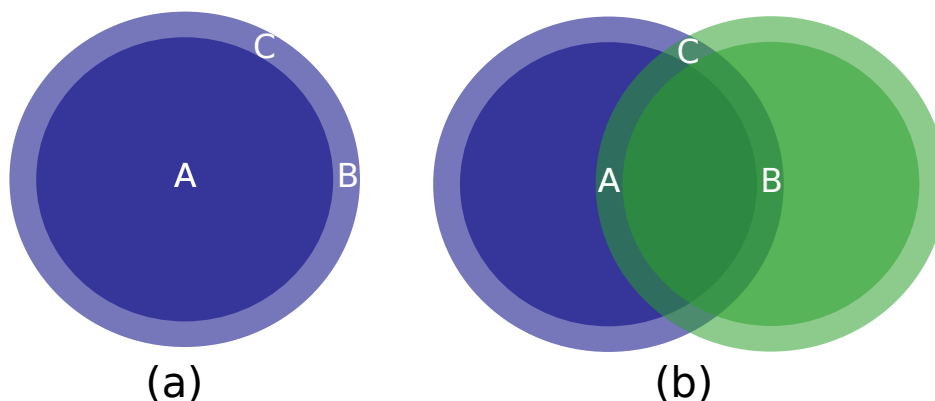


Figure 4.19: High traffic problem in dynamic ring width with explicit ack.

Third and selected method: dynamic ring using node density estimation The previous two methods have issues, hence they cannot be used to dynamically adjust the ring width. Here, we present the third method, the dynamic ring with DEDeN, which is the method we select for the dynamic ring.

This method takes as input the number N denoting the required ring neighbors per hop. During the network initialization, nodes perform the **local density** estimation using a density estimator. One such estimator is DEDeN Arrabal et al. (2018a), referenced in 2.2.1.

We fix N for all rings and let the ring adapt its width to the environment. In Fig. 4.20, $N = 5$ ring neighbors, which results in a thick ring in the sparse region and a thin ring in the dense region.

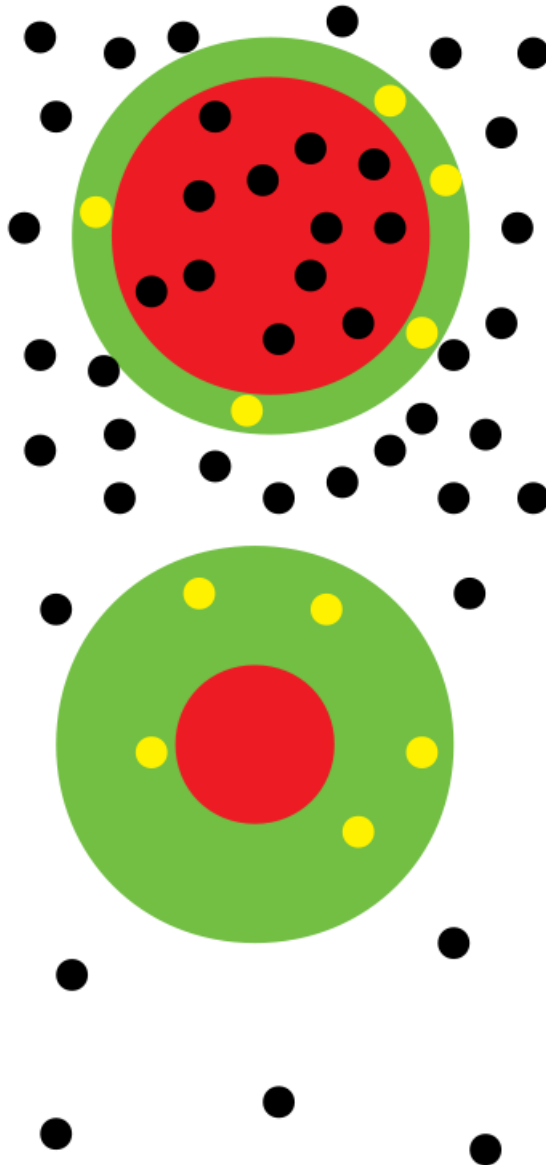


Figure 4.20: Simplified illustration of the dynamic ring: the ring adapts its width to the density to include 5 ring neighbors. Forwarders (yellow), nodes (black dots), rings (green) and inner discs (red).

We recall that $rangeBig$ is the communication range. Instead, $rangeSmall$ corresponds to the desired number of ring neighbors. Hence, the ratio of ring neighbors N to the neighbors L (= local density above) should be equal to the ratio of the ring to the communication circle:

$$N/L = RingArea/circleArea \quad (4.1)$$

$$N/L = \pi(rangeBig^2 - rangeSmall^2)/(\pi rangeBig^2) \quad (4.2)$$

hence

$$rangeSmall = \sqrt{rangeBig^2 - N * rangeBig^2 / L} \tag{4.3}$$

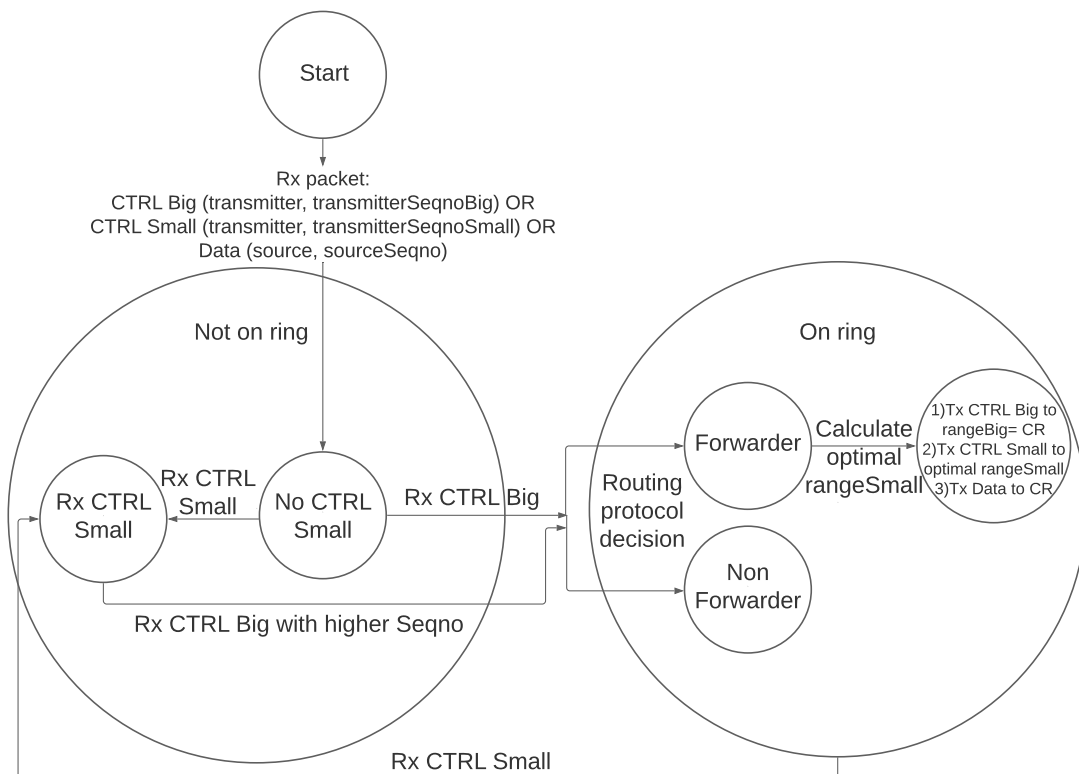


Figure 4.21: State diagram for dynamic ring with DEDeN: node states based on packet reception from one transmitter.

The ring computation is presented in Algo. 3 and the state diagram (Fig. 4.21) represents the dynamic ring. The *rangeSmall* value is set directly using a formula. It works also for heterogeneous networks (node densities are different in different parts of the network) and for different propagation models (e.g., unit disc and shadowing models). However, if the topology changes with time, the local density changes too, and thus *rangeSmall* needs to be recomputed during runtime.

Algorithm 3: Dynamic ring width with DEDeN.

Data: N = desired number of ring neighbours per node L = number of neighbours per node = local density $rangeBig$ = default communication range

sourceID = identifier of source node (first transmitter node)

transmitterID = identifier of current transmitter node

seqNo = sequence number

ctrlBigSeqNo = seqNo of high-power control packet = 0

ctrlSmallSeqNo = seqNo of low-power control packet = 0

dataSeqNoMap = [sourceID, seqNo]

amIOnRingMap = [transmitterID, ctrlBigSeqNo, ctrlSmallSeqNo]

countAckMap = [sourceID, seqNo, rangeSmall] needToSendControl = true

Result: Find appropriate ring width for forwarders

```

1 Upon packet reception (type, sourceID, seqNo, transmitterID)
2 if type is DATA then
3   if dataSeqNoMap[sourceID] does not exist OR dataSeqNoMap[sourceID] <
   seqNo then
4     // no packet has been seen from this source before OR seqNo of
   this packet is higher than the highest already seen seqNo from
   this source
5     dataSeqNoMap[sourceID] = seqNo // insert new sourceID OR update
   the highest already seen seqNo from this source
6     if call amIOnRing AND routing protocol selects me as forwarder then
7       call forwardDataPackets
8     end
9   end
10 else if type is CONTROL-BIG then
11   ctrlBigSeqNo[transmitterID] = seqNo
12 else if type is CONTROL-SMALL then
13   ctrlSmallSeqNo[transmitterID] = seqNo
14 bool function amIOnRing
    // I am on the ring if: (I received controlBig from this transmitter
    and did NOT receive controlSmall from the same transmitter) OR (I
    received controlBig from this transmitter with higher seqNo than
    controlSmall)
15 return (ctrlBigSeqNo[transmitterID] exists AND ctrlSmallSeqNo[transmitterID] does
    not exist) OR (ctrlBigSeqNo[transmitterID] > ctrlSmallSeqNo[transmitterID]);

```

```

15 function forwardDataPacket
    // N/L = RingArea/circleArea
16 rangeSmall =  $\sqrt{\text{rangeBig}^2 - N * \text{rangeBig}^2 / L}$ 
17 if needToSendControl then
18     send ControlBig to rangeBig
19     send ControlSmall to rangeSmall
20     needToSendControl = false
21 send Data
22 if countAckMap[sourceID,seqNo] not found in countAckMap then
23     insert [sourceID, seqNo, rangeSmall] in countAckMap // use same rangeSmall
        for all packets from the same source or for only one packet seqNo

```

4.5.3/ EVALUATION OF DYNAMIC RING

This section presents how the dynamic ring with DEDeN is applied to four routing protocols: pure flooding, probabilistic flooding, backoff flooding and SLR, and how they compare to traditional routing protocols.

4.5.3.1/ SCENARIOS

The scenario is the same as Section 4.4, we repeat it in Table 4.10. Again, a source node in the top of the network generates a CBR flow of 50 packets. The source either floods the whole network, or transmits to one destination node (found in the bottom). Since a node sends controls only once before the very first forwarded data packet, the cost of the control packets fades out over 50 data packets.

Table 4.10: Simulation parameters.

Parameter	Value
Size of simulated area	6 mm * 6 mm
Number of nodes	10 000
Communication range	1 000 μ m
RangeBig	1 000 μ m
RangeSmall	variable
Data packet size	1 003 bit
Control packet sizes	101, 102 bit

RangeBig is set to the default communication range (to increase the forwarding progress),

and `rangeSmall` value is dynamically chosen by nodes depending on the local density, according to Eq. 4.2.

The dynamic ring proposed algorithm is implemented in three flooding schemes: pure flooding, probabilistic flooding and backoff flooding, and one destination-oriented scheme: SLR. For backoff flooding, the maximum number of data copies received in a time window must not exceed 2 packets in order for the node to forward (*redundancy* = 2). For probabilistic flooding, nodes forward packets with a static probability *proba* and discard it otherwise. The probability value is set to the minimum probability that gives 100% delivery in each scenario that is 6% for without the ring and 10% with dynamic ring (found through testing).

The dynamic ring scheme starts with the DEDeN initialization phase in order for nodes to know their local density and compute their `rangeSmall` values. We recall that DEDeN initialization can be repeated when the network changes its topology. The CBR flow starts after the DEDeN and SLR initialization phases, to not interfere with them.

Again, we avoid forwarding loops 4.3.1.1, as seen in Algo. 3.

The evaluation uses the 4 routing protocols above with 2 variants each (without the ring and with dynamic ring), and for 10 different random number generator seeds for the back-off time before transmission. This results in 80 simulations with 50 data packets each.

Dynamic ring with DEDeN We recall that in the dynamic ring, the ring is set at the start (at the first data packet) as in the original ring. Afterwards, the dynamic ring uses density information from DEDeN density estimator to automatically adapt the ring width (`rangeSmall`) in order to include N ring neighbors in the ring per hop. In the particular case where the local density is smaller than N , the `rangeSmall` value is set to zero and all neighbors become ring neighbors. For the following simulations, we use $N = 60$ for all the routing protocols. This value includes non-forwarders and forwarders; non-forwarders are not only nodes that previously forwarded a copy of the data packet, but also nodes that are not chosen by the routing scheme to forward.

Table 4.11 shows the final comparison of the average values of the 10 runs with 50 packets each for all the different combinations of the routing schemes. The web site³ regenerates results along with simulation's description.

³<http://eugen.dedu.free.fr/bitsimulator/nanocom22>

Table 4.11: Evaluation results in a 10 000 node network averaged for 10 runs and 50 packets each.

	Without ring	With dynamic ring
Pure flooding:		
forwarders per packet	10 000	1 949.2
receivers per packet	10 000	10 000
Probabilistic flooding:		
	<i>proba</i> = 6%	<i>proba</i> = 10%
forwarders per packet	601.59	273.512
receivers per packet	9 999.9	9 999.47
Backoff flooding:		
forwarders per packet	79.934	52.242
receivers per packet	9 999.97	9 999.55
SLR:		
forwarders per packet	901.688	129.116
Destination reached	100%	100%

4.5.3.2/ EFFECT OF DYNAMIC RING ON PURE FLOODING

Fig. 4.22 confirms that the dynamic ring assigns indeed ring widths (*rangeSmall*) to nodes, depending on their local density. The higher the density, the higher the *rangeSmall* value is, and the thinner the ring width is. When the local density is very high, the *rangeSmall* value approaches the communication range (10^6 nm). However, when the density ≈ 120 (that is double the number of ring neighbors), the *rangeSmall* value is approximately half the communication range.

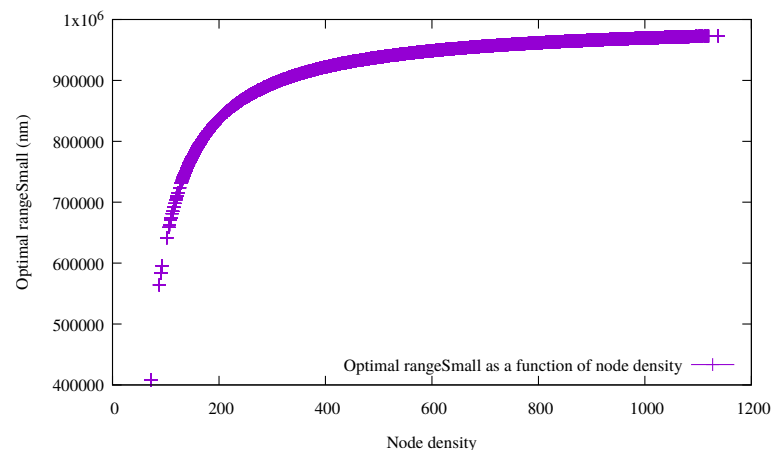


Figure 4.22: The dynamic ring with DEDeN in pure flooding assigning different *rangeSmall* values for nodes depending on their density.

Table 4.11 also confirms the expectations: the number of senders per packet is reduced by 80%, from 10 000 to 1949.2, with 100% delivery rate. Fig. 4.23 shows the placement of the forwarders on rings.

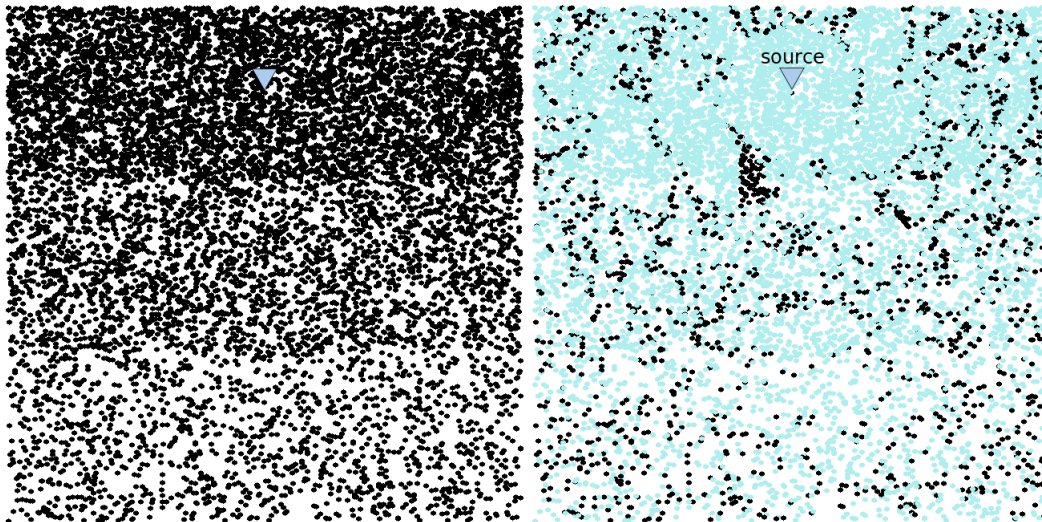


Figure 4.23: Pure flooding without (left) and with the dynamic ring with DEDeN (right); forwarders in black, receivers in blue, first packet of the first run only.

4.5.3.3/ EFFECT OF DYNAMIC RING ON PROBABILISTIC FLOODING

In probabilistic flooding, dynamic ring neighbors become forwarders if they receive the data packet for the first time and if their generated random probability is less than the static probability *proba*.

Table 4.11 shows that the probabilistic dynamic ring is efficient in reducing the number of forwarders per packet by 54% from 601 to 273, while the delivery rate is of 99.9%. Fig. 4.24 shows the difference in the placement of forwarders from random (left) to on rings (right).

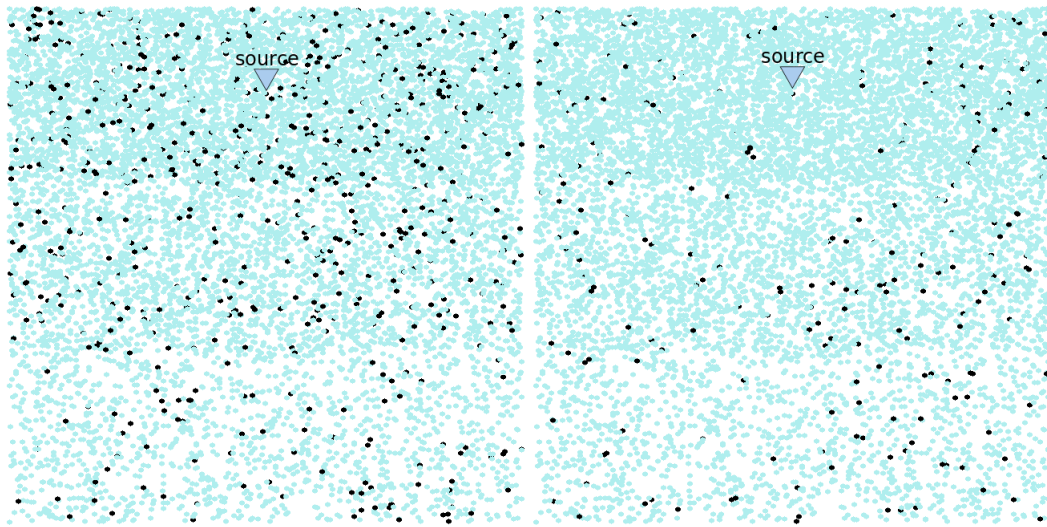


Figure 4.24: Probabilistic flooding without (left) and with the dynamic ring with DEDeN (right); forwarders in black, receivers in blue, first packet of the first run only.

4.5.3.4/ EFFECT OF DYNAMIC RING ON BACKOFF FLOODING

The dynamic ring improves backoff flooding as seen in Table 4.11, where the number of relay nodes per packet decreases by 34% (from 79.9 to 52.2), with almost all nodes receiving the packet (99.99%). Fig. 4.25 shows fewer and better placed forwarders with the dynamic ring (right) compared to no ring (left). This is an exceptional result, given that backoff flooding is already a highly efficient flooding.

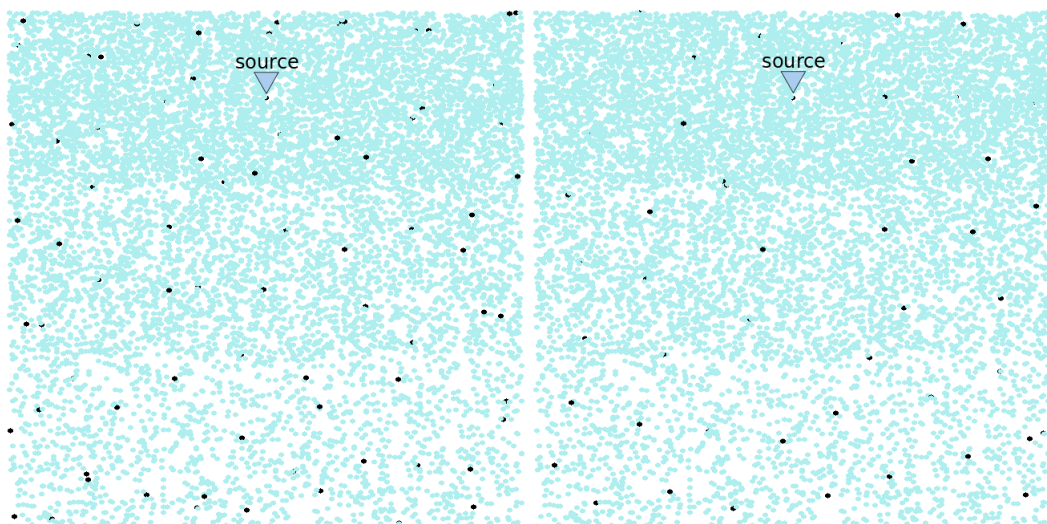


Figure 4.25: Backoff flooding without (left) and with the dynamic ring with DEDeN (right); forwarders in black, receivers in blue, first packet of the first run only.

4.5.3.5/ EFFECT OF DYNAMIC RING ON SLR

Table 4.11 shows that the number of forwarders is reduced by 85%, from 901 (without the ring) to 129 (with the dynamic ring), while keeping 100% successful packet delivery. Fig. 4.26 visually shows this reduction and the optimized placement of forwarders on border of ranges.

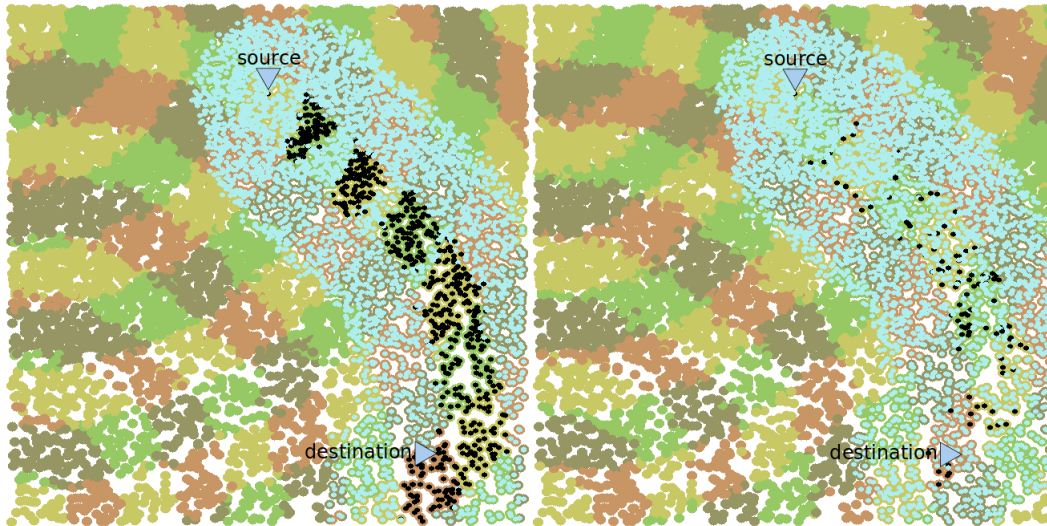


Figure 4.26: SLR without (left) and with the dynamic ring with DEDeN (right); forwarders in black, receivers in blue, first packet of the first run only.

To conclude, the dynamic ring allows to optimize all the presented routing protocols by choosing a ring width value. The dynamic ring selects forwarders on border of communication ranges in rings and significantly reduces the number of forwarders per packet while keeping 100% delivery rate to the destination(s).

4.5.4/ CONCLUSION OF DYNAMIC RING

Section 4.5 presents an optimization for the routing schemes in dense nanonetworks, using an improved method of the ring: the dynamic ring. Classical acknowledgment methods that count the number of acknowledgments from the original ring to update its width, are proved not to work in the context of electromagnetic nanonetworks.

The dynamic ring scheme with a density estimator automatically selects a ring width value for each node. The scheme is implemented in BitSimulator below four routing protocols: three flooding schemes and one destination-oriented scheme. The results are compared using two metrics: the number and placement of forwarders and the packet delivery rate. They show that the scheme generally selects forwarding nodes found at the

border of communication ranges and reduces the number of forwarders per packet, while maintaining a successful packet delivery.

4.6/ CONCLUSION

The first contribution of this dissertation is summarized here. The ring, in all of its forms, is an interesting approach that can be integrated into existing routing protocols, in order to make them behave efficiently in (resource-constrained) ultra-dense networks. Three variants of the ring were presented and analyzed. The original ring defines a simple ring at each forwarder. In the expanded ring, the multi-hop nature of the ring is enhanced and forwarders are rather placed in the rings and never in the inner discs. The dynamic ring thins or thickens the ring depending on the local density of the forwarder. In all the presented results, the rings show a great deduction of the number of forwarders, with a successful packet delivery.

TRANSPORT LAYER: BETA PARAMETER IN NANONETWORKS

5.1/ INTRODUCTION

In electromagnetic nanonetworks, the nanoscale, the THz band and the dense deployment of nodes call for the design of novel protocols for all the network layers. Unfortunately, recent research has focused on designing routing protocols for nanonetworks, while neglecting the transport layer.

For the physical layer, some modulation schemes have been proposed, especially TS-OOK and its variant RD TS-OOK, that we previously discussed in detail in 2.2.2.2. The problem with TS-OOK is that selecting the optimal symbol rate $\beta = T_s/T_p$ Jornet and Akyildiz (2014) is complex. If $\beta = 1$, all the symbols of a nanodevice are transmitted in burst and only one nanodevice can access the channel at a time. When we increase β , multiple nanodevices can access the channel simultaneously and the throughput of each of them is thus reduced Aliouat et al. (2021).

Pulses (bits 1) have a short duration of $T_p=100$ fs to reduce the probability of collisions Pujol et al. (2011). Using a big time between pulses T_s allows receivers to decode each T_s instead of sensing the channel continuously. A big T_s also permits for multiple nanodevices to transmit simultaneously over the THz channel, and for receiver to receive packets in parallel, and that is different from the sequential nature of receptions at the macroscale communications. When received, bits from different transmitters may overlap in time and collide. Contrarily to macroscale communications, in nanonetworks catastrophic collisions only occur when the bit 0 is replaced by a bit 1, and hence some data packets are altered along the route Dhoutaut et al. (2018).

To minimize collisions Pujol et al. (2011), RD TS-OOK makes each transmitting node select its own β randomly from a pool of co-prime rate codes, instead of using the same rate for all nodes as in TS-OOK. β value is included in the transmitting Data Symbol Rate

(DSR) field in the Transmission Request (TR) packet generated by the transmitter during the handshaking process in the MAC protocol PHLAME Pujol et al. (2011).

Congestion in THz nanonetworks is worth studying since it becomes severe in ultra-dense networks. As seen later, congestion (large number of ignored packet events) in Table 5.2 causes packet loss in Table 5.3. In nanonetworks, the low-power nanonodes are unable to consume the wide THz bandwidth as they send short pulses of $T_p=100$ fs, hence congestion does not arise from the large THz shared channel. Instead, the congestion arises from the **limited buffers of nodes**, and that it is determined at the node level by measuring the buffer level: when the number of packets being received by a node exceeds its capacity, the node is congested Arrabal et al. (2019). In other words, congestion is the buffer overflow and collision is packets with bits that have been altered. The main source of congestion and collision is the high number of communicated packets, which goes back to the high number of forwarders. Forwarders may be condensed in the same flow, as in inefficient routing protocols. They could be at the intersection of many flows, which form a congestion zone.

The contribution of this chapter is to draw the reader's attention to carefully select appropriate values for β (and thus the modulation scheme) and for the source packet rate, as they affect the congestion and collisions, in order to achieve a good delivery ratio with less costs.

In the rest of this chapter, Section 5.2 presents the related work. Section 5.3 selects the simulation software and describes the scenario. Section 5.3.2 analyzes the results of the simulations. Finally, Section 5.4 concludes the chapter.

5.2/ RELATED WORK

We first present works on congestion control in nanonetworks, then in the broader field of wireless sensor networks, and finally in classical IP networks.

In general, congestion control mechanisms can be divided into two categories: traffic control by limiting the transmissions (decreasing source rate or congested nodes rate, etc.), and resource control by turning-on network resources (alternative routes, duty cycling, etc.) Kafi et al. (2014).

The transport layer of THz **nanonetworks** remains largely unexplored. We found only two articles on congestion control in electromagnetic nanonetworks. One is congestion control by deviation routing, where data packets deviate from the original route to avoid the congestion zone Arrabal et al. (2019). The other is an energy-efficient transport layer protocol for electromagnetic and molecular body area nanonetwork, where the sender upon receiving a "halt" signal stops the packet transmission for a predefined time Alam

et al. (2017); this scheme uses routing tables in a low density scenario (up to 100 nodes), so it is unfeasible in ultra-dense scenarios.

Nanonetworks, on the other hand, share similar aspects with WSNs. In a survey on WSNs Kafi et al. (2014), some protocols use the source packet rate for congestion control: FUSION combines multiple congestion control techniques and one is source limiting where the hop-by-hop back-pressure reaches the source to decrease its rate Hull et al. (2004). This scheme is costly in ultra-dense nanonetworks, as it generates a new traffic and consumes the energy and memory resources of nanodevices. The Congestion Detection and Avoidance in Sensor Networks (CODA) is a protocol where the source waits for constant acknowledgments from the sink using “regulate bit” in event packets Wan et al. (2011). The dense deployment of nanonodes makes CODA costly as well (high network traffic). In the context of nanonetworks, the relationship between the source rate and congestion is not studied. In this chapter, we do not propose a dynamic source packet rate congestion control, but rather study the influence of source rate on congestion in the context of THz nanonetworks. It is also important to recall that the congestion in nanonetworks is caused by the limitations of a nanodevice and the dense deployment of nodes, and not from the (THz very wide) band channel. Also, in an ultra-dense nanonetwork, a nanonode cannot maintain full neighborhood or network knowledge, and the location information may not be available given that embedding hardware modules (such as GPS and RSSI) is complex at the nanoscale. This is different from macroscale wireless networks and this makes traditional congestion control mechanisms unfeasible in THz nanonetworks.

Finally, in **IP networks**, when packets are lost, TCP controls the congestion by limiting the traffic at the source. ECN, that extends TCP/IP, makes intermediate routers mark packets in a pre-congestion phase, to also decrease the source traffic Ramakrishnan et al. (2001).

Pulse-based modulations in the THz band, found in 2.2.2.2, use the symbol rate β . We propose to adjust the β value along with source packet rate to control congestion and collisions in THz nanonetworks.

To the best of our knowledge, this is the first paper that addresses the relationship between β and congestion.

5.3/ SIMULATION

5.3.1/ SCENARIOS

We assume that nanonodes are homogeneous: they all radiate the same power and share the same characteristics of processing power and energy. Another assumption is

that nanoantennas are omnidirectional.

Table 5.1 presents the simulation parameters that we selected for the scenario. The scenario describes a 2D nanonetwork of 20 000 nodes distributed in a square area of 36 mm², over 3 horizontal equal bands of different densities: 10 000, 6000 and 4000 nodes per band, as seen in Fig. 5.1.

Table 5.1: Simulation parameters.

Parameter	Value
Size of simulated area	6 mm * 6 mm
Number of nodes	20 000
Communication range	900 μ m
Data packet size	1000 bit
Number of flows	5
Number of packets per flow	100
Routing protocol	SLR backoff
Communication range for SLR addressing phase	250 μ m
Backoff redundancy	20
MCR	3
Pulse duration T_p	100 fs
MaxBitError	0

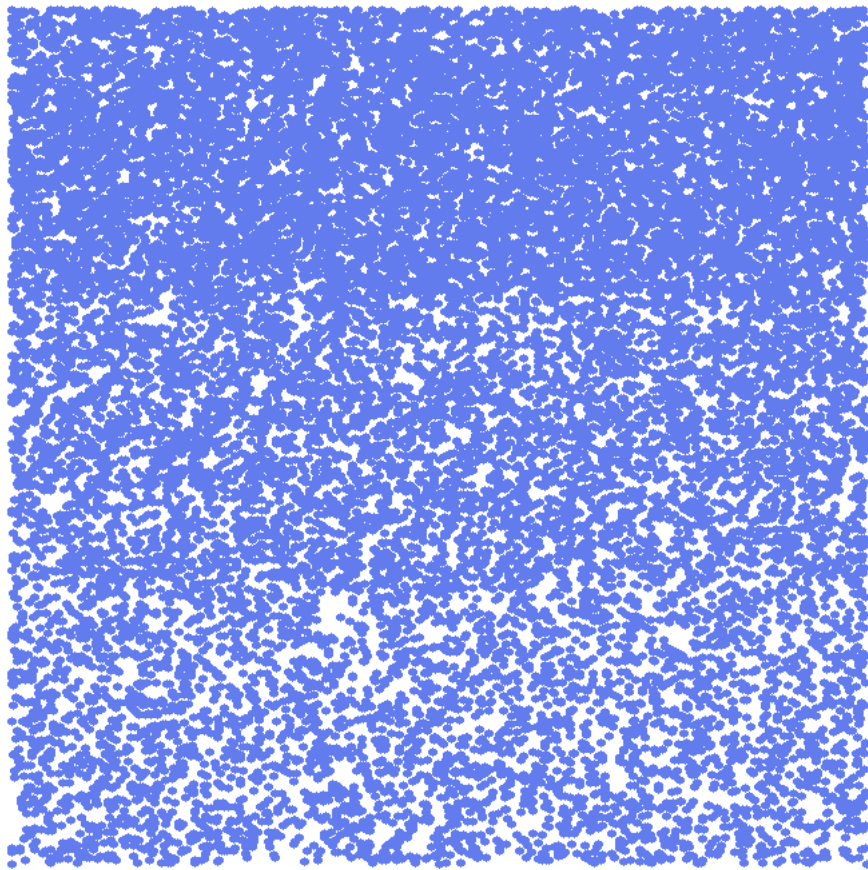


Figure 5.1: Nodes distribution in the network (without routing).

The communication range is $900\ \mu\text{m}$, and hence the multi-hop communications are done over $6\ \text{mm}/900\ \mu\text{m} \approx 6.6$ hops in each dimension. Nodes use the normal shadowing propagation model 21.

5 CBR flows (source-destination pairs) exist in the scenario, shown in blue in Fig. 5.2. Each source nodes emits 100 packets (of 1000 bits each) to its corresponding destination node, thus avoiding statistical bias. The 100 packets differ in their random backoff time before transmission, that depends on the node's local density. Source nodes start emitting at the same time. Destination nodes are close to each other so they form a destination zone where the 5 flows intersect and cause a congestion zone. We use the best unicast routing scheme, SLR backoff Arrabal et al. (2019), where two routing protocols (SLR and backoff flooding) are merged.

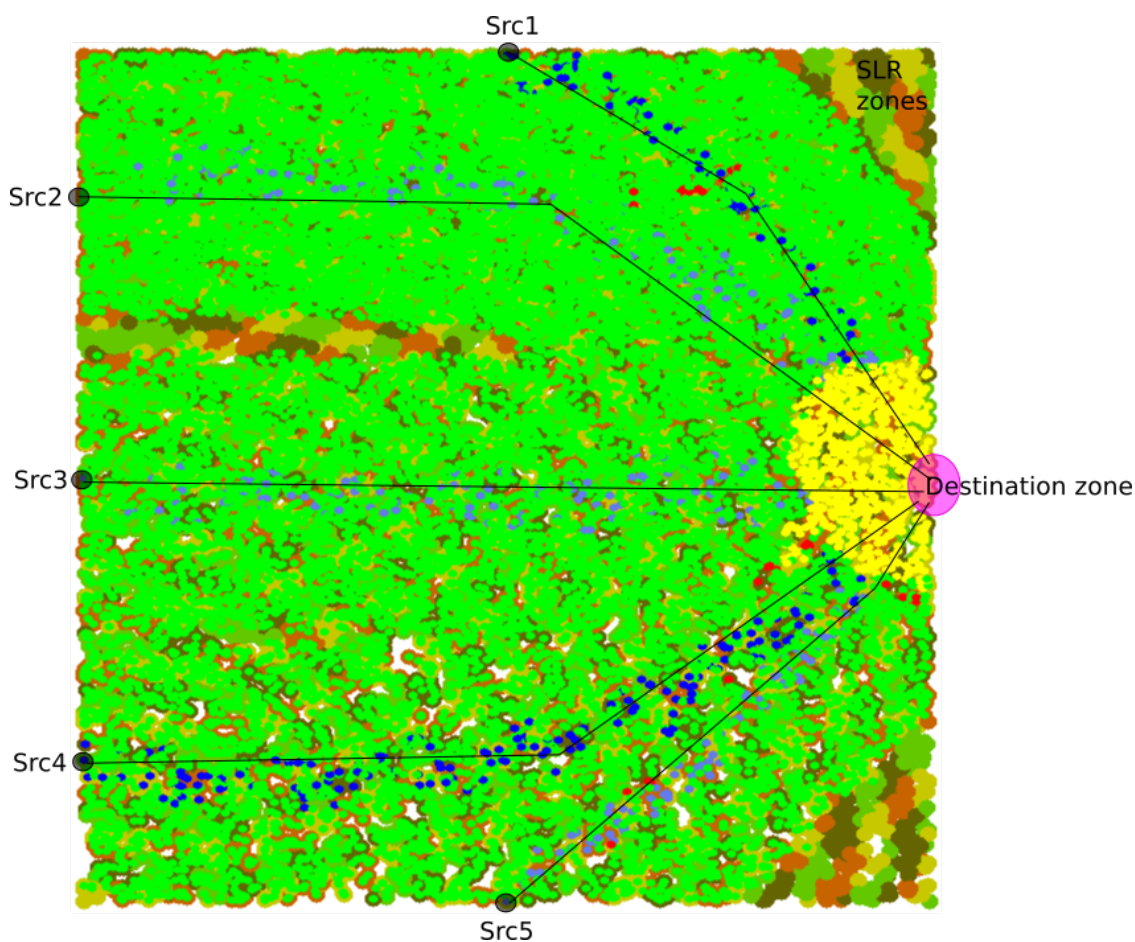


Figure 5.2: Scenario with $\beta=1000$ and source inter-packet interval= 10^5 ns: 5 flows intersecting at destination zone causing a congestion zone (right). Only first packet of each flow is shown. Forwarders are in blue, receivers in green, nodes with ignore in yellow, and nodes with collisions in red. SLR zones in the background.

In the SLR backoff protocol, forwarding nodes are on the path between the source and destination (as in SLR) and have also received less than N data copies in the time window (as in backoff flooding). We set the backoff redundancy N (the number of copies) to 20 to ensure good delivery to the destination(s) and to create congestion. During the SLR addressing phase, nodes only use a fraction of their sending power, and hence a smaller communication range of $250 \mu\text{m}$, creating SLR mini-zones, i.e., zones smaller than communication range.

Similarly to other work, forwarders relay packets they receive the first time 4.3.1.1.

We recall all the node's constraints by the parameter MCR (3.3.1).

We remind that MaxBitError as the maximum number of altered bits in a collided packet before it is considered damaged and is discarded (3.3.1). The rationale is that error correction codes, such as SBN (Simple Block Nanocode for nanocommunications) Zainuddin et al. (2016), can correct up to a given number of bits per packet. Also, we consider

that not all collisions are destructive: only bits 0 colliding with bits 1 are altered (cf. “there are no collisions between silences, and collisions between pulses and silences are only harmful from the silence perspective” Pujol et al. (2011)).

For regeneration of results: please check¹.

5.3.2/ EFFECT OF BETA AND PACKET RATE ON NANOCOMMUNICATIONS

In order to study the effects of the symbol rate β and source packet rate (or alternatively source inter-packet interval) on communication, three metrics are used: the number of ignore events, the number of collision events, and the percentage of delivery at each destination node. The source inter-packet interval sets the time between the sending of the first bit of two consecutive packets and can be modified only if the application permits it.

We change β for all nodes in the routing phase only (for data packets only). This is because modifying β in the SLR and DEDeN initialization phases results in different SLR zones and local densities respectively, and causes a faulty comparison, as multiple variables are being changed simultaneously; in these two initialization phases we set β to 1000, a value given in the literature (“the ratio between the time between pulses and the pulse duration is kept constant and equal to $\beta = 1000$ ” Jornet and Akyildiz (2014)).

The packet generated by the source crosses multiple hops and is retransmitted by many forwarders to get to the destination. This makes nodes receive the same packet multiple times (the first received packet and its copies). A large number of nodes (along the path between the source-destination pairs) receive the data packets and their copies, and thus a huge number of packets are processed, some of them may be ignored, collided or received successfully. Each event generated in the simulations corresponds to one data copy of one node, which further explains the high number of events in Table 5.2.

5.3.2.1/ EFFECT OF SYMBOL RATE BETA AND SOURCE PACKET RATE ON IGNORE AND COLLISION

Table 5.2 shows how different combinations of β and source packet rate affect the number of ignore and collision events. For instance, the same source inter-packet interval of 100 000 ns for node β values of 100, 1000 and 10 000 causes 74 070, 88 138 and 3 980 873 ignore events, and 418 553, 45 139 and 19 718 collisions, respectively. In other words, the lower the β value, the lower the number of ignores and the higher the number of collisions. This is also seen in Fig. 5.3, where $\beta=100$ exhibits fewer ignores at the congestion zone (yellow) and more collisions (red) than $\beta=1000$, in Fig. 5.2. The explana-

¹<http://eugen.dedu.free.fr/bitsimulator/icpads22>

tion of this result is that when reducing β , the time between pulses T_s is reduced too, and symbols are processed faster and thus packets get out faster from buffers (lower ignores). Smaller values of β also mean that fewer simultaneous transmitters share the channel, but more collisions occur at the receiver because symbols of multiple packets are likely to overlap in time.

Table 5.2: Number of ignore and collision events for 5 flows of 100 packets each in a network of 20 000 nodes.

	Ignore events	Collision events
$\beta=10$:		
source inter-packet=10 ns	9 352 176	17 097 957
$\beta=100$:		
source inter-packet= 10^2 ns	7 334 666	1 687 428
source inter-packet= 10^3 ns	4 339 230	2 023 881
source inter-packet= 10^4 ns	105 023	471 747
source inter-packet= 10^5 ns	74 070	418 553
source inter-packet= 10^6 ns	74 070	418 553
$\beta=1000$:		
source inter-packet= 10^3 ns	6 658 649	161 758
source inter-packet= 10^4 ns	3 819 608	198 475
source inter-packet= 10^5 ns	88 138	45 139
source inter-packet= 10^6 ns	82 603	41 179
$\beta=10\,000$:		
source inter-packet= 10^3 ns	9 277 891	11 843
source inter-packet= 10^4 ns	7 109 044	14 494
source inter-packet= 10^5 ns	3 980 873	19 718
source inter-packet= 10^6 ns	93 691	4 544

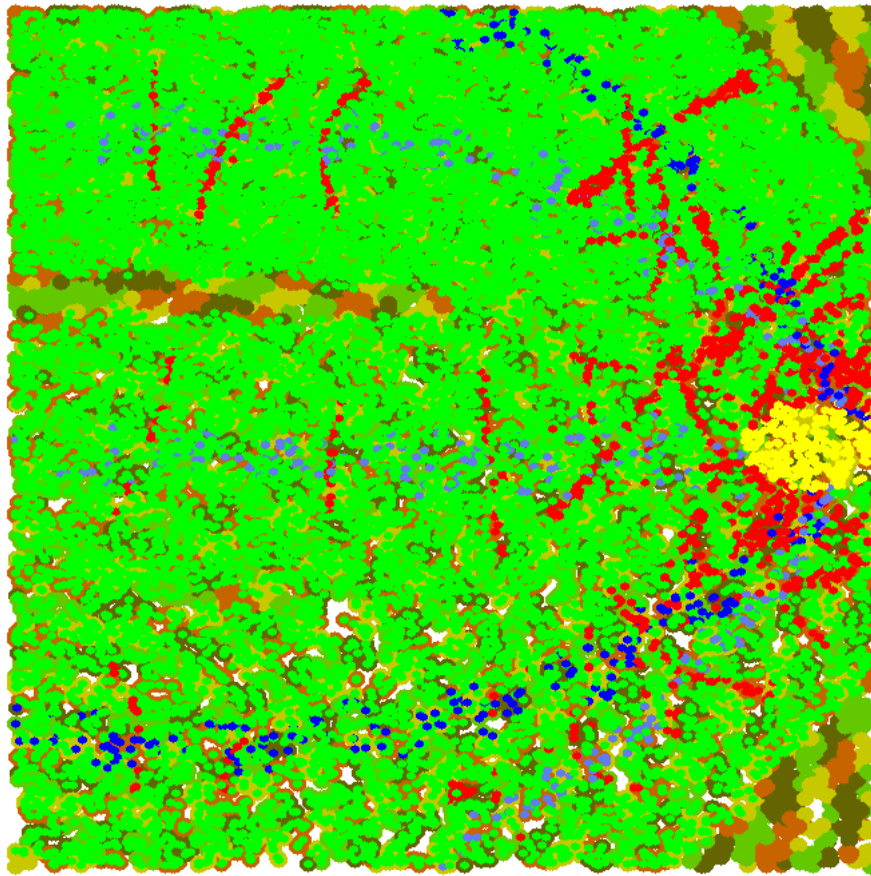


Figure 5.3: Scenario used, with $\beta=100$ and source inter-packet interval= 10^5 ns. Only first packet of each flow is shown.

In the same Table 5.2, for a given β value, 1000 for example, for different source inter-packet intervals, of 1000, 10 000, 100 000 and 1 000 000, the number of ignores are respectively: 6 658 649, 3 819 608, 88 138 and 82 603, and collisions are 161 758, 198 475, 45 139 and 41 179. This means that lower values for the source inter-packet interval induce higher ignore and higher collisions, as expected because of the high number of packets present in the network, which fills buffers faster and leads to higher chances of collisions as bits from many packets are likely to collide.

To sum up, lower β values increase the chances of collisions, but reduce the congestion (buffer overflow), and vice-versa; lower source inter-packet intervals stimulate congestion and collisions, and vice-versa.

5.3.2.2/ EFFECT OF BETA AND SOURCE PACKET RATE ON PACKET DELIVERY

A 100% (full) packet delivery is achieved when the destination receives the 100 packets from its corresponding source.

Table 5.3 shows the delivery percentage at each of the five destination nodes. When

comparing with Table 5.2, we can conclude that the symbol rate/source packet rate pair that results in high levels of ignores (in the scale of million events) makes the destinations lose some packets. Packet collision is more tolerated than packet ignore, as certain packets can be altered along the route, but others arrive successfully to the destinations.

Table 5.3: Percentage of packet delivery by each destination node for 5 flows of 100 packets each in a network of 20 000 nodes.

Destination	1	2	3	4	5
$\beta=10$:					
source inter-pkt=10 ns	13%	18%	18%	13%	15%
$\beta=100$:					
source inter-pkt= 10^2 ns	21%	21%	22%	13%	18%
source inter-pkt= 10^3 ns	82%	88%	84%	76%	75%
source inter-pkt= 10^4 ns	100%	100%	100%	100%	100%
source inter-pkt= 10^5 ns	100%	100%	100%	100%	100%
source inter-pkt= 10^6 ns	100%	100%	100%	100%	100%
$\beta=1000$:					
source inter-pkt= 10^3 ns	17%	21%	20%	13%	15%
source inter-pkt= 10^4 ns	77%	82%	88%	76%	79%
source inter-pkt= 10^5 ns	100%	100%	100%	100%	100%
source inter-pkt= 10^6 ns	100%	100%	100%	100%	100%
$\beta=10\ 000$:					
source inter-pkt= 10^3 ns	5%	4%	4%	3%	5%
source inter-pkt= 10^4 ns	17%	21%	19%	19%	16%
source inter-pkt= 10^5 ns	78%	88%	90%	74%	77%
source inter-pkt= 10^6 ns	100%	100%	100%	100%	100%

In other words, the high congestion induced by non-optimal selected values for β and source rate prevents packets to reach the destination(s).

5.3.2.3/ EFFECT OF DYNAMIC BETA ON IGNORE, COLLISION AND PACKET DELIVERY

In TS-OOK modulation, all the nodes use the same β value, of 1000 in our simulations; given that the distance between two consecutive bits is the same, packets which collide in one pulse collide in all pulses Pujol et al. (2011); Shrestha et al. (2016). In contrast, in RD TS-OOK, a variant of TS-OOK, transmitters select their own β , randomly from co-prime numbers, aiming to minimize the chances of collisions per packet Pujol et al. (2011). We have implemented this part of RD TS-OOK in BitSimulator and assigned to each node a random number from three choices right before each transmission, i.e., a dynamic β .

The three choices are taken from the literature: 1009, 1013 and 1019 (“the RD TS-OOK symbol rates are randomly chosen by each node from a pool of pairwise co-prime rate codes in the order of 1000 (e.g., 1009, 1013, 1019)” Pujol et al. (2011)). We chose values close to 1000 also because we want to test the dynamicity, and not the different value of β . As a corollary, given that β values are bound to nodes, this means that a packet is transmitted with **different** β as it is routed from node to node.

Table 5.4 presents the influence of dynamic β (TS-OOK and RD TS-OOK) on ignore, collision and packet delivery.

Table 5.4: Comparison results between TS-OOK and RD TS-OOK for 5 flows of 100 packets each in a network of 20 000 nodes.

	Ignore	Collision	Delivery to dest
source inter-packet= 10^5 ns			
TS-OOK $\beta=1000$:			
MaxBitError=0	88 138	45 139	100%
MaxBitError=5	83 756	46 014	100%
RD TS-OOK (dynamic β):			
MaxBitError=0	102 820	1 756 377	100%
MaxBitError=5	99 909	30 610	100%

For the same source inter-packet interval of 100 000, β in the order of 1000 (fixed for TS-OOK: 1000, and random for RD TS-OOK: 1009, 1013, 1019) ensures 100% delivery to the destination(s) and give similar values for the ignore events. Here, we can also see the relationship between the ignores and the delivery, as low levels of ignore ensure good percentage of delivery.

For the collisions, we remind that, RD TS-OOK is designed to reduce the collisions by desynchronizing the transmitters. However, Table 5.4 shows that the collisions in RD TS-OOK (1 756 377) are notably higher than TS-OOK (45 139), when no bit error is tolerated (MaxBitError=0). To confirm that, compared to TS-OOK, RD TS-OOK causes fewer error bits per packet, but more collided packets, we make nodes accept a few error bits. Therefore, when an error correction code of up to 5 bits (MaxBitError=5) is used, RD TS-OOK outperforms TS-OOK: 30 610 collision events (for packets with more than 5 bit errors) for RD TS-OOK compared to 46 014 collisions for TS-OOK.

In brief, RD TS-OOK and TS-OOK give similar numbers of ignores and collisions, as their β are close to each other (close to 1000), no matter if they are dynamic or not. However, RD TS-OOK causes fewer collisions than TS-OOK (fewer bit errors per packet that can be fixed by error correction codes).

5.4/ CONCLUSION

Protocols for all the different layers are being developed in nanonetworks, but the transport layer remains the least explored Lemic et al. (2021) and thus new congestion control protocols are required.

This chapter analyzes the effects of fixed and dynamic symbol rate of nodes β along with the source packet rate. The results of this chapter show that β (and consequently the modulation scheme) and the source rate affect the congestion and collisions. If a congestion is detected in the nanonetwork, users should verify the β and source rate values. Users are encouraged to choose lower source rate (if the application allows it) to avoid congestion, i.e., the source sends then pauses then sends then pauses etc. They are also encouraged to select a lower β value (if the nanomachine hardware permits it) that causes less congestion (buffer overflow), as it makes a faster processing of symbols and packets, which then results in a good packet delivery to the destination(s), even if there are many collisions on the route.

6

REPRODUCIBILITY

6.1/ INTRODUCTION

Reproducibility and research integrity are keys for any scientific study. Reproducibility is the ability to reproduce the same (or similar) results of an experiment when repeating it Popper (2005), so that the study is reliable and trustworthy. In all of the proposed contributions, the results were produced by the network simulator BitSimulator and can be reproduced.

6.2/ DETAILS OF CONTRIBUTION

To guarantee the reproducibility, BitSimulator Dhoutaut et al. (2018) uses random number generator (RNG) seeds. A scenario that runs with a certain seed must give the same result if repeated with the same seed. To ensure good statistics and analysis, a scenario is run multiple times with different seeds. In BitSimulator, three seeds are defined and their initial values are set for :

- The genericNodesRNGSeed, which is the random placement of the nodes.
- The backoffRNGSeed, which sets the sending time inside the waiting window of backoff-based routing protocols (e.g., Backoff flooding, SLR backoff).
- The payloadRNGSeed, which is the random bits of the packet payload.

In the following, we give an example of one of my contributions and how the reproducibility was managed.

6.2.1/ REPRODUCIBILITY EXAMPLE

In this section, we take the reproducibility of my second contribution 5 as an example that can be found here ¹. The results of the simulations are three tables Table 5.2, Table 5.3 and Table 5.4. To reproduce these tables, in the directory of BitSimulator, we only need to have the scenario file (e.g., scenario.xml) and the bash shell script file (e.g., beta.sh). We launch the shell file beta.sh to run the scenario multiple times, each time we change beta, the source inter-packet interval, TS-OOK or RD TS-OOK, or maxBitError 3.3.1. In the other contributions, for faster simulations, we also ran another shell file (e.g., par.sh) that permits to run multiple codes from the main shell file in parallel, to make use of the multiple cores.

The output is a text file that contains the results of the three tables, as seen in Fig. 6.1.

```

Table1:
beta= 1000 and interval between packets= 100 000 ns: 88138 ignore 45139 collision
beta= 10 and interval between packets= 10 ns: 9352176 ignore 17097957 collision
beta= 100 and interval between packets= 100 ns: 7334666 ignore 1687428 collision
beta= 100 and interval between packets= 1000 ns: 4339230 ignore 2023881 collision
beta= 100 and interval between packets= 10 000 ns: 105023 ignore 471747 collision
beta= 100 and interval between packets= 100 000 ns: 74070 ignore 418553 collision
beta= 100 and interval between packets= 1 000 000 ns: 74070 ignore 418553 collision
beta= 1 000 and interval between packets= 1 000 ns: 6658649 ignore 161758 collision
beta= 1 000 and interval between packets= 10 000 ns: 3819608 ignore 198475 collision
beta= 1 000 and interval between packets= 1 000 000 ns: 82603 ignore 41179 collision
beta= 10 000 and interval between packets= 1 000 ns: 9277891 ignore 11843 collision
beta= 10 000 and interval between packets= 10 000 ns: 7109044 ignore 14494 collision
beta= 10 000 and interval between packets= 100 000 ns: 3980873 ignore 19718 collision
beta= 10 000 and interval between packets= 1 000 000 ns: 93691 ignore 4544 collision
Table2:
beta= 1000 and interval between packets= 100 000 ns: 100 100 100 100 100
beta= 10 and interval between packets= 10 ns: 13 18 18 13 15
beta= 100 and interval between packets= 100 ns: 21 21 22 13 18
beta= 100 and interval between packets= 1000 ns: 82 88 84 76 75
beta= 100 and interval between packets= 10 000 ns: 100 100 100 100 100
beta= 100 and interval between packets= 100 000 ns: 100 100 100 100 100
beta= 100 and interval between packets= 1 000 000 ns: 100 100 100 100 100
beta= 1 000 and interval between packets= 1 000 ns: 17 21 20 13 15
beta= 1 000 and interval between packets= 10 000 ns: 77 82 88 76 79
beta= 1 000 and interval between packets= 1 000 000 ns: 100 100 100 100 100
beta= 10 000 and interval between packets= 1 000 ns: 5 4 4 3 5
beta= 10 000 and interval between packets= 10 000 ns: 17 21 19 19 16
beta= 10 000 and interval between packets= 100 000 ns: 78 88 90 74 77
beta= 10 000 and interval between packets= 1 000 000 ns: 100 100 100 100 100
Table3:
beta= 1000 and interval between packets= 100 000 ns and maxerror= 0: 88138 ignore 45139 collision 100 delivery
beta= 1000 and interval between packets= 100 000 ns and maxerror= 5: 83756 ignore 46014 collision 100 delivery
RD TSOOK and interval between packets= 100 000 ns and maxerror= 0: 102820 ignore 1756377 collision 100 delivery
RD TSOOK and interval between packets= 100 000 ns and maxerror= 5: 99909 ignore 30610 collision 100 delivery

```

Figure 6.1: The reproducible table results of the contribution in Chapter 5

6.3/ CONCLUSION

Reproducibility has been a major factor in this research. All the contributions' results can be reproduced with the subsequent websites:

- Ring Hoteit et al. (2022b):

<http://eugen.dedu.free.fr/bitsimulator/wcnc22>

¹<http://eugen.dedu.free.fr/bitsimulator/icpads22>

- Expanded Ring Hoteit et al. (2022c):
<http://eugen.dedu.free.fr/bitsimulator/iwcmc22>
- Dynamic Ring Hoteit et al. (2022d):
<http://eugen.dedu.free.fr/bitsimulator/nanocom22>
- Beta Hoteit et al. (2022a):
<http://eugen.dedu.free.fr/bitsimulator/icpads22>



GENERAL CONCLUSION AND FUTURE WORK

CONCLUSION AND SUMMARY OF THE PHD THESIS

This thesis studied wireless nanocommunications and communications in large-scale ultra-dense ad hoc networks. The proposed protocols and methodologies are summarized in this section. In the introduction, we first introduced large-scale wireless ad hoc networks and nanonetworks enabled by the THz and nanotechnology. We also brought light to vivid nanonetwork applications that can re-engineer the world and that can become reality, if researchers focus on developing protocols for nanonetworks. We then illustrated a nanomachine and outlined its constraints in resources due to its tiny size. The nanomachine cannot perform complex applications if it is alone, so the need for network densification is stressed. Additionally, networks in general are being densified and if resources are limited, the question arises on how the existing protocol stack can cope with these challenges. The state of the art section focuses on the different layers: the physical, MAC, routing and transport layers of nanonetworks. The state of the art and a proposed tree also show the lack of sufficient research on the scalability of routing protocols in ultra-dense ad hoc networks. Also, the transport layer of nanonetworks is unexplored. Based on this, we define the goal of this dissertation: the scalability and reliability of communication protocols under resource constraints. The programming and simulation environment section compares the available electromagnetic nanonetwork simulators, selects BitSimulator as the most convenient for this study and provides a user guide for BitSimulator. The contribution section then discusses mainly the ring, in all its forms (basic, expanded and dynamic), that can be applied to nanonetworks and large-scale ad hoc networks in general, then the other contribution corresponds to the THz nanonetworks only where a featured parameter β is studied along with the source rate. The contributions are analyzed and simulated using BitSimulator. The reproducibility section highlights one of the strengths of research that features BitSimulator and that is the ability to reproduce results of study. Finally, we draw some conclusions and future perspectives for this dissertation.

7.1/ CONTRIBUTIONS

The contributions are revisited here. The first contribution in the network layer of electromagnetic nanonetworks and (resource-limited) ultra-dense ad hoc networks, is the ring scheme that selects the forwarders on the border of the communication ranges on each transmitting hop. The expanded ring then redefines the ring and makes only the rings forward, while discarding the inner discs. The dynamic ring automatically adapts the original ring's width to the local density. The ring schemes optimize the forwarder selection keeping a good packet delivery ratio. Therefore, the ring reduces the energy consumption of the network and prolongs the network's lifetime, as data transmission consumes a lot of resources. The second contribution is in the transport layer of electromagnetic nanonetworks, showing a relationship between the symbol and packet rates and the congestion in nanonetworks.

7.2/ PERSPECTIVES

Future perspectives about electromagnetic nanonetworks are given in this section, along with a simplified novel approach of communication for routing in nanonetworks.

Mobility of nanodevices is one challenge that need to be addressed while designing protocols, as some applications involve the mobility in body fluids or in environmental water, etc.

In the transport layer, the theoretical analysis of the effect of β on nanonetworks is important. The influence of β and the source rate on the **delay** can be studied. Future research can also be directed towards designing novel **congestion control** protocols for nanonetworks. They can be dynamic source rate limiting traffic and dynamic β based on node buffer fill level.

Future work should also concentrate on finding the **optimal number and distribution of forwarders** in the network, so that the resources are not wasted on redundant retransmissions. In a nanonetwork, NP-hard problems (to solve the optimal number of forwarders) are too complex to achieve, but we hope to still find solutions to diminish the number of forwarders and this is what inspired the **Mobile forwarder**.

Mobile forwarder The proposed paradigm of communication in the community of nanonetworks is mainly multi-hop communication. In the usual multi-hop fashion, in order to broadcast a message to the whole network, the source node transmits the data packets to its 1-hop forwarders which, in turn, transmit them to 2-hop forwarders and so on, until reaching all the nodes. In this section, we inspire a novel form of communication

that we call “Mobile forwarder”. “Mobile forwarder” benefits from the high density aspect of a nanonetwork and makes a forwarding nanorouter (less constrained than a nanonode) responsible for covering zones while moving in the network. We can imagine an in-body application, where a gateway to the outside world tries to communicate (transmit or receive) a message (or an order) with a static nanonetwork in a diseased organ in the human body. The gateway passes the message to a mobile forwarding nanorouter, so that the latter delivers the data to the diseased organ. The forwarding nanorouter then releases the data packets to nodes in a communication range, moves then serves the next communication region until reaching the whole network. The nanorouter may follow a mobility model that corresponds to the diseased organ. To avoid energy deficiency due to mobility, the mobile forwarding nanorouter may harvest energy from the environment (e.g, temperature or blood) or more nanorouters may be connected with the gateway.

Final Word The IoT and the IoNT will require connecting devices densely, which will make research on scalability even more relevant. Nanonetworks remain an undiscovered and exciting topic of research. The constraints imposed by these networks make the design of protocols challenging, and more realistic constraints will show on the surface when nanodevices are finally built.

BIBLIOGRAPHY

- [Afsharinejad et al. 2016] AFSHARINEJAD, Armita ; DAVY, Alan ; JENNINGS, Brendan: **“Dynamic channel allocation in electromagnetic nanonetworks for high resolution monitoring of plants”**. In *Nano Communication Networks* 7 (2016), pages 2–16
- [Akyildiz and Jornet 2010a] AKYILDIZ, Ian F. ; JORNET, Josep M.: **“Electromagnetic wireless nanosensor networks”**. In *Nano Communication Networks* 1 (2010), number 1, pages 3–19
- [Akyildiz and Jornet 2010b] AKYILDIZ, Ian F. ; JORNET, Josep M.: **“The internet of nano-things”**. In *IEEE Wireless Communications* 17 (2010), number 6, pages 58–63
- [Akyildiz et al. 2011] AKYILDIZ, Ian F. ; JORNET, Josep M. ; PIEROBON, Massimiliano: **“Nanonetworks: A new frontier in communications”**. In *Communications of the ACM* 54 (2011), number 11, pages 84–89
- [Alam et al. 2017] ALAM, Mayisha ; NURAIN, Novia ; TAIRIN, Suraiya ; AL ISLAM, ABM A.: **“Energy-efficient transport layer protocol for hybrid communication in body area nanonetworks”**. In *2017 IEEE Region 10 Humanitarian Technology Conference (R10-HTC)*. Dhaka, Bangladesh : IEEE, December 2017, pages 674–677
- [Ali and Abu-Elkheir 2015] ALI, Najah A. ; ABU-ELKHEIR, Mervat: **“Internet of nano-things healthcare applications: Requirements, opportunities, and challenges”**. In *11th Int. Conf. on Wireless and Mobile Computing, Networking and Communications (WiMob)*. Los Alamitos, CA, USA : IEEE, October 2015, pages 9–14
- [Aliouat et al. 2021] ALIOUAT, Lina ; RAHMANI, Mohammed ; MABED, Hakim ; BOURGEOIS, Julien: **“Enhancement and performance analysis of channel access mechanisms in terahertz band”**. In *Nano Communication Networks* 29 (2021), pages 100364
- [Alvarez et al. 2016] ALVAREZ, Jennifer L. ; RICE, Mark ; SAMSON, John R. ; KOETS, Michael A.: **“Increasing the capability of CubeSat-based software-defined radio applications”**. In *2016 IEEE aerospace conference IEEE (event)*, 2016, pages 1–10
- [Arrabal et al. 2019] ARRABAL, Thierry ; BÜTHER, Florian ; DHOUTAUT, Dominique ; DEDU, Eugen: **“Congestion Control by Deviation Routing in Nanonetworks”**. In *6th ACM International Conference on Nanoscale Computing and Communication (NanoCom)*. Dublin, Ireland : ACM/IEEE, September 2019, pages 1–6

- [Arrabal et al. 2018a] ARRABAL, Thierry ; DHOUTAUT, Dominique ; DEDU, Eugen: **“Efficient density estimation algorithm for ultra dense wireless networks”**. In *International Conference on Computer Communications and Networks (ICCCN)*. Hangzhou, China : IEEE, July 2018, pages 1–9
- [Arrabal et al. 2018b] ARRABAL, Thierry ; DHOUTAUT, Dominique ; DEDU, Eugen: **“Efficient multi-hop broadcasting in dense nanonetworks”**. In *17th IEEE International Symposium on Network Computing and Applications (NCA)*. Cambridge, MA, USA : IEEE, November 2018, pages 385–393
- [Awasthi et al. 2016] AWASTHI, Amruta ; AWASTHI, Anshul ; RIORDAN, Daniel ; WALSH, Joseph: **“Non-invasive sensor technology for the development of a dairy cattle health monitoring system”**. In *Computers* 5 (2016), number 4, pages 23
- [Boillot et al. 2015] BOILLOT, Nicolas ; DHOUTAUT, Dominique ; BOURGEOIS, Julien: **“Going for large scale with nano-wireless simulations”**. In *2nd ACM International Conference on Nanoscale Computing and Communication (NanoCom)*. Boston, MA, USA : ACM, September 2015, pages 1–2
- [Cai et al. 2005] CAI, Ying ; HUA, Kien A. ; PHILLIPS, Aaron: **“Leveraging 1-hop neighborhood knowledge for efficient flooding in wireless ad hoc networks”**. In *IEEE International Conference on Performance, Computing and Communications (IPCCC)*. Phoenix, AZ, USA : IEEE, April 2005, pages 347–354
- [Canovas-Carrasco et al. 2020] CANOVAS-CARRASCO, Sebastian ; ASOREY-CACHEDA, Rafael ; GARCIA-SANCHEZ, Antonio-Javier ; GARCIA-HARO, Joan ; WOJCIK, Krzysztof ; KULAKOWSKI, Pawel: **“Understanding the applicability of terahertz flow-guided nano-networks for medical applications”**. In *IEEE Access* 8 (2020), pages 214224–214239
- [Clausen and Jacquet 2003] CLAUSEN, Thomas ; JACQUET, Philippe: **“Optimized link state routing protocol (OLSR)”**. 2003. – Research Report
- [Correll et al. 2017] CORRELL, Nikolaus ; DUTTA, Prabal ; HAN, Richard ; PISTER, Kristofer: **“Wireless robotic materials”**. In *Proceedings of the 15th ACM Conference on Embedded Network Sensor Systems*, 2017, pages 1–6
- [Del Monte 2017] DEL MONTE, Louis A.: *Nanoweapons: A Growing Threat to Humanity*. U of Nebraska Press, 2017
- [Devreese 2007] DEVREESE, Jozef T.: **“Importance of nanosensors: Feynman’s vision and the birth of nanotechnology”**. In *MRS bulletin* 32 (2007), number 9, pages 718–725

- [Dhoutaut et al. 2018] DHOUTAUT, Dominique ; ARRABAL, Thierry ; DEDU, Eugen: **“Bit-Simulator, an electromagnetic nanonetworks simulator”**. In *5th ACM/IEEE International Conference on Nanoscale Computing and Communication (NanoCom)*. Reykjavik, Iceland : ACM/IEEE, September 2018, pages 1–6
- [Donohoe et al. 2015] DONOHOE, Michael ; BALASUBRAMANIAM, Sasitharan ; JENNINGS, Brendan ; JORNET, Josep M.: **“Powering in-body nanosensors with ultrasounds”**. In *IEEE Transactions on Nanotechnology* 15 (2015), number 2, pages 151–154
- [Dressler and Fischer 2015] DRESSLER, Falko ; FISCHER, Stefan: **“Connecting in-body nano communication with body area networks: Challenges and opportunities of the Internet of Nano Things”**. In *Nano Communication Networks* 6 (2015), number 2, pages 29–38
- [Ducrocq et al. 2013] DUCROCQ, Tony ; MITTON, Nathalie ; HAUSPIE, Michaël: **“Energy-based clustering for wireless sensor network lifetime optimization”**. In *2013 IEEE wireless communications and networking conference (WCNC)* IEEE (event), 2013, pages 968–973
- [Farrow et al. 2014] FARROW, Nicholas ; SIVAGNANADASAN, Naren ; CORRELL, Nikolaus: **“Gesture based distributed user interaction system for a reconfigurable self-organizing smart wall”**. In *Proceedings of the 8th International Conference on Tangible, Embedded and Embodied Interaction*, 2014, pages 245–246
- [Fraga-Lamas et al. 2016] FRAGA-LAMAS, Paula ; FERNÁNDEZ-CARAMÉS, Tiago M. ; SUÁREZ-ALBELA, Manuel ; CASTEDO, Luis ; GONZÁLEZ-LÓPEZ, Miguel: **“A review on internet of things for defense and public safety”**. In *Sensors* 16 (2016), number 10, pages 1644
- [Füßler et al. 2003] FÜSSLER, Holger ; WIDMER, Jörg ; KÄSEMANN, Michael ; MAUVE, Martin ; HARTENSTEIN, Hannes: **“Contention-based forwarding for mobile ad hoc networks”**. In *Ad Hoc Networks* 1 (2003), number 4, pages 351–369
- [Geim and Novoselov 2010] GEIM, Andre K. ; NOVOSELOV, Konstantin S.: **“The rise of graphene”**. In *Nanoscience and technology: a collection of reviews from nature journals*. World Scientific, 2010, pages 11–19
- [Goody and Yung 1995] GOODY, Richard M. ; YUNG, Yuk L.: *Atmospheric radiation: theoretical basis*. Oxford university press, 1995
- [Han et al. 2008] HAN, Jongyoon ; FU, Jianping ; SCHOCH, Reto B.: **“Molecular sieving using nanofilters: past, present and future”**. In *Lab on a Chip* 8 (2008), number 1, pages 23–33

- [Hills et al. 2019] HILLS, Gage ; LAU, Christian ; WRIGHT, Andrew ; FULLER, Samuel ; BISHOP, Mindy D. ; SRIMANI, Tathagata ; KANHAIYA, Pritpal ; HO, Rebecca ; AMER, Aya ; STEIN, Yosi ; OTHERS: **“Modern microprocessor built from complementary carbon nanotube transistors”**. In *Nature* 572 (2019), number 7771, pages 595–602
- [Hossain et al. 2018] HOSSAIN, Zahed ; XIA, Qing ; JORNET, Josep M.: **“TeraSim: An ns-3 extension to simulate Terahertz-band communication networks”**. In *Nano Communication Networks* 17 (2018), September, pages 36–44
- [Hoteit et al. 2022a] HOTEIT, Farah ; DEDU, Eugen ; SEAH, Winston K. ; DHOUTAUT, Dominique: **“Influence of beta and source packet rate on electromagnetic nanocommunications”**. In *IEEE International Conference on Parallel and Distributed Systems (ICPADS)*. Nanjing, China : IEEE, December 2022, pages 7
- [Hoteit et al. 2022b] HOTEIT, Farah ; DEDU, Eugen ; SEAH, Winston K. ; DHOUTAUT, Dominique: **“Ring-based forwarder selection to improve packet delivery in ultra-dense networks”**. In *IEEE Wireless Communications and Networking Conference (WCNC)*. Austin, TX, USA : IEEE, April 2022, pages 2709–2714
- [Hoteit et al. 2022c] HOTEIT, Farah ; DHOUTAUT, Dominique ; SEAH, Winston K. ; DEDU, Eugen: **“Dynamic ring-based forwarder selection to improve packet delivery in ultra-dense nanonetworks”**. In *9th ACM International Conference on Nanoscale Computing and Communication (ACM NanoCom)*. Barcelona, Catalunya, Spain : ACM, October 2022, pages 7
- [Hoteit et al. 2022d] HOTEIT, Farah ; DHOUTAUT, Dominique ; SEAH, Winston K. ; DEDU, Eugen: **“Expanded ring-based forwarder selection to improve packet delivery in ultra-dense nanonetworks”**. In *International Wireless Communications and Mobile Computing Conference (IWCMC)*. Dubrovnik, Croatia : IEEE, June 2022, pages 1406–1410
- [Hughes and Correll 2014] HUGHES, Dana ; CORRELL, Nikolaus: **“A soft, amorphous skin that can sense and localize textures”**. In *2014 IEEE International Conference on Robotics and Automation (ICRA)* IEEE (event), 2014, pages 1844–1851
- [Hull et al. 2004] HULL, Bret ; JAMIESON, Kyle ; BALAKRISHNAN, Hari: **“Mitigating congestion in wireless sensor networks”**. In *Proceedings of the 2nd international conference on Embedded networked sensor systems*. New York, NY, USA : Association for Computing Machinery, 2004, pages 134–147
- [Initiative] INITIATIVE, National N.: *Size of the Nanoscale*. <https://www.nano.gov/nanotech-101/what/nano-size>. – National Nanotechnology Initiative

- [Iovine et al. 2017] IOVINE, Renato ; LOSCRÌ, Valeria ; PIZZI, Sara ; TARPARELLI, Richard ; VEGNI, Anna M.: **“Electromagnetic nanonetworks for sensing and drug delivery”**. In *Modeling, Methodologies and Tools for Molecular and Nano-scale Communications*. Springer, 2017, pages 473–501
- [James et al. 2015] JAMES, Ashish ; MADHUKUMAR, A.S. ; ADACHI, Fumiyuki: **“Efficient multihop transmission scheme for error-free relay forwarding in cooperative networks”**. In *Wireless Communications and Mobile Computing* 15 (2015), number 4, pages 755–769
- [Javaid et al. 2021] JAVAID, Mohd ; HALEEM, Abid ; SINGH, Ravi P. ; RAB, Shanay ; SUMAN, Rajiv: **“Exploring the potential of nanosensors: A brief overview”**. In *Sensors International* 2 (2021), pages 100130
- [Jeong et al. 2022] JEONG, Youngdo ; JIN, Soyeong ; PALANIKUMAR, L ; CHOI, Huyeon ; SHIN, Eunhye ; GO, Eun M. ; KEUM, Changjoon ; BANG, Seunghwan ; KIM, Dongkap ; LEE, Seungho ; OTHERS: **“Stimuli-Responsive Adaptive Nanotoxin to Directly Penetrate the Cellular Membrane by Molecular Folding and Unfolding”**. In *Journal of the American Chemical Society* 144 (2022), number 12, pages 5503–5516
- [Johnson et al. 2007] JOHNSON, David ; HU, Yin-chun ; MALTZ, David: **“The dynamic source routing protocol (DSR) for mobile ad hoc networks for IPv4”**. 2007. – Research Report
- [Jornet and Akyildiz 2010a] JORNET, Josep M. ; AKYILDIZ, Ian F.: **“Channel capacity of electromagnetic nanonetworks in the terahertz band”**. In *2010 IEEE international conference on communications IEEE (event)*, 2010, pages 1–6
- [Jornet and Akyildiz 2010b] JORNET, Josep M. ; AKYILDIZ, Ian F.: **“Graphene-based nano-antennas for electromagnetic nanocommunications in the terahertz band”**. In *4th European Conference on Antennas and Propagation*. Barcelona, Spain : IEEE, April 2010, pages 1–5
- [Jornet and Akyildiz 2011] JORNET, Josep M. ; AKYILDIZ, Ian F.: **“Channel modeling and capacity analysis for electromagnetic wireless nanonetworks in the terahertz band”**. In *IEEE Transactions on Wireless Communications* 10 (2011), number 10, pages 3211–3221
- [Jornet and Akyildiz 2012a] JORNET, Josep M. ; AKYILDIZ, Ian F.: **“The internet of multimedia nano-things”**. In *Nano Communication Networks* 3 (2012), number 4, pages 242–251
- [Jornet and Akyildiz 2012b] JORNET, Josep M. ; AKYILDIZ, Ian F.: **“Joint energy harvesting and communication analysis for perpetual wireless nanosensor net-**

- works in the terahertz band**". In *IEEE Transactions on Nanotechnology* 11 (2012), number 3, pages 570–580
- [Jornet and Akyildiz 2014] JORNET, Josep M. ; AKYILDIZ, Ian F.: **"Femtosecond-Long Pulse-Based Modulation for Terahertz Band Communication in Nanonetworks"**. In *IEEE Transactions on Communications* 62 (2014), May, number 5, pages 1742–1753
- [Kafi et al. 2014] KAFI, Mohamed A. ; DJENOURI, Djamel ; BEN-OTHTMAN, Jalel ; BADACHE, Nadjib: **"Congestion control protocols in wireless sensor networks: A survey"**. In *IEEE Communications Surveys & Tutorials* 16 (2014), March, number 3, pages 1369–1390
- [Karp and Kung 2000] KARP, Brad ; KUNG, Hsiang-Tsung: **"GPSR: Greedy perimeter stateless routing for wireless networks"**. In *6th Annual Int. Conf. on Mobile computing and networking (MobiCom)*. Boston, MA, USA : ACM, August 2000, pages 243–254
- [Kiraly et al. 2018] KIRALY, Brian ; RUDENKO, Alexander N. ; WEERDENBURG, Werner M. van ; WEGNER, Daniel ; KATSNELSON, Mikhail I. ; KHAJETOORIANS, Alexander A.: **"An orbitally derived single-atom magnetic memory"**. In *Nature communications* 9 (2018), number 1, pages 1–8
- [Kleinrock and Kamoun 1977] KLEINROCK, Leonard ; KAMOUN, Farouk: **"Hierarchical routing for large networks performance evaluation and optimization"**. In *Computer Networks (1976)* 1 (1977), number 3, pages 155–174
- [Kleinrock and Silvester 1978] KLEINROCK, Leonard ; SILVESTER, John: **"Optimum Transmission Radii for Packet Radio Networks or Why Six is a Magic Number"**. In *National Telecommunications Conference*. Piscataway, NJ, USA : IEEE, December 1978, pages 4.3.1–4.3.5
- [Lamonaca et al. 2018] LAMONACA, Francesco ; SCIAMMARELLA, PF ; SCURO, Carmelo ; CARNI, DL ; OLIVITO, RS: **"Internet of things for structural health monitoring"**. In *2018 Workshop on Metrology for Industry 4.0 and IoT IEEE (event)*, 2018, pages 95–100
- [Lemic et al. 2021] LEMIC, Filip ; ABADAL, Sergi ; TAVERNIER, Wouter ; STROOBANT, Pieter ; COLLE, Didier ; ALARCÓN, Eduard ; MARQUEZ-BARJA, Johann ; FAMAËY, Jeroen: **"Survey on terahertz nanocommunication and networking: A top-down perspective"**. In *IEEE Journal on Selected Areas in Communications* 39 (2021), number 6, pages 1506–1543
- [Leveziel et al. 2022] LEVEZIEL, Maxence ; HAOUAS, Wissem ; LAURENT, Guillaume J. ; GAUTHIER, Michaël ; DAHMOUCHE, Redwan: **"MiGriBot: A miniature parallel robot**

- with integrated gripping for high-throughput micromanipulation”. In *Science Robotics* 7 (2022), number 69, pages eabn4292
- [Li et al. 2022] LI, Haipeng ; MERKL, Padryk ; SOMMERTUNE, Jens ; THERSLEFF, Thomas ; SOTIRIOU, Georgios A.: “**SERS Hotspot Engineering by Aerosol Self-Assembly of Plasmonic Ag Nanoaggregates with Tunable Interparticle Distance**”. In *Advanced Science* (2022), pages 2201133
- [Liang et al. 2014] LIANG, Chunchao ; LIM, Sunho ; MIN, Manki ; WANG, Wei: “**Geometric broadcast without GPS support in dense wireless sensor networks**”. In *2014 IEEE 11th Consumer Communications and Networking Conference (CCNC)* IEEE (event), 2014, pages 405–410
- [Liaskos et al. 2018] LIASKOS, Christos ; NIE, Shuai ; TSIOLIARIDOU, Ageliki ; PITSILLIDES, Andreas ; IOANNIDIS, Sotiris ; AKYILDIZ, Ian: “**A new wireless communication paradigm through software-controlled metasurfaces**”. In *IEEE Communications Magazine* 56 (2018), June, number 9, pages 162–169
- [Liaskos et al. 2015] LIASKOS, Christos ; TSIOLIARIDOU, Ageliki ; PITSILLIDES, Andreas ; AKYILDIZ, Ian F. ; KANTARTZIS, Nikolaos V. ; LALAS, Antonios X. ; DIMITROPOULOS, Xenofontas ; IOANNIDIS, Sotiris ; KAFESAKI, Maria ; SOUKOULIS, C.M.: “**Design and Development of Software Defined Metamaterials for Nanonetworks**”. In *IEEE Circuits and Systems Magazine* 15 (2015), number 4, pages 12–25
- [Liaskos et al. 2016] LIASKOS, Christos ; TSIOLIARIDOU, Angeliki ; IOANNIDIS, Sotiris ; KANTARTZIS, Nikolaos ; PITSILLIDES, Andreas: “**A deployable routing system for nanonetworks**”. In *2016 IEEE International Conference on Communications (ICC)*. Kuala Lumpur, Malaysia : IEEE, 2016, pages 1–6
- [Lueth et al. 2022] LUETH, Knud L. ; HASAN, Mohammad ; SINHA, Satyajit ; ANNASWAMY, Sharmila ; WEGNER, Philipp ; BRUEGGE, Fernando ; KULEZAK, Matthieu: “**A comprehensive 114-page report on the current state of the Internet of Things, incl. market update forecast, latest trends, IT spending update, and more**” / IOT ANALYTICS. May 2022. – Research Report
- [Mabed 2017] MABED, Hakim: “**Enhanced spread in time on-off keying technique for dense Terahertz nanonetworks**”. In *2017 IEEE Symposium on Computers and Communications (ISCC)* IEEE (event), 2017, pages 710–716
- [Mabed and Bourgeois 2018] MABED, Hakim ; BOURGEOIS, Julien: “**A flexible medium access control protocol for dense terahertz nanonetworks**”. In *Proceedings of the 5th ACM International Conference on Nanoscale Computing and Communication*, 2018, pages 1–7

- [Maccari et al. 2018] MACCARI, Leonardo ; MAISCHBERGER, Mirko ; CIGNO, Renato L.: **“Where have all the MPRs gone? On the optimal selection of Multi-Point Relays”**. In *Ad Hoc Networks* 77 (2018), pages 69–83. – ISSN 1570-8705
- [McEvoy and Correll 2016] MCEVOY, Michael ; CORRELL, Nikolaus: **“Shape change through programmable stiffness”**. In *Experimental Robotics* Springer (event), 2016, pages 893–907
- [McEvoy and Correll 2015] MCEVOY, Michael A. ; CORRELL, Nikolaus: **“Materials that couple sensing, actuation, computation, and communication”**. In *Science* 347 (2015), number 6228, pages 1261689
- [Mohammad and Shubair 2019] MOHAMMAD, Hadeel ; SHUBAIR, Raed M.: **“Nanoscale Communication: State-of-Art and Recent Advances”**. In *arXiv e-prints* (2019), May, pages arXiv–1905
- [Neupane 2014] NEUPANE, Semanta R.: *Routing in resource constrained sensor nanonetworks*. Tampere, Finland, Tampere University of Technology, Master Thesis, 2014
- [Oppermann et al. 2004] OPPERMANN, Ian ; HÄMÄLÄINEN, Matti ; IINATTI, Jari: *UWB: theory and applications*. John Wiley & Sons, 2004
- [Panichpapiboon and Cheng 2013] PANICHPAPIBOON, Sooksan ; CHENG, Lin: **“Ir-responsible forwarding under real intervehicle spacing distributions”**. In *IEEE Transactions on Vehicular Technology* 62 (2013), June, number 5, pages 2264–2272
- [Perkins et al. 2003] PERKINS, Charles ; BELDING-ROYER, Elizabeth ; DAS, Samir: **“Ad hoc on-demand distance vector (AODV) routing”**. 2003. – Research Report
- [Pešović et al. 2010] PEŠOVIĆ, Uroš M ; MOHORKO, Jože J ; BENKIČ, Karl ; ČUČEJ, Žarko F: **“Single-hop vs. Multi-hop–Energy efficiency analysis in wireless sensor networks”**. In *18th telecommunications forum, TELFOR*, 2010, pages 471–474
- [Piro et al. 2013] PIRO, Giuseppe ; GRIECO, Luigi A. ; BOGGIA, Gennaro ; CAMARDA, Pietro: **“Nano-Sim: simulating electromagnetic-based nanonetworks in the network simulator 3”**. In *6th International ICST Conference on Simulation Tools and Techniques (SimuTools)*. Cannes, France : ACM, March 2013, pages 203–210
- [Popper 2005] POPPER, Karl: *The logic of scientific discovery*. Routledge, 2005
- [Profita et al. 2015] PROFITA, Halley ; FARROW, Nicholas ; CORRELL, Nikolaus: **“Flutter: An exploration of an assistive garment using distributed sensing, computation and actuation”**. In *Proceedings of the Ninth International Conference on Tangible, Embedded, and Embodied Interaction*, 2015, pages 359–362

- [Pujol et al. 2011] PUJOL, Joan C. ; JORNET, Josep M. ; PARETA, Josep S.: **“PHLAME: A physical layer aware MAC protocol for electromagnetic nanonetworks”**. In *2011 IEEE Conference on Computer Communications Workshops (INFOCOM WKSHPS)*. Shanghai, China : IEEE, April 2011, pages 431–436
- [Ramakrishnan et al. 2001] RAMAKRISHNAN, K. ; FLOYD, Sally ; BLACK, David: *The Addition of Explicit Congestion Notification (ECN) to IP*. September 2001
- [Rappaport et al. 2011] RAPPAPORT, Theodore S. ; MURDOCK, James N. ; GUTIERREZ, Felix: **“State of the art in 60-GHz integrated circuits and systems for wireless communications”**. In *Proceedings of the IEEE* 99 (2011), number 8, pages 1390–1436
- [Reina et al. 2015] REINA, Daniel G. ; TORAL, Sergio ; JOHNSON, Princy ; BARRERO, Federico: **“A survey on probabilistic broadcast schemes for wireless ad hoc networks”**. In *Ad Hoc Networks* 25 (2015), February, pages 263–292
- [Ren et al. 2019] REN, Aifeng ; ZAHID, Adnan ; YANG, Xiaodong ; ALOMAINY, Akram ; IMRAN, Muhammad A. ; ABBASI, Qammer H.: **“Terahertz (THz) application in food contamination detection”**. In *Nano-Electromagnetic Communication at Terahertz and Optical Frequencies: Principles and Applications* (2019), pages 77
- [Rikhtegar and Keshtgary 2013] RIKHTEGAR, Negar ; KESHTGARY, Manijeh: **“A brief survey on molecular and electromagnetic communications in nano-networks”**. In *International Journal of Computer Applications* 79 (2013), number 3
- [Rossi et al. 2008] ROSSI, Dario ; FRACCHIA, Roberta ; MEO, Michela: **“VANETs: Why use beaconing at all?”**. In *IEEE International Conference on Communications (ICC)*. Beijing, China : IEEE, May 2008, pages 2745–2751
- [Saeed et al. 2021] SAEED, Nasir ; LOUKIL, Mohamed H. ; SARIEDDEEN, Hadi ; AL-NAFFOURI, Tareq Y. ; ALOUINI, Mohamed-Slim: **“Body-centric terahertz networks: Prospects and challenges”**. In *IEEE Transactions on Molecular, Biological and Multi-Scale Communications* (2021)
- [Sahin et al. 2021] SAHIN, Emre ; DAGDEVIREN, Orhan ; AKKAS, Mustafa A.: **“An Evaluation of Internet of Nano-Things Simulators”**. In *6th International Conference on Computer Science and Engineering (UBMK)*. Ankara, Turkey : IEEE, 2021, pages 670–675
- [Sarycheva et al. 2018] SARYCHEVA, Asia ; POLEMI, Alessia ; LIU, Yuqiao ; DANDEKAR, Kapil ; ANASORI, Babak ; GOGOTSI, Yury: **“2D titanium carbide (MXene) for wireless communication”**. In *Science advances* 4 (2018), number 9, pages eaau0920

- [Shrestha et al. 2016] SHRESTHA, Anish P. ; YOO, Sang-Jo ; CHOI, Hyoung J. ; KWAK, Kyung S.: **“Enhanced rate division multiple access for electromagnetic nanonetworks”**. In *IEEE Sensors Journal* 16 (2016), number 19, pages 7287–7296
- [Singh et al. 2018] SINGH, Pankaj ; KIM, Byung-Wook ; JUNG, Sung-Yoon: **“TH-PPM with non-coherent detection for multiple access in electromagnetic wireless nanocommunications”**. In *Nano Communication Networks* 17 (2018), pages 1–13
- [Smith et al. 2012] SMITH, Richard ; ARCA, A ; CHEN, X ; MARQUES, L ; CLARK, M ; AYLOTT, J ; SOMEKH, M: **“Design and fabrication of nanoscale ultrasonic transducers”**. In *Journal of Physics: Conference Series* Volume 353 IOP Publishing (event), 2012, pages 012001
- [Soliman et al. 2021] SOLIMAN, Wasim G. ; SWATHI, Ch ; YASASVI, T ; PRIYA, B K. ; REDDY, D A.: **“Review on poly (ethylene oxide)-based electrolyte and anode nanomaterials for the internet of things node-level lithium-ion batteries”**. In *Materials Today: Proceedings* 42 (2021), pages 429–435
- [Sun et al. 2000] SUN, Min-Te ; FENG, Wu-Chi ; LAI, Ten-Hwang ; YAMADA, Kentaro ; OKADA, Hiromi ; FUJIMURA, Kikuo: **“GPS-based message broadcast for adaptive inter-vehicle communications”**. In *IEEE Conference on Vehicular Technology (VTC)* Volume 6. Boston, MA, USA : IEEE, September 2000, pages 2685–2692
- [Suzuki and Budiman 2013] SUZUKI, Junichi ; BUDIMAN, Harry: **“Robustness in TDMA scheduling for neuron-based molecular communication”**. In *Proceedings of the 8th International Conference on Body Area Networks*, 2013, pages 478–483
- [Tairin et al. 2017] TAIRIN, Suraiya ; NURAIN, Novia ; AL ISLAM, ABM A.: **“Network-level performance enhancement in wireless nanosensor networks through multi-layer modifications”**. In *International Conference on Networking, Systems and Security (NSysS)*. Dhaka, Bangladesh : IEEE, 2017, pages 75–83
- [Tang et al. 2019] TANG, Ning ; ZHOU, Cheng ; XU, Lihuai ; JIANG, Yang ; QU, Hemi ; DUAN, Xuexin: **“A fully integrated wireless flexible ammonia sensor fabricated by soft nano-lithography”**. In *ACS sensors* 4 (2019), number 3, pages 726–732
- [Tseng et al. 2021] TSENG, Ethan ; COLBURN, Shane ; WHITEHEAD, James ; HUANG, Luocheng ; BAEK, Seung-Hwan ; MAJUMDAR, Arka ; HEIDE, Felix: **“Neural nano-optics for high-quality thin lens imaging”**. In *Nature communications* 12 (2021), number 1, pages 1–7
- [Tseng et al. 2002] TSENG, Yu-Chee ; NI, Sze-Yao ; CHEN, Yuh-Shyan ; SHEU, Jang-Ping: **“The Broadcast Storm Problem in a Mobile Ad Hoc Network”**. In *Wireless Networks* 8 (2002), March, number 2–3, pages 153–167

- [Tsioliariidou et al. 2017] TSIOLIARIDOU, Ageliki ; LIASKOS, Christos ; DEDU, Eugen ; IOANNIDIS, Sotiris: **“Packet routing in 3D nanonetworks: A lightweight, linear-path scheme”**. In *Nano Communication Networks* 12 (2017), June, pages 63–71
- [Tsioliariidou et al. 2015] TSIOLIARIDOU, Ageliki ; LIASKOS, Christos ; IOANNIDIS, Sotiris ; PITSILLIDES, Andreas: **“CORONA: A Coordinate and Routing system for Nanonetworks”**. In *2nd ACM International Conference on Nanoscale Computing and Communication*. Boston, MA, USA : ACM, 2015, pages 1–6
- [Tsioliariidou et al. 2016] TSIOLIARIDOU, Ageliki ; LIASKOS, Christos ; IOANNIDIS, Sotiris ; PITSILLIDES, Andreas: **“Lightweight, self-tuning data dissemination for dense nanonetworks”**. In *Nano Communication Networks* 8 (2016), pages 2–15
- [Vavouris et al. 2018] VAVOURIS, Apostolos K. ; DERVISI, Foteini D. ; PAPANIKOLAOU, Vasilis K. ; KARAGIANNIDIS, George K.: **“An energy efficient modulation scheme for body-centric nano-communications in the THz band”**. In *2018 7th International Conference on Modern Circuits and Systems Technologies (MOCASST) IEEE (event)*, 2018, pages 1–4
- [Wan et al. 2011] WAN, Chieh-Yih ; EISENMAN, Shane B. ; CAMPBELL, Andrew T.: **“Energy-efficient congestion detection and avoidance in sensor networks”**. In *ACM Transactions on Sensor Networks (TOSN)* 7 (2011), February, number 4, pages 1–31
- [Wang 2012] WANG, Zhong L.: *Self-powered nanosensors and nanosystems*. 2012
- [Witt and Turau 2005] WITT, Matthias ; TURAU, Volker: **“BGR: Blind geographic routing for sensor networks”**. In *Third International Workshop on Intelligent Solutions in Embedded Systems IEEE (event)*, 2005, pages 51–61
- [Wong and Dia 2017] WONG, Kaufui ; DIA, Sarah: **“Nanotechnology in batteries”**. In *Journal of Energy Resources Technology* 139 (2017), number 1
- [Yang et al. 2020] YANG, Ke ; BI, Dadi ; DENG, Yansha ; ZHANG, Rui ; RAHMAN, Muhammad Mahboob U. ; ALI, Najah A. ; IMRAN, Muhammad A. ; JORNET, Josep M. ; ABBASI, Qammer H. ; ALOMAINY, Akram: **“A comprehensive survey on hybrid communication in context of molecular communication and terahertz communication for body-centric nanonetworks”**. In *IEEE Transactions on Molecular, Biological and Multi-Scale Communications* 6 (2020), number 2, pages 107–133
- [Yang et al. 2015] YANG, Ke ; PELLEGRINI, Alice ; MUNOZ, Max O. ; BRIZZI, Alessio ; ALOMAINY, Akram ; HAO, Yang: **“Numerical analysis and characterization of THz propagation channel for body-centric nano-communications”**. In *IEEE Transactions on Terahertz Science and technology* 5 (2015), number 3, pages 419–426

- [Zahid et al. 2020] ZAHID, Adnan ; ABBAS, Hasan T. ; REN, Aifeng ; ALOMAINY, Akram ; IMRAN, Muhammad A. ; ABBASI, Qammer H.: **“Application of terahertz sensing at nano-scale for precision agriculture”**. In *Wireless Automation as an Enabler for the next Industrial Revolution* (2020), pages 241–257
- [Zainuddin et al. 2016] ZAINUDDIN, Muhammad A. ; DEDU, Eugen ; BOURGEOIS, Julien: **“SBN: Simple Block Nanocode for nanocommunications”**. In *ACM International Conference on Nanoscale Computing and Communication*. New York City, NY, USA : ACM, September 2016 (3), pages 1–7
- [Zakharov et al. 2012] ZAKHAROV, Dmitry ; LEBEDEV, Gor ; IRZHAK, Artemy ; AFONINA, Veronika ; MASHIROV, Alexey ; KALASHNIKOV, Vladimir ; KOLEDV, Viktor ; SHELYAKOV, Alexander ; PODGORNYY, Dmitry ; TABACHKOVA, Natalia ; OTHERS: **“Submicron-sized actuators based on enhanced shape memory composite material fabricated by FIB-CVD”**. In *Smart materials and structures* 21 (2012), number 5, pages 052001
- [Zanella et al. 2014] ZANELLA, Andrea ; BUI, Nicola ; CASTELLANI, Angelo ; VANGELISTA, Lorenzo ; ZORZI, Michele: **“Internet of things for smart cities”**. In *IEEE Internet of Things journal* 1 (2014), number 1, pages 22–32
- [Zhang et al. 2017] ZHANG, Rui ; YANG, Ke ; ABBASI, Qammer H. ; QARAQE, Khalid A. ; ALOMAINY, Akram: **“Analytical characterisation of the terahertz in-vivo nano-network in the presence of interference based on TS-OOK communication scheme”**. In *IEEE Access* 5 (2017), pages 10172–10181
- [Zhang et al. 2016] ZHANG, Rui ; YANG, Ke ; ALOMAINY, Akram ; ABBASI, Qammer H. ; QARAQE, Khalid ; SHUBAIR, Raed M.: **“Modelling of the terahertz communication channel for in-vivo nano-networks in the presence of noise”**. In *2016 16th Mediterranean Microwave Symposium (MMS)* IEEE (event), 2016, pages 1–4
- [Zhang 2019] ZHANG, Xingcai: **“Nanowires pin neurons: a nano “moon landing””**. In *Matter* 1 (2019), number 3, pages 560–562

LIST OF FIGURES

1.1	The integrated nanodevice's hardware architecture. Source: Mohammad and Shubair (2019).	5
1.2	Nanosensor. Source: Allied Market Research.	6
1.3	A spray-on nanoantenna. Source: Sarycheva et al. (2018).	6
1.4	Nanotweezers. Source: Zakharov et al. (2012).	7
1.5	Carbon nanotubes. Source: Stefan Diller/ Science Photo Library.	8
1.6	Prototype of an integrated nanosystem including a nanogenerator (energy harvester). Source: Wang (2012).	9
1.7	In-body nanocommunications. Source: Yang et al. (2020).	10
1.8	Examples of robotic materials McEvoy and Correll (2015), A: a facade that changes its opacity and color by hand gesture recognition Farrow et al. (2014), B: a dress that localizes the direction of incoming sounds and displays them to its wearer by localized flutter Profita et al. (2015), C: a beam that changes its shape using variable stiffness control McEvoy and Correll (2016) and D: a robotic skin that can sense and localize textures Hughes and Correll (2014).	12
1.9	Classification of routing protocols in wireless ad hoc networks.	14
2.1	Comparison between modulations: Jornet and Akyildiz (2014), Pujol et al. (2011), Mamed and Bourgeois (2018), Vavouris et al. (2018), user1 in blue and user2 in red. Source: Lemic et al. (2021).	21
2.2	Comparison between SLR (black) and CORONA (yellow) routing protocols for a communicating source and destination nodes in a given space. Source: Tsioliariidou et al. (2017).	25
3.1	Interactions among main C++ classes. Source: Dhoutaut et al. (2018).	29
3.2	VisualTracer's global mode: 30 000 neighbors receiving a few packets over time (4 very small time steps). Source: Dhoutaut et al. (2018).	32

3.3	VisualTracer's global mode: Propagation delay causing deferred reception. Source: Dhoutaut et al. (2018).	33
3.4	VisualTracer's individual mode: four flows scenario, collisions in red. Source: Dhoutaut et al. (2018).	33
4.1	Ring principle: only nodes in the ring (between rangeBig and rangeSmall) are potential forwarders of the packet sent by the center.	42
4.2	The communication range of the source hop without (left) and with the shadowing (right).	44
4.3	Proportion of packets received at a given distance from the center node with CR = 900 μ m and different values of std deviation.	44
4.4	Pure flooding without (left) and with the ring (right).	48
4.5	Cumulative number of forwarding nodes over time in pure flooding without and with the ring with 10 000 nodes.	49
4.6	Forwarders in backoff flooding without (left) and with the ring (right).	50
4.7	Cumulative number of forwarding nodes over time in backoff flooding without and with the ring with 10 000 nodes.	50
4.8	SLR without (left) and with the ring (right).	51
4.9	Cumulative number of forwarding nodes over time in SLR without and with the ring with 10 000 nodes.	52
4.10	Cumulative number of receiving nodes over time in pure flooding without and with the ring with 10 000 nodes.	53
4.11	Cumulative number of receiving nodes over time in backoff flooding without and with the ring with 10 000 nodes.	53
4.12	Arrival time at destination node in SLR for each packet sequence number with 10 000 nodes (all ten CBR packets for only seed=0 shown).	54
4.13	Simplified illustration of original ring (left) vs. expanded ring (right). Pink regions contain potential forwarders.	57
4.14	Envisioned goal by the expanded ring: forwarders at the first hop are in the inner black ring and forwarders at the second hop are in the external black ring. Nodes (black dots), rings (green) and inner discs (red).	58
4.15	State diagram of expanded ring.	60
4.16	Pure flooding without ring (left) and with (right) the expanded ring for the first packet of the first run (forwarders are in black, receivers are in light blue).	63

4.17	SLR without (left) and with (right) the expanded ring for the first packet for the first run (forwarders are in black, receivers are in light blue).	64
4.18	Drawbacks of dynamic ring with implicit ack: only the pink areas include new forwarders that will send the data packets counted as acknowledgments.	66
4.19	High traffic problem in dynamic ring width with explicit ack.	67
4.20	Simplified illustration of the dynamic ring: the ring adapts its width to the density to include 5 ring neighbors. Forwarders (yellow), nodes (black dots), rings (green) and inner discs (red).	68
4.21	State diagram for dynamic ring with DEDeN: node states based on packet reception from one transmitter.	69
4.22	The dynamic ring with DEDeN in pure flooding assigning different rangeS-small values for nodes depending on their density.	73
4.23	Pure flooding without (left) and with the dynamic ring with DEDeN (right); forwarders in black, receivers in blue, first packet of the first run only. . . .	74
4.24	Probabilistic flooding without (left) and with the dynamic ring with DEDeN (right); forwarders in black, receivers in blue, first packet of the first run only.	75
4.25	Backoff flooding without (left) and with the dynamic ring with DEDeN (right); forwarders in black, receivers in blue, first packet of the first run only.	75
4.26	SLR without (left) and with the dynamic ring with DEDeN (right); forwarders in black, receivers in blue, first packet of the first run only.	76
5.1	Nodes distribution in the network (without routing).	82
5.2	Scenario with $\beta=1000$ and source inter-packet interval= 10^5 ns: 5 flows intersecting at destination zone causing a congestion zone (right). Only first packet of each flow is shown. Forwarders are in blue, receivers in green, nodes with ignore in yellow, and nodes with collisions in red. SLR zones in the background.	83
5.3	Scenario used, with $\beta=100$ and source inter-packet interval= 10^5 ns. Only first packet of each flow is shown.	86
6.1	The reproducible table results of the contribution in Chapter 5	91

LIST OF TABLES

4.1	Simulation parameters.	45
4.2	Results with 10 000 nodes.	48
4.3	Average packet transmission time for 10 000 nodes.	52
4.4	Total data traffic generated for 10 000 nodes.	55
4.5	Evaluation results for 20 000 nodes.	55
4.6	Reduction of the number of forwarders from without to with the ring, for both networks of 10 000 and 20 000 nodes.	56
4.7	Average delivery ratio with ring in a network of 10 000 nodes vs. 20 000 nodes.	56
4.8	Simulation parameters.	61
4.9	Evaluation results with 10 000 nodes averaged for 10 runs and 50 packets each.	62
4.10	Simulation parameters.	71
4.11	Evaluation results in a 10 000 node network averaged for 10 runs and 50 packets each.	73
5.1	Simulation parameters.	81
5.2	Number of ignore and collision events for 5 flows of 100 packets each in a network of 20 000 nodes.	85
5.3	Percentage of packet delivery by each destination node for 5 flows of 100 packets each in a network of 20 000 nodes.	87
5.4	Comparison results between TS-OOK and RD TS-OOK for 5 flows of 100 packets each in a network of 20 000 nodes.	88

LIST OF ABBREVIATIONS

- **AODV:** Ad hoc On Demand Distance Vector. 21, 22
- **CBR:** Constant BitRate. 46, 54, 61, 71, 72, 82, 111
- **CODA:** Congestion Detection and Avoidance in Sensor Networks. 80
- **CORONA:** Coordinate and Routing system for Nanonetworks. 24, 25, 110
- **CR:** Communication Range. 43, 44, 46, 61, 111
- **DDS:** Drug Delivery System. 10
- **DEDeN:** Density Estimator for Dense Networks. 17, 23, 30, 32, 46, 49, 67, 69, 71–76, 84, 112
- **DEROUS:** Deployable Routing System for Nanonetworks. 24
- **DSR:** Dynamic Source Routing. 22
- **EM:** Electromagnetic. 6, 18, 27, 28
- **GPS:** Global Positioning System. 22, 23, 39, 40, 80
- **IoNT:** Internet of Nano Things. 3, 4, 6, 8, 13, 37, 97
- **IoT:** Internet of Things. 3, 13, 37, 97
- **MAC:** Medium Access Control. 19, 40, 43, 67, 79, 95
- **MCR:** Maximum Concurrent Receptions. 31, 83
- **mmWave:** Millimeter Wave. 9
- **MPR:** MultiPoint Relay. 22, 65
- **OLSR:** Optimized Link State Routing Protocol. 22
- **OOK:** On-Off Keying. 19

- **PHLAME:** Physical Layer Aware MAC Protocol for Electromagnetic Nanonetworks. 79
- **PPM:** Pulse Position Modulation. 20
- **RD TS-OOK:** Rate Division Time Spread On-Off Keying. 20, 78, 87, 88, 91, 113
- **RREQ:** Route Request. 22
- **RSSI:** Received Signal Strength Indicator. 40, 80
- **SDM:** Software-Defined Metamaterial. 11
- **SINR:** Signal to Interference plus Noise Ratio. 19
- **SLR:** Stateless Linear-path Routing. 24, 25, 28, 32, 46–48, 51–56, 60–64, 71–73, 76, 81–84, 90, 110–112
- **SRH-TSOOK:** Symbol rate Hopping TSOOK. 20
- **THz:** TeraHertz. 9–13, 18, 19, 37, 38, 78–80, 95
- **TS-OOK:** Time Spread On-Off Keying. 19, 20, 26–28, 30, 31, 38, 45, 78, 87, 88, 91, 113
- **VANET:** Vehicular Ad hoc Network. 40
- **WSN:** Wireless Sensor Network. 22, 37, 38, 80

Title: Methodologies and cross-layer protocols in electromagnetic nanonetworks and ultra-dense wireless ad hoc networks

Keywords: Routing, Congestion, Nanonetwork, Dense network, Scalability

Abstract:

With the densification of wireless ad hoc networks and the proliferation of connected objects in the Internet of Things (IoT), each device has a huge neighborhood. The further evolution of wireless communications defines the nanoscale and ultra-dense electromagnetic nanonetworks. Tiny nanodevices connect in a massively dense nanonetwork in the Terahertz band, to overcome the constraints of single devices and to execute complex tasks. In the future, nanonetworks will re-engineer humans and the world providing a wide range of applications, such as in-body communications and software defined metamaterials, etc. The motivation of this thesis is the lack of viable routing protocols for ultra-dense wireless ad hoc networks

and more specifically resource-constrained networks (e.g., nanonetworks). This dissertation evaluates the applicability of traditional protocols in these large scale networks and designs methodologies and scalable protocols. This thesis also highlights the unique behaviors of nanonetworks, resulting from the Terahertz channel and the Time Spread On-Off Keying modulation (TS-OOK), such as the "beta" parameter that influences the congestion, an important problem to study for large scale networks. To validate the proposed protocols, we use a nanonetwork simulator "BitSimulator", that is convenient for the study and that permits the implementation of the proposed network protocols as well as to assess the ideas.

Titre : Méthodologies et protocoles cross-layer dans les nanoréseaux électromagnétiques et les réseaux ad hoc sans fil ultra-denses

Mots-clés : Routage, Congestion, Nanoréseau, Réseau Dense, Scalabilité

Résumé :

Avec la densification des réseaux sans fil ad hoc et la prolifération des objets connectés dans l'Internet des objets (IoT), chaque machine a un énorme voisinage. L'évolution des communications sans fil définit l'échelle nanométrique et les nanoréseaux électromagnétiques ultra-denses. De minuscules nanomachines se connectent dans un nanoréseau massivement dense dans la bande TéraHertz, afin de surmonter les contraintes des dispositifs individuels et d'exécuter des tâches complexes. À l'avenir, les nanoréseaux restructureront les humains et le monde en fournissant un large éventail d'applications, comme des communications à l'intérieur du corps et des métamatériaux définis par logiciel, etc. La motivation de cette thèse est le manque de protocoles de routage viables pour les réseaux ad hoc sans

fil ultra-denses et plus spécifiquement pour les réseaux à ressources limitées (par exemple les nanoréseaux). Cette thèse évalue l'applicabilité des protocoles traditionnels dans ces réseaux à grande échelle et conçoit des méthodologies et des protocoles évolutifs. Cette thèse met également en évidence les comportements uniques des nanoréseaux, résultant du canal TéraHertz et de la modulation Time Spread On-Off Keying (TS-OOK), comme le paramètre "beta" qui influence la congestion, un problème important à étudier dans les réseaux à grande échelle. Pour valider les protocoles proposés, nous utilisons un simulateur de nanoréseau "BitSimulator", qui est convenable pour l'étude et qui permet l'implémentation des protocoles de réseau proposés ainsi que l'évaluation des idées.